UNIVERSITAT AUTÒNOMA DE BARCELONA

FACULTY OF MEDICINE

DEPARTMENT OF PEDIATRICS, OBSTETRICS & GYNECOLOGY

PREVENTIVE MEDICINE AND PUBLIC HEALTH

L-CARNITINE THERAPY PRESERVES ENDOTHELIAL FUNCTION IN A LAMB MODEL OF INCREASED PULMONARY BLOOD FLOW

A dissertation presented by

Angela Aramburo Caragol

in partial fulfillment of the requirements for the degree of

Doctor of Philosophy in Medical Sciences

Doctoral Thesis Director:

Carlos Rodrigo Gonzalo de Liria MD, PhD

Doctorate Program in Pediatrics, Obstetrics & Gynecology

2020

CONTRIBUTIONS:

* These authors contributed equally

ABSTRACT:

Title: L-carnitine therapy improves endothelial function in a lamb model of increased pulmonary blood flow.

Background: Congenital heart disease (CHD) with increased pulmonary blood flow (PBF) results in a progressive pulmonary vascular endothelial dysfunction that is partly dependent on decreased nitric oxide (NO) signaling. In a lamb model of CHD with increased PBF, we have shown a disruption in carnitine homeostasis, associated with mitochondrial dysfunction and decreased eNOS/HSP90 interactions that contribute to eNOS uncoupling, increased superoxide levels, and decreased bioavailable NO. Thus, we undertook this study to test the hypothesis that L-carnitine therapy would maintain carnitine homeostasis, mitochondrial function and NO signaling in our lamb model of increased PBF.

Methods: Methods: 13 fetal lambs underwent in-utero placement of an aorto-pulmonary graft (shunt). Immediately following spontaneous delivery, lambs received daily treatment with oral L-carnitine (n=7; 100 mg/kg/day) or its vehicle (n=6). An additional group of eleven lambs with normal PBF served as controls.

Results: At 4-weeks of age, L-carnitine-treated shunt lambs had decreased levels of acyl-carnitine and a reduced acyl-carnitine/free carnitine ratio compared to vehicle-treated shunt lambs. These changes correlated with increased carnitine acetyl-transferase (CrAT) protein and enzyme activity, as well as decreased levels of nitrated CrAT. The lactate/pyruvate ratio was also decreased in L-carnitine-treated shunt lambs. Furthermore, Hsp70 protein levels were significantly decreased in L-carnitine-treated shunt lambs, which

correlated with a significant increase in eNOS/Hsp90 interactions, NOS activity, and NOx levels, as well as with a significant decrease in eNOS derived superoxide. Further, acetylcholine significantly decreased left pulmonary vascular resistance (PVR) only in L-carnitine-treated shunt lambs.

Conclusions: Early L-carnitine therapy may improve and/or attenuate the decline in endothelial function noted in children with CHD associated with pulmonary overflow and thus has potentially important clinical implications that warrant further investigation.

Keywords: heart defects, congenital; pulmonary circulation; hypertension, pulmonary; endothelium, vascular; oxidative stress; carnitine; mitochondria; nitric oxide; animal model; animal research.

LIST OF ABBREVIATIONS

AC	Acycarnitine
Ach	Acetylcholine
ADMA	Asymmetric Dimethylarginine
ASD	Atrial Septal Defect
ATP	Adenosine Triphosphate
AVT	Acute Vasodilatory Testing
BH$_4$	Tetrahydrobiopterin
CACT	Carnitine Acylcarnitine Translocase
cAMP	Cyclic Adenosine Monophosphate
cGMP	Guanosine-3', 5'-Cyclic Monophosphate
CCS	Congenital Cardiac Shunt
CHD	Congenital Heart Disease
CPB	Cardiopulmonary By-Pass
CPT	Carnitine Palmitoyl Transferase
CrAT	Carnitine Acetyl Transferase
ECM	Extracellular Matrix
EDTA	Ethylene Diamine Tetraacetic Acid
eNOS	Endothelial Nitric Oxide Synthase
ET1	Endothelin-1
GTP	Guanosine-5'-Triphosphate
HES	Haematoxylin eosin staining
HSP	Heat Shock Protein
IV	Intravenous
IM	Intramuscular
iNO	Inhaled Nitric Oxide
L-NAME	Nitro-L-Arginine Methyl Ester hydrochloride
NO	Nitric Oxide
NOx	Nitrite and Nitrate

NOS	Nitric Oxide Synthase
PA	Pulmonary Artery
PAH	Pulmonary Arterial Hypertension
PAWP	Pulmonary Artery Wedge Pressure
PAP	Pulmonary Arterial Pressure
PBF	Pulmonary Blood Flow
PDA	Patent Ductus Arteriosus
PDE	Phosphodiesterase
PGI$_2$	Prostaglandin I$_2$
PH	Pulmonary Hypertension
PHVD	Pulmonary Hypertensive Vascular Disease
PPARγ	Peroxisome Proliferator-Activated Receptor gamma
PPRE	PPRA Response Element
PVD	Pulmonary Vascular Disease
PVR	Pulmonary Vascular Resistance
PVRI	Pulmonary Vascular Resistance Index
ROS	Reactive oxygen species
SMC	Smooth Muscle Cell
SO$_2$	Oxyhemoglobin Saturation
SOD-2	Superoxide Dismutase-2
SVC	Superior Vena Cava
SVR	Systemic Vascular Resistance
TGA	Transposition of Great Arteries
TXA$_2$	Thromboxane A$_2$
UCP-2	Uncoupling Protein-2
VSD	Ventricular Septal Defect
WSPH	World Symposium on Pulmonary Hypertension

LIST OF FIGURES

LIST OF TABLES

TABLE OF CONTENTS

INTRODUCTION

1 <u>INTRODUCTION</u>

1.1 PULMONARY HYPERTENSION AND CONGENITAL HEART DISEASE

1.1.1 Concepts and epidemiology

Pulmonary hypertension is a fatal, relatively rare and highly heterogeneous pathophysiological disorder that results in elevated mean pulmonary arterial pressure (mPAP), right ventricular dysfunction, left ventricular compression and heart failure(2). Despite PH can present at any age and involve multiple clinical conditions, outside the immediate post-natal period, congenital heart disease (CHD) is the first cause of PH in the pediatric population with 3 million children estimated at risk worldwide(3-5).

Congenital heart disease (CHD) affects approximately 8/1,000 live births. These defects are characterized by a heterogeneous group of abnormal connections between the cardiac chambers and vessels with different hemodynamic consequences and, hence, varying need for follow-up and interventions(6).

A wide range of CHD can lead to PH through two main pathogenic mechanisms:

   1) Congenital systemic-to-pulmonary cardiac shunts (CCS) that result in increased pulmonary blood flow (PBF), elevated pulmonary vascular reactivity (PVR)[1] and *pre-capillary PH*;

   2) Left side heart disease that results in an elevated pulmonary artery wedge pressure (PAWP) and *post-capillary PH.*

According to recent data from nationwide registries in Europe and USA, the vast majority of PH associated with CHD corresponds to *pre-capillary PH* secondary to repairable CCS(5, 7, 8) with an estimated incidence of 21.9 cases per million children(4). Despite major advances in our understanding and management of

CHD in recent decades, *pre-capillary PH* remains a major complication of CCS around the globe, increasing perioperative morbidity and mortality of surgical repair or even preventing it completely when disease is advanced. Sadly the latter continues to be a common scenario nowadays, as still only a fraction of at risk children worldwide are offered timely access to surgical or percutaneous defect closure(3).

1.1.2 Hemodynamic definition of Pulmonary Hypertension (PH)

Since the 1st World Symposium on Pulmonary Hypertension (WSPH) in 1973, PH in adults and children had been arbitrarily defined as mPAP $\geqslant$25mmHg at rest measured by right heart catheterization(9). Based on new data on mPAP in healthy individuals(10), the 6th WSPH Task Force (Nice, 2018) has recently redefined PH as mPAP >20mmHg, together with an elevated PVR (*pre-capillary pH*) and/or PAWP (*post-capillary PH*) (Table 1)(11).

Table 1: 6th WSPH Hemodynamic definitions of pulmonary hypertension		
Definitions	**Characteristics**	**Clinical groups #**
Pre-capillary PH	mPAP >20 mmHg PAWP $\leqslant$15 mmHg PVR $\geqslant$3 WU	1, 3, 4 and 5
Isolated post-capillary PH	mPAP >20 mmHg PAWP >15 mmHg PVR <3 WU	2 and 5
Combined pre- and post-capillary PH	mPAP >20 mmHg PAWP >15 mmHg PVR $\geqslant$3 WU	2 and 5
PVR= [(mPAP-PAWP)/cardiac ouput]. WU: Wood Units. #: Group 1: PAH; group 2: PH due to left heart disease; group 3: PH due to lung diseases and/or hypoxia; group 4: PH due to pulmonary artery obstructions; group 5: PH with unclear and/or multifactorial mechanisms.		

Adapted from Simmoneau et al.(11)

Thus, the newly proposed WSPH PH definition mandates the assessment of PVR by right heart catheterization, with accurate measurement of cardiac output and PAWP. Importantly, the new definition excludes cases of isolated elevated mPAP seen e.g. with high cardiac output or with unrestricted CCS at an early stage when PVR is not yet elevated [mPAP= PBF x PVR].

The 6th WSPH Task Force agreed to apply the new PH definition to infants from 3 months of age (when mPAP falls to adult levels after post-natal transition) to adulthood, advising in pediatrics to index PVR (PVRI≥ 3 WU/m^2) (12).

1.1.3 Clinical classification and terminology of PH associated with CHD

Two main clinical classifications of PH associated with CHD currently exist: a) the *Panama classification of Pediatric Pulmonary Hypertensive Vascular Disease,* and b) the *6th WSPH clinical classification of PH.*

a) The *Panama classification of Pediatric Pulmonary Hypertensive Vascular Disease (PHVD)*, which followed the 2,011 Pulmonary Vascular Research Institute meeting (Panama), proposed a clinical classification of what they called *PHVD* specifically focused on issues and disease entities relevant to children and emphasizing the impact of developmental physiology (Table 2).

TABLE 2. Panama classification of PHVD (2011)	
Category	**Pediatric PHVD category**
1	Prenatal or developmental pulmonary hypertensive vascular disease
2	Perinatal pulmonary vascular maladaptation
3	**Pediatric cardiovascular disease:** 3.1 Systemic to pulmonary shunts (CCS) 3.2 Post-operative pulmonary arterial hypertension (PAH) 3.3 PVD following staged palliation for single ventricle physiology 3.4 PHVD with congenital abnormalities of the pulm. arteries/veins 3.5 Pulmonary venous hypertension

4	Bronchopulmonary dysplasia
5	Isolated pediatric PHVD (isolated pediatric pulm. arterial hypertension)
6	Multifactorial pulmonary hypertensive vascular disease in congenital malformation syndromes
7	Pediatric lung disease
8	Pediatric thromboembolic disease
9	Pediatric hypobaric hypoxic exposure
10	Pediatric PVD associated with other system disorders

From Cerro et al.(13)

Pediatric cardiovascular disease (category 3) was divided in 5 sub-categories, each of them with several subgroups (Table 3). The term *PHVD* was introduced at the time to exclude children with PH without elevated PVR, as well as to account for patients with high PVRI despite a normal mPAP, as seen in some children with single ventricle physiology post-cavo-pulmonary anastomosis(13).

TABLE 3. Panama classification of PHVD: Pediatric Cardiovascular Disease	
Category 3	**Pediatric cardiovascular disease**

3.1	**Systemic to pulmonary shunts (CCS)**
	3.1.1. PAH associated with systemic to pulmonary shunt with increased PVRI, no R-L shunt
	   3.1.1.1. Operable
	   3.1.1.2. Inoperable
	3.1.2 Classical Eisenmenger syndrome
	   3.1.2.1. Eisenmenger–Simple lesion (ASD, VSD, PDA)
	   3.1.2.2. Eisenmenger–Complex lesion (Truncus, TGA/VSD, single ventricle)
	3.1.3. Small defect with elevated pulmonary arterial pressure/PVRI out of proportion to the size of the defect
	   Coexistent with pulmonary hypoplasia
	   Coexistent with inherited or idiopathic PHVD

3.2	**Post-operative PAH** 3.2.1. Closure of shunt with 3.2.1.1 persistent increase in PVRI>3 WU.m2

	3.2.1.2 recurrent increase in PVRI>3 WU.m2
	3.2.2. Arterial or atrial switch for TGA with intact ventricular septum
	3.2.3. Repair of left heart obstruction
	3.2.4. Repair of tetralogy of Fallot
	3.2.5. Repair of pulmonary atresia with VSD and MAPCA's
	3.2.6. Surgical aorto-pulmonary shunt
3.3	**Pulmonary vascular disease following staged palliation for single ventricle physiology**
	3.3.1. After stage 1 (PA banding, modified Norwood, hybrid procedure, aorto-pulmonary or ventricular pulmonary shunt, stenting PDA)
	3.3.2. After SVC to PA anastomosis (Glenn)
	3.3.3. After total cavo-pulmonary anastomosis (Fontan)
3.4	**Pediatric PHVD (PPHVD) associated with congenital abnormalities of the pulmonary arteries/veins**
	3.4.1. PPHVD associated with congenital abnormalities of the pulmonary arteries
	3.4.1.1. Origin of a pulmonary artery from the aorta
	3.4.1.2. Unilateral isolation/ductal origin/"absence" of a pulmonary artery
	3.4.2. PPHVD associated with congenital abnormalities of the pulmonary veins
	3.4.2.1. Scimitar Complex
	3.4.2.2. Pulmonary vein stenosis
	3.4.2.3. Cantú syndrome
3.5	**Pulmonary venous hypertension**
	3.5.1. Pulmonary venous hypertension due to congenital left heart inflow or outflow disease:
	Aortic stenosis, aortic incompetence, mitral stenosis, mitral regurgitation, supramitral ring, pulmonary vein obstruction, cor triatriatum, endocardial fibroelastosis, left ventricular hypoplasia/Shone's complex, congenital cardiomyopathy, restrictive atrial septum in hypoplastic left heart syndrome
	3.5.2. Pulm. venous hypertension due to acquired left heart disease:
	Left sided Valvar Heart Disease (rheumatic/postendocarditis/rheumatoid arthritis)
	Restrictive /Dilated /Hypertrophic Cardiomyopathy
	Constrictive pericardial disease

From Cerro et al.(13)

b) The *6th WSPH clinical classification of PH* categorizes adults and children with

PH associated with CHD in 3 clinical subgroups (Table 4):

- Congenital heart defects/shunts leading to *pre-capillary PH* (subgroup 1.4.4)

- Congenital left-side heart diseases leading to *post-capillary PH* (subgroup 2.4)

- Complex CHD (subgroup 5.4)

Table 4. 6th WSPH updated clinical classification of pulmonary hypertension
1. PAH
1.1 Idiopathic PAH
1.2 Heritable PAH
1.3 Drug- and toxin-induced PAH
1.4 PAH associated with:
1.4.1 Connective tissue disease
1.4.2 HIV infection
1.4.3 Portal hypertension
1.4.4 Congenital heart disease
1.4.5 Schistosomiasis
1.5 PAH long-term responders to calcium channel blockers
1.6 PAH with overt features of venous/capillaries involvement
1.7 Persistent PH of the newborn syndrome
2. PH due to left heart disease
2.1 PH due to heart failure with preserved left ventricular ejection fraction
2.2 PH due to heart failure with reduced left ventricular ejection fraction
2.3 Valvular heart disease
2.4 Congenital/acquired cardiovascular conditions leading to post-capillary PH
3. PH due to lung diseases and/or hypoxia
3.1 Obstructive lung disease
3.2 Restrictive lung disease
3.3 Other lung disease with mixed restrictive/obstructive pattern
3.4 Hypoxia without lung disease
3.5 Developmental lung disorders
4. PH due to pulmonary artery obtructions
4.1 Chronic thromboembolic PH
4.2 Other pulmonary artery obstructions
5. PH with unclear and/or multifactorial mechanisms
5.1 Haematological disorders
5.2 Systemic and metabolic disorders
5.3 Others
5.4 Complex congenital heart disease

From Simonneau et al.(11)

The term *pulmonary arterial hypertension* (PAH) in the 6th WSPH classification describes a group of patients (clinical group 1) with *pre-capillary PH* (mPAP >20 mmHg with PVR ≥ 3 WU) in the absence of other causes of *pre-capillary PH* such as lung diseases (group 3) or pulmonary artery obstructions (group 4)(14). The term PAH refers to different forms of PH that share a similar clinical picture and virtually identical pathological changes of the lung microcirculation(15). This broad PAH category includes the CCS.

Congenital left heart inflow or outflow diseases (clinical sub-group 2.4 of the 6th WSPH classification) include congenital cardiomyopathies, and post-capillary obstructive lesions, such as obstructed total anomalous pulmonary venous drainage, cor triatriatum or mitral and aortic stenosis.

Of note, an additional widely used term in the pediatric PH nomenclature is *pulmonary vascular disease* (*PVD*). PVD is considered a broader and more inclusive term than PH or PAH in that it also includes abnormalities of pulmonary vascular tone, reactivity, growth, and structure that may exist without the development of increased mPAP or PVR, as seen at times in children with single ventricle physiology or with CCS at an early stage. PVD is also commonly used to refer to all PAH forms (WSPH clinical group 1), as well as pediatric diseases of the lung circulation(16).

From here onwards, PVD will be the term used in this manuscript to refer to the molecular, functional, histologic and clinical pulmonary vascular abnormalities associated with congenital systemic-to-pulmonary cardiac shunts (CCS).

1.2 PULMONARY VASCULAR DISEASE (PVD) ASSOCIATED WITH CONGENITAL CARDIAC SHUNTS

1.2.1 Natural history of PVD in CCS and Eisenmenger syndrome

The pulmonary circulation is a highly specialized vascular system that has evolved to provide an extensive surface area for gas exchange(17). Despites it receives the entire cardiac output during each cardiac cycle, more than any other organ in the body, normal adult pulmonary circulation is a low-pressure low-resistance system, properties that are critical to prevent damage to the gas exchange barrier and optimize the efficiency of the right ventricle. During fetal life, however, lungs are filled with amniotic fluid and pulmonary circulation is a high-pressure, high-resistance, low-capacitance system. Post-natal changes in the pulmonary circulation result in an initial rapid drop of the PVR, that usually continues until it reaches adult levels between 2 and 8 weeks of life [PVR ≈20% of systemic vascular resistance (SVR)].

Consequently, CCS initially manifest as systemic-to-pulmonary (left-to-right) shunts that result in progressively increasing PBF as PVR gradually drops. Depending on the defect anatomic characteristics, CCS may lead to early congestive heart failure in infancy (e.g. tachycardia, tachypnea, hepatomegaly or failure to thrive). In addition, the increased shear stress associated with the CCS cause early structural and functional changes to the pulmonary vasculature that, despite reversible in most instances with early repair, put children at risk of perioperative life-threatening episodes of acute reactive pulmonary vasoconstriction (pulmonary hypertensive crisis) with subsequent hypoxemia, acidosis, right heart failure and low cardiac output state that significantly increase their morbidity and mortality risk(18).

When CCS are not corrected within usually the first two years of life, chronic exposure to increase pulmonary blood flow +/- pressure leads to irreversible structural pulmonary vascular remodeling and dysfunction that result in increased

tone and PVR. These changes usually correlate with a decrease in the degree of left-to-right shunting and an improvement of heart failure symptoms may be observed(19).

As PVD progresses PVR continues to rise until it approaches or exceeds SVR. At this point shunt direction reverts (right-to-left) and cyanosis appears. This irreversible end-stage disease, known as Eisenmenger syndrome, usually contraindicates defect closure and leads to death secondary to hypoxemia and myocardial failure at around the third or fourth decade of life(20) (Figure 1).

Figure 1: Diagram of the natural history of PVD associated to CCS
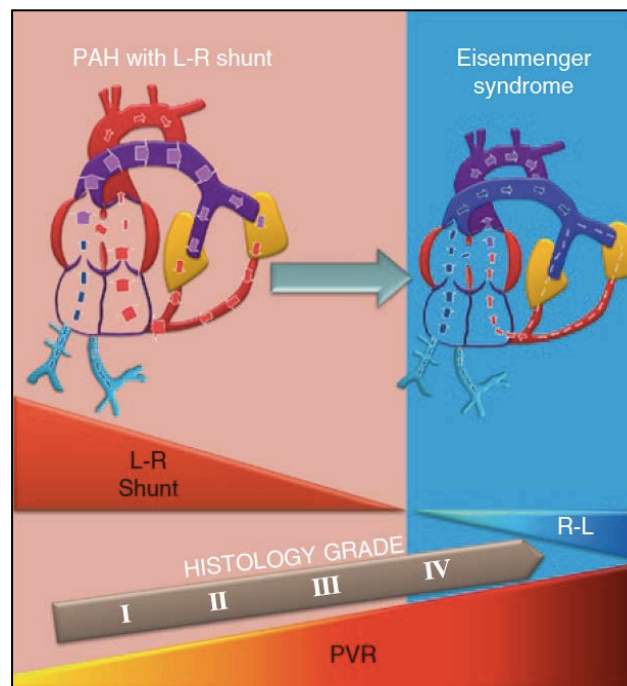
From: Pulmonary Hypertension in Adult Congenital Heart Disease(21)

It is important to notice that despite all CCS eventually lead to irreversible PVD, a wide range of CCS lesions exist, with different defects evolving differently depending on the degree of increased PBF they cause, but most importantly on the concomitant presence or not of increased pressure(22). Thus, increase in PBF only causes a laminar shear stress that seems to differ to the laminar and

circumferential (pressure) shear stress induced by high flow and pressure lesions. Thus, simple post-tricuspid shunts such as VSD (Figure 2) or ductus arteriosus (Figure 3a) develop in general PVD more rapidly than pre-tricuspid shunts like atrial septal defects (Figure 3b), which are increased-flow-alone lesions that usually do not result in increased PVR until the third decade of life.

Figure 2: Ventricular septal defect
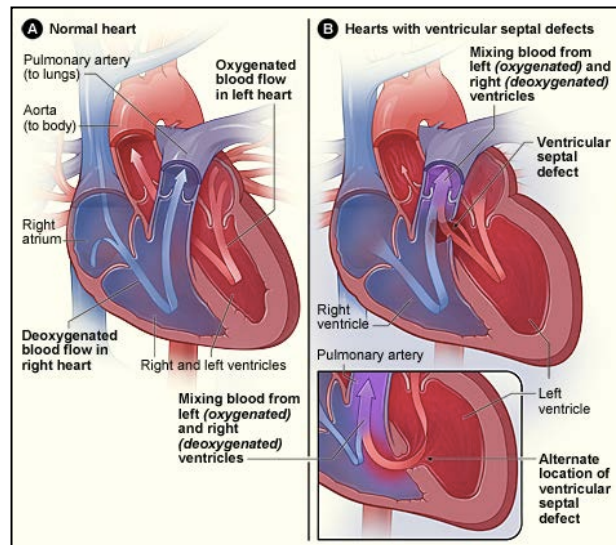
A. Normal heart; B. Hearts with ventricular septal defects. Image courtesy of Pediatric Cardiothoracic Surgery, University California San Francisco

Figure 3: Ductus arteriosus (a) and atrial septal defect (b)
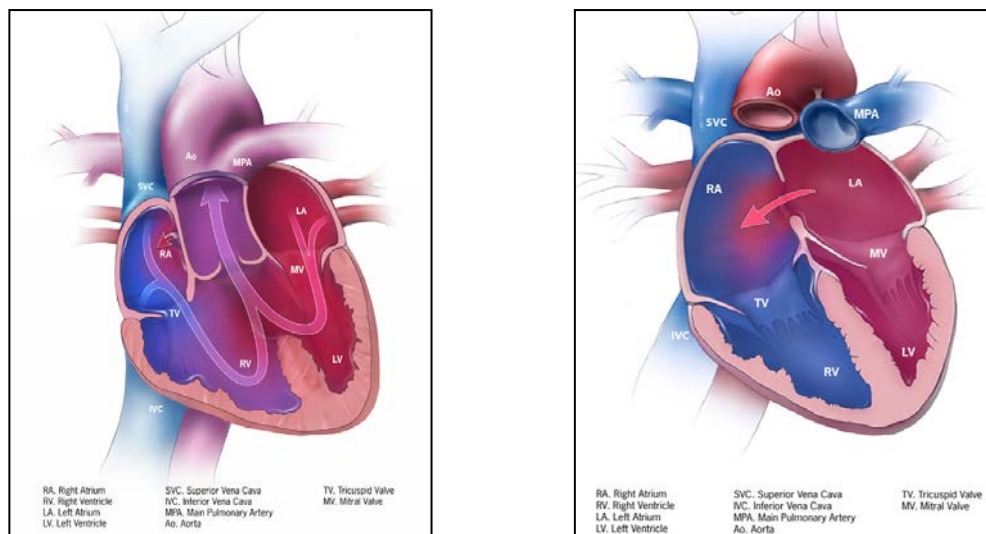
Images from Center for Disease Control and Prevention (https://www.cdc.gov/ncbddd/).

On the contrary, some complex CHD such as truncus arteriosus, transposition of the great arteries with VSD and complete atrio-ventricular canal defects are of particular high risk for the development of severe PVD if untreated in the first year of life(22, 23). There is, however, great variability in the clinical presentation and prognosis among patients with same CHD. Interestingly, infants with genetic disorders, such as trisomy 2, may develop advanced PVD more rapidly(24). Consequently, knowing the natural history of each CCS has obvious implications in the follow-up and timing of the repair, being the status of the pulmonary vasculature often the principal determinant of the clinical course and potential operability(24). Even so, whether PAP and/or PVR will eventually return to normal or remain elevated after surgical repair is frequently uncertain, as determined by the morphometric and histologic changes of the pulmonary vasculature at the time of the repair. In fact, lung biopsy and the assessment of the degree of arteriopathy were used for years to define the feasibility of surgery and reversibility of PVD(25, 26). Nowadays, a less invasive approach is advised and when uncertainty about operability potential exists, an acute vasodilator testing in the catheterization laboratory with the use of potent pulmonary vasodilators such as oxygen and inhaled nitric oxide (iNO) is often performed. Nevertheless, specific criteria for defining a positive acute vascular testing response or specific hemodynamic targets that predict reversibility of PVD and good long-term prognosis following defect closure remain lacking.

The 6th WSPH Pediatric Task Force has provided a consensus guidance for assessing the operability of CCS(12) (Table 5), however authors acknowledge that other factors beyond the hemodynamic measurements and response to acute vascular testing should be consider together in the assessment, highlighting an

obvious need for further research on the topic. These factors include age, type of

cardiac lesion, comorbidities, resting and exercise saturations, clinical history and

response to targeted PH therapy.

Table 5: Guidance for assessing operability in PVD associated with CHD		
PVRI (WU/m^2)	PVR (WU)	Correctability/favourable long-term outcome
<4	<2.3	Yes
4-8	2.3-4.6	Individual patient evaluation in tertiary centers
>8	>4.6	No
WU: Wood Units. Special considerations include: age of patient, type of defect, comorbidities, resting or exercise-induced desaturation and PVD therapy (treat with intent-to-repair approach has not been proven).		

From Rosenzweig et al.(12)

1.2.2 Anatomical, pathophysiological and clinical classifications of CCS

To better describe the wide heterogeneity in anatomic lesions as well as in clinical

manifestations of PVD, anatomical-pathophysiological and clinical classifications

of CCS have been proposed by the consecutive World Symposium of Pulmonary

Hypertension meetings. The latest 6th WSPH has recently classified CCS from an

anatomical-pathophysiological point of view(15) according not only to factors

relevant in the progression of PVD such as anatomical type and dimension, but

also based on direction of shunt, association with other cardiac or extra-cardiac

anomalies, and status of anatomical repair (Table 6).

TABLE 6. Anatomical-pathophysiological classification of CCS associated with PVD.
1. Type:

1.1 Simple pre-tricuspid shunts
  1.1.1 Atrial septal defect (ASD)
    1.1.1.1 Ostium secundum
    1.1.1.2 Sinus venosus
    1.1.1.3 Ostium primum
  1.1.2 Total or partial unobstructed anomalous pulmonary venous return
1.2 Simple post-tricuspid shunts
  1.2.1 Ventricular septal defect (VSD)
  1.2.2 Patent ductus arteriosus
1.3 Combined shunts
   Describe combination and define predominant defect
 	
1.4 Complex congenital heart disease
  1.4.1 Complete atrioventricular septal defect
  1.4.2 Truncus arteriosus
  1.4.3 Single ventricle physiology with unobstructed pulmonary blood flow
  1.4.4 Transposition of the great arteries with VSD (without pulmonary stenosis) and/or patent ductus arteriosus
  1.4.5 Other

2. Dimension (specify for each defect if >1 congenital heart defect exists):

2.1 Haemodynamic (specify Qp/Qs)[a]
  2.1.1 Restrictive (pressure gradient across the defect)
  2.1.2 Non-restrictive
2.2 Anatomic[b]
  2.2.1 Small to moderate (ASD ≤2.0 cm and VSD ≤1.0 cm)
  2.2.2 Large (ASD >2.0 cm and VSD >1.0 cm)

3. Direction of shunt:

3.1 Predominantly systemic-to-pulmonary
  3.2 Predominantly pulmonary-to-systemic
  3.3 Bidirectional

4. Associated cardiac and extra cardiac abnormalities
5. Repair status:

5.1 Unoperated
  5.2 Palliated (specify type of operation/s, age at surgery)
  5.3 Repaired (specify type of operation/s, age at surgery)

a. Ratio of pulmonary (Qp) to systemic (Qs) blood flow; b. The size applies to adult patients

Adapted from Galié et al.(15)

In addition, for clinical practice use and taking into account the natural history of PVD, the 6th WSPH clinical classification of CCS has described four distinct phenotypes that differed in management and responses to treatment: Eisenmenger syndrome; PAH associated with relevant systemic-to-pulmonary shunts, which may be correctable or non-correctable depending on the status of pulmonary vasculature; PAH with coincidental defects; and PAH after defect correction (Table 7).

Table 7. Clinical classification of PAH with congenital heart disease/defects
1. Eisenmenger's syndrome
Includes all large intra- and extra-cardiac defects, which begin as systemic-to-pulmonary shunts and progress with time to severe elevation of PVR and to reversal (pulmonary-to-systemic) or bidirectional shunting; cyanosis, secondary erythrocytosis, and multiple organ involvement are usually present.

2. PAH associated with prevalent systemic-to-pulmonary shunts
  • Correctable[a]
  • Non-correctable
Includes moderate to large defects; PVR is mildly to moderately increased; systemic-to-pulmonary shunting is still prevalent, whereas cyanosis at rest is not a feature.

3. PAH with small/coincidental defects[b] Marked elevation in PVR in the presence of small cardiac defects, which themselves do not account for the development of elevated PVR; the clinical picture is very similar to idiopathic PAH. Closing the defects is contra-indicated.
4. PAH after defect correction Congenital heart disease is repaired, but PAH either persists immediately after correction or recurs/develops months or years after correction in the absence of significant postoperative hemodynamic lesions.
PAH: pulmonary arterial hypertension; PVR: pulmonary vascular resistance. [a] With surgery or intravascular percutaneous procedure. [b] The simple defect diameter measured by echocardiography may be not sufficient for defining the hemodynamic relevance of the defect and also the pressure gradient, the shunt size and direction, and the pulmonary to systemic flows ratio should be considered.

Adapted from Galié et al.(15)

1.2.3 Histopathology of PVD associated to CCS

1.2.3.1 Normal pulmonary arterial tree

The wall of the pulmonary arteries consists in three main cellular layers (tunica externa or adventitia, tunica media and tunica intima) embedded in and supported by extracellular matrix (Figure 4). The composition of the wall as well as the contribution of each layer to the total wall thickness, however, varies from the proximal pulmonary artery trunk to the smallest extra-alveolar arteries, with a gradual loss of musculature. The adventitial surface of the arteries in the broncho-vascular bundle is tethered to the surface of the adjacent airway on one face and to alveolar septal networks on the other. The adventitia is loosely organized, comprised of extracellular matrix (ECM) proteins, fibroblasts or other interstitial cells, vasa vasorum, and a neuronal network. The tunica media has two components: the external elastic lamina and smooth muscle cells.

Figure 4: Structure of the pulmonary arterial wall
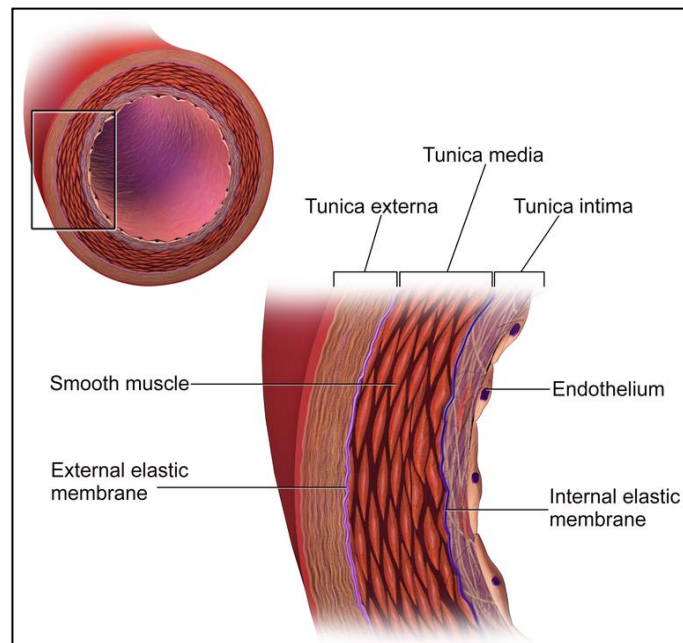
From Blaussen..com(27)

Based on the presence and number of elastic lamina and the degree of

muscularity, pulmonary arteries can be classified as elastic, transitional (with features of both elastic and muscular), muscular, partially muscular or non-muscular. The thin tunica intima consists of a non-fenestrated monolayer of endothelial cells lining the vessel lumen, as well as a sub-endothelial interstitium that extends to the internal elastic lamina(17). Based on the relationship of the pulmonary vasculature to surrounding lung tissue, pulmonary arteries can also be divided into 1) those external to (pre-acinar) vs. those within the respiratory acinus of the lung (intra-acinar); 2) those external to (extra-alveolar) vs. those within the alveolar compartment; and 3) those upstream to the alveolar capillary bed (pre-capillary). Intra-acinar arteries are associated with respiratory bronchioles, alveolar ducts and alveolar walls, i.e. the airways involved in gas exchange (Figure 5)(17).

Figure 5: Normal pulmonary arterial tree
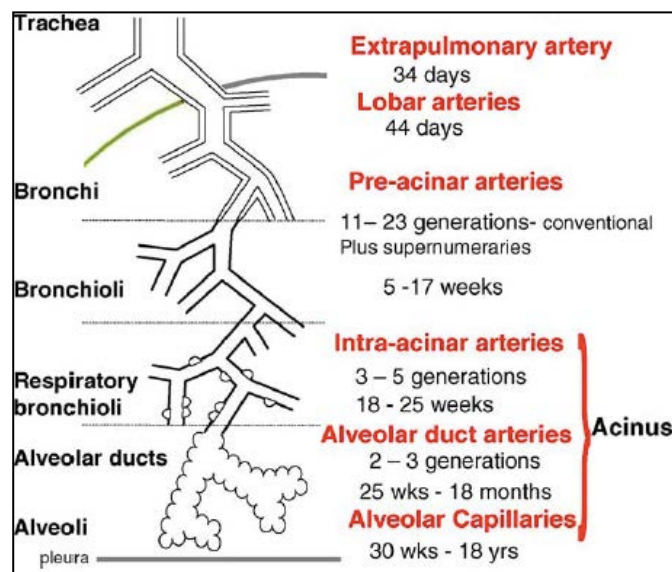
Adapted from Hislop et al.(28)

In the normal human fetus, the pre-acinar arteries and those at the level of the terminal bronchioles are muscular, whereas the intra-acinar arteries are either partially muscular or non-muscular. Arteries at the alveolar duct and wall levels are non-muscular. The immediate postnatal period is characterized by rapid

recruitment of small alveolar duct and wall vessels and progressive dilatation of muscular arteries and wall thinning that reaches adult levels within a few days and by four months has included the largest PA at the hilum.

Although most alveolar duct arteries become partially muscularized, most alveolar wall arteries remain non-muscular even in the adult. Pre-capillary (alveolar duct and alveolar wall) arteries proliferate through the neonatal period and early infancy, accompanying the proliferation of alveoli and the ratio of alveoli to arteries is used as a measure of arterial growth. The ratio of alveoli to arteries decreases from the newborn value of 20:1 to the value of 6–8:1, which is first achieved in early childhood and persists through adulthood(29).

1.2.3.2 Pulmonary arterial histologic changes associated to CCS

In 1958, Heath and Edwards described for the first time the progressive histologic changes that occur in the intima and media of pulmonary arteries and arterioles exposed from birth to elevated PAP as a consequence of large post-tricuspid shunts (e.g. VSD, large patent ductus arteriosus), pointing out potential differences with pre-tricuspid shunts (e.g. ASD).

These structural changes were so stereotyped that authors could group them into six different histologic grades, often seen irregularly distributed throughout the lung(30). Thus, they described a medial artery hypertrophy (Grade I) that progresses to intimal proliferation (cellular neointima formation, grade II) and fibrosis (occlusive neointimal formation, grade III) resulting in arterial lumen occlusion. With advancement of the disease, a progressive generalised dilation of the muscular arteries (plexiform lesions) and fibroelastosis (Grade IV) is observed, which leads to thinning and fibrosis of the media with cavernous and angiomatoid

formation (Grade V) and ultimately to necrotizing arteritis (Grade VI) (Figure 6 and

7, Table 8).

Figure 6: Heath–Edwards histologic classification of PVD: grades I–III
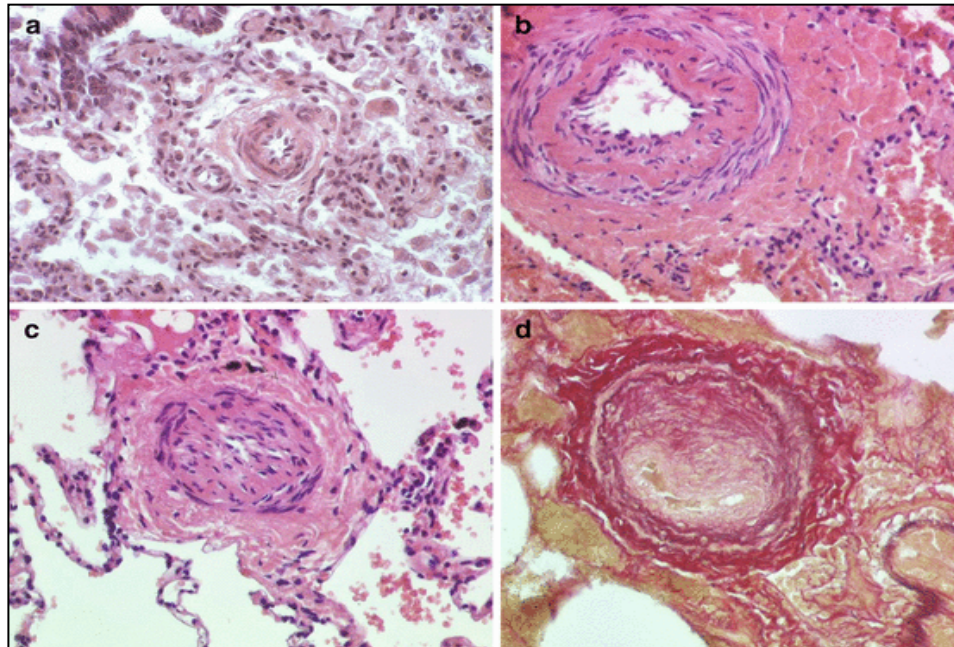
Lung biopsies: a) Grade I: small arteries with hypertrophy of the media. Haematoxylin eosin staining (HES), original magnification (OM) Åx10. b) Grade II: artery with intimal smooth muscle cell proliferation, medial hypertrophy and increased adventitia fibrosis. HES, OM Åx20. c) Grade III: sub-occlusive concentric intimal proliferation, thinning of the media and fibrosis of the adventitia. HES OM Åx20. d) Grade III: obstructive eccentric fibrocellular intimal proliferation. Elastic fibre Van Gieson staining,OM Åx20. From K. Dimopoulos et al.(21).

Figure 7: Heath–Edwards histologic classification of PVD: grades IV-VI
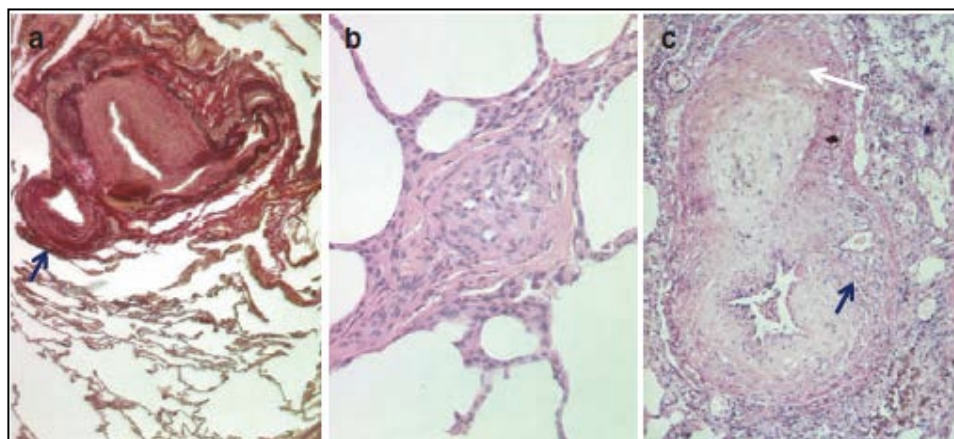
Lung biopsies: a) Grade IV: severe arterial dilatation and sub-occlusive fibrosis. Elastic fibre Van Gieson staining, OM Åx10. b) Grade V: typical plexiform lesion. HES, OM Åx20. c) Grade VI: typical aneurysmatic lesion, with occlusion of the lumen and fibrinoid necrosis (white arrow) of the parietal wall and neo-angiogenetic proliferative aspect (black arrow). From K. Dimopoulos et al.(21).

Table 8. Heath & Edwards Grades of PVD associated with CCS						
	1	2	3	4	5	6
Type of intimal reaction	None					
		Cellular				
			Fibrous & fibroelastic			
				Plexiform lesion		
State of media of arteries and arterioles	Hypertrophied					
		Some generalized dilatation				
			Local "dilatation lesions"			
					Pulmonary	
						Necrotizing

While authors considered grade-I changes simply an integral part of the various structural and functional alterations seen with large CCS, grades-II to VI changes seem to occur as a result of raised PAP and are present in all forms of hypertensive PVD, whatever the etiology. Further work with patients with CCS who underwent surgical repair led Heath and Edwards to suggest that histologic grade ≤III was potentially reversible, whereas >grade IV likely was not(31).

Two decades after the Heath-Edwards classification was published, Rabinovitch et al, using a newly developed quantitative method, analysed the vascular structure in lung tissue biopsies obtained at time of surgical repair from patients with CCS aged 2 days to 30 years, who either had pulmonary hypertension or in whom it would be likely to develop if the lesion were not corrected(32). Authors of this seminal work described three new structural progressive grades of PVD, and importantly correlated the quantitative morphologic data with preoperative pulmonary haemodynamic data (Table 9, Figure 8), suggesting for the first time

how structural alterations in the pulmonary arteries produce hemodynamic changes.

Table 9. Lung biopsy in CHD: a morphometric approach to PVD	
Grade	**Lung biopsy findings**
A	Extension of muscle into peripheral arteries normally non-muscular, either as a solitary finding or associated with a mild increase in the medial wall thickness of the normally muscular arteries (≤1.5 times normal)
B	Extension as in grade A but greater medial hypertrophy - Mild: Medial wall thickness is greater than 1.5 but less than 2 times normal - Severe: Medial wall thickness is 2 times normal or greater
C	Feature of B (severe), with a decreased number of peripheral arteries relative to alveoli and usually decreased arterial size - Mild: More than half of the normal number of arteries is present - Severe: Half of the normal number of arteries or less is observed

From Suesaowalak et al.(19) and adapted from Rabinovitch et al.(33)

Thus, grade A (found in all patients with increased PBF) was defined as an abnormal extension of muscle into peripheral normally non-muscular arteries. Grade B was defined as grade A with an additional increase in the percentage medial wall thickness of the small intra-acinar arteries. Grade B was found to correlate invariably with elevated PAP (usually greater than half that of the systemic level) when wall thickness was more than twice normal. Grade C, found in a minority of patients only, was defined as grade B with a further reduction in the number of small arteries relative to the alveolar concentration and correlated with moderate-to-severe PVR elevation (>3.5 Wood Units/m^2). Grade C was invariably present in Heath-Edwards grade ≥III, but was also observed in less severe forms (grade I and II), perhaps due to insufficient growth of new arteries compared to alveoli in young children(21). Grade A and B were considered refinements of Heath-Edwards grade I (medial hypertrophy), whereas Grade C was thought to be

a new finding reflecting the failure of the arteries to proliferate normally and indicative of more severe disease. Authors felt not only that Grade C preceded obliterative PVD, but also that could potentially identify patients in whom PVD would progress after repair.

Figure 8: Peripheral pulmonary arterial development
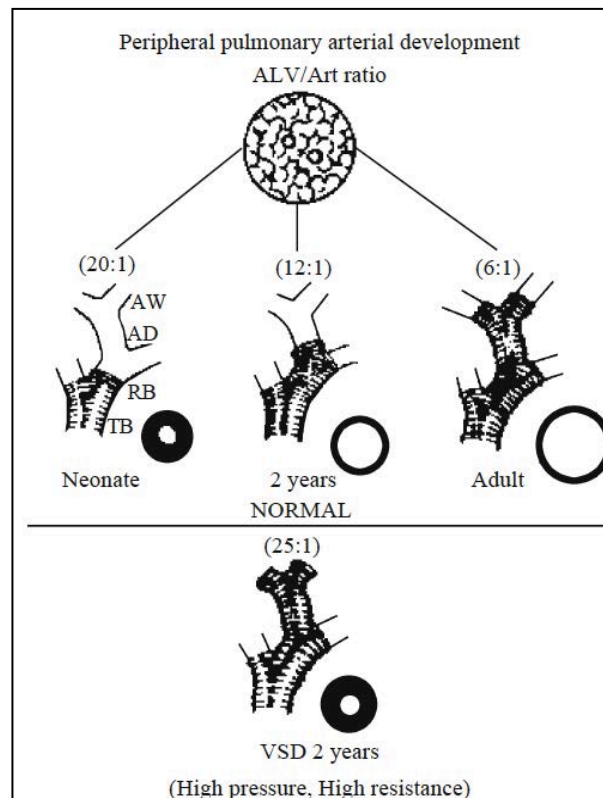
A summary of schema showing morphometric changes of extension of muscle into peripheral arteries, percent wall thickness and artery number (alveolar arterial ratio (ALV/Art)) as they relate to age. Above panel is normal development. Bottom shows abnormalities in all three features in the 2-year-old child with a hypertensive ventricular septal defect (VSD). TB: artery accompanying a terminal bronchiolus; RB: artery accompanying a respiratory bronchiolus; AD: artery accompanying an alveolar duct; AW: artery accompanying an alveolar wall. From Suesaowalak et al(19) and adapted from Rabinovitch et al.(33).

Moreover, Rabinovitch et al study next the correlation between lung biopsy findings at the time of surgical repair and postoperative pulmonary hemodynamic findings (immediately and 1 year after) in 74 patients with large CCS frequently complicated by PH(33). Authors found that one-year after the repair, PAP and/or PVR was normal in all patients whose conditions were corrected before 9 months of age regardless of the severity of pulmonary vascular changes, suggesting that

after repair there is both regression of the structural changes as well as subsequent growth of new vessels. PAP and PVR, however, remained elevated in all patients whose conditions were repaired after 2 years of age with grade C morphometric findings or increased to a severe degree if associated with Heath-Edwards grade ≥III.

While both ground-breaking and still largely used, no histologic classification is perfect, and we now know biopsy findings cannot be interpreted in isolation. As discussed before, previous routine lung biopsies have been abandoned in the last years, as in practice most patients fall between the two extremes of mild medial hypertrophy (reversible) and extensive dilatation lesions (irreversible) and therefore clinical and haemodynamic data are the determinants of operability(21).

1.2.4 Pathobiology of PVD associated to CCS

Although the chronic changes in vascular morphology secondary to CCS are well described, the early determinants of PVD remain incompletely understood. The currently accepted paradigm is that increased pulmonary flow and/or pressure cause aberrant mechanical forces in the pulmonary arterial bed that trigger an increased vascular reactivity and tone with progressive vascular remodelling. Compelling evidence to date supports the unifying hypothesis that secondary endothelial injury is the earliest hallmark of this complex process(24).

1.2.4.1 Increased pulmonary pressure and/or flow leading to early endothelial injury

A few landmark human studies published more than three decades ago laid the groundwork for the current unifying hypothesis of early endothelial injury in the pathobiology of PVD associated with CCS.

Rabinovitch et al(34) studied lung biopsy samples of children with CCS with different histologic grades of PVD. Using scanning electron microscopy, authors demonstrated alterations in surface characteristics and intra-cytoplasmatic composition of the endothelial cell, which were already present at very early stages of the disease and suggested heightened metabolic function. The authors next showed that endothelial von Willebrand factor production was altered in children with CCS, suggesting not only early ultra-structural but also functional abnormalities of the endothelial cells(34).

Further on, in 1993 Celermajer et al(35) studied in the cardiac catheterization laboratory the pulmonary arterial vasodilatory response to three increasing doses of acetylcholine (an endothelium-dependent vasodilator) and sodium nitroprusside (an NO donor and therefore endothelium-independent vasodilator) in three groups of children: healthy controls; young children with CCS and increased PBF but normal calculated PVR; and older children with established PVD defined as a PVR ≥6WU. Authors showed that children with advanced PVD had a poor pulmonary vasodilatory response to either of the vasodilators as opposed to controls. Interestingly, children with increased PBF only dilated normally in response to nitroprusside but demonstrated a blunted response to acetylcholine, indicating an endothelium not capable of producing NO to the same extent as healthy controls. This relevant study proofed not only that endothelium-dependant relaxation could be demonstrated in-vivo, but also that was impaired very early in children with CCS (before their baseline PAP or PVR increased significantly), explaining why even reversible PVD can contribute to morbidity and mortality.

Also in 1993, Hanley et al(36) assessed the best surgical repair timing for children with truncus arteriousus. Children with this CHD are known to be at particular high

risk for postoperative pulmonary hypertension and at the time delaying surgery a few weeks after birth (until PVR had dropped) was thought to be protective. Authors showed, however, that the earlier the patients were operated the lower postoperative PAP and the fewer pulmonary hypertensive episodes patients had. The study highlighted that minimizing, with an early repair, the time the pulmonary endothelial cell layer is exposed to increased PBF and the subsequent shear stress is associated with improved postoperative pulmonary vascular morbidity.

All these observations, supported by subsequent relevant animal work, led to the current unifying hypothesis that, in CCS the initial insult of increased pressure and/or flow causes cause a shear stress on the pulmonary vasculature that leads to endothelial injury and disruption of its regulatory mechanisms, resulting eventually in PAH and its associated increased PVR. These alterations in endothelial function occur extremely early and precede the structural changes and the elevation of PAP(24).

1.2.4.2 Consequences of the endothelial injury

There is strong evidence that, endothelial injury leads to an imbalance of vasoactive factors, alterations in the extracellular matrix of the pulmonary arterial wall and to oxidative stress. These events, together with likely many other, such as dysregulation of potassium channels, increased expression of adhesion molecules and a local release of chemokines, cytokines growth factors and transcriptional factors(37, 38), ultimately result in the two fundamental features of PVD: pulmonary vasoconstriction and pulmonary vascular remodelling.

1.2.4.2.1 Alterations in vasoactive factors

The most important consequence of endothelial injury is the decreased ability of

the endothelium to mediate vasodilation. Since Furchgott et al(39) discovered in 1980 the obligatory role of functional endothelial cells in the relaxation of arterial smooth muscle in response to acetylcholine, pointing out the existence of an *endothelial-derived relaxing factor (EDRF)* and the interaction between the two histologic arterial wall layers, major advances have been made in our understanding of how the pulmonary vascular endothelium is a key determinant of the pulmonary vascular tone, regulated by a complex interaction of vasoactive substances produced locally by the vascular endothelium(24).

Three of the main endothelial-derived vasoactive mediators shown to be disturbed in patients with PVD are: nitric oxide (NO), prostacyclin and endothelin-1. These substances are capable of producing vascular relaxation and/or constriction, at the same time as to modulate thrombogenesis and induce and/or inhibit SMC migration and replication(40-45). The three of them are current therapeutic target options for patients with pulmonary hypertension(38). A schematic view of the pathways activated by these three substances is shown in Figure 9.

NO, identified in 1987 by Ignarro et al as Furchgott's previously described *EDRF*(46), is a potent endothelium-derived vasodilator synthesized by the oxidation of the guanidine nitrogen moiety of L-arginine following activation of the endothelial nitric oxide synthase (eNOS). Basal NO release is a crucial mediator of both pulmonary and systemic resting vascular tone. After certain stimuli, such as shear stress or the receptor binding of specific endothelium-dependant vasodilators (such as acetylcholine, ATP or bradykinin), NO is synthesized and released from the endothelial cell.

NO then diffuses into pulmonary arterial SMCs and activates soluble guanylate cyclase (sGC), which catalyzes the production of guanosine-3', 5'-cyclic

monophosphate (cGMP) from guanosine-5'-triphosphate (GTP). cGMP is a second messenger that maintains pulmonary arterial SMC relaxation through activation of a cGMP-dependent protein kinase and ultimately reducing the inward flux of calcium ions. cGMP is removed by the enzyme cyclic nucleotide phophodiesterases (PDE) 5 to yield the inactive product 5'GMP. In addition to its vasodilating activity, the NO-cGMP signal transduction pathway is an important inhibitor of SMC proliferation and platelet activation(24).

Figure 9: The three main endothelial pathways disturbed in PVD
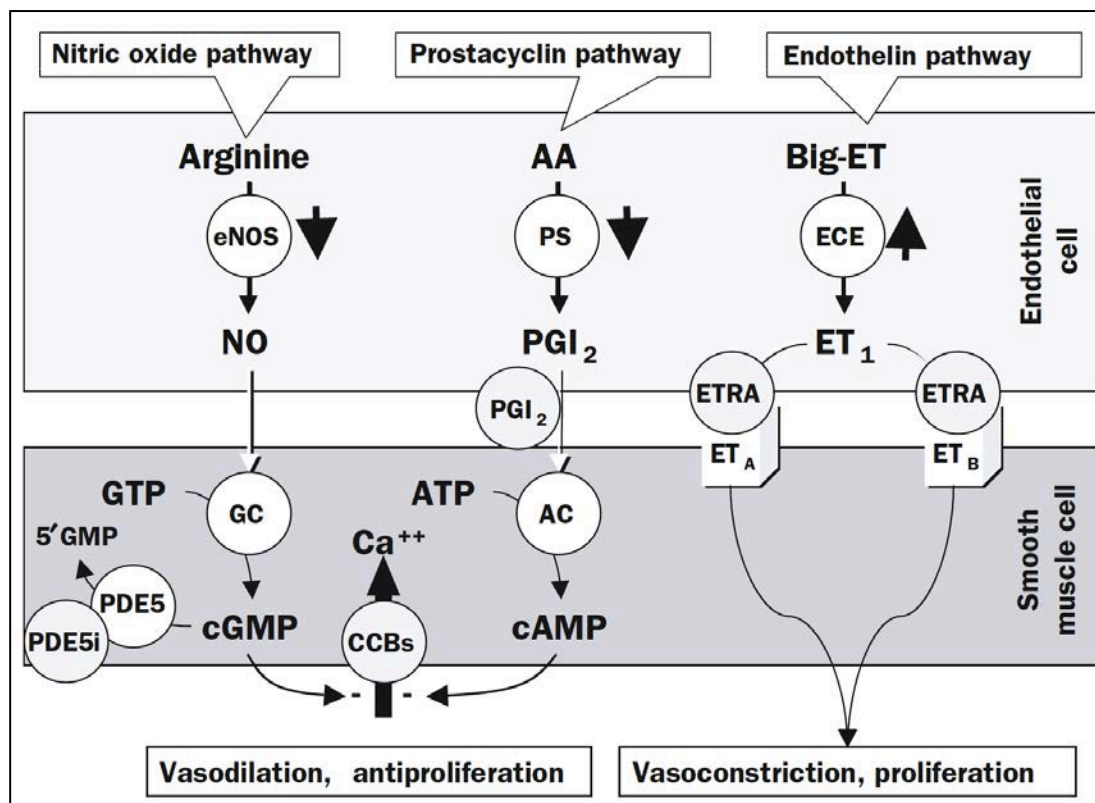
From McGoon al.(47)

Prostacyclin [i.e. prostaglandin I$_2$ (PGI$_2$)] is another pulmonary vasodilator catalyzed from arachidonic acid by prostacyclin synthase (PS) in the endothelial cells. Once it diffuses to the pulmonary arterial SMCs, PGI$_2$ stimulates adenylate cyclase (AC), increasing the production of cyclic adenosine monophosphate (cAMP) from adenosine triphosphate (ATP). cAMP acts as a second messenger

that, similarly to NO, constitutively maintains pulmonary arterial relaxation and inhibition of SMC proliferation and platelet activation(47).

Endothelin-1 (ET1) is the most potent endothelium-derived vasoconstrictor with important mitogenic properties. The precursor big-ET (i.e., pro-ET) is converted to ET1 (a 21–amino acid peptide) in the endothelial cells by the endothelin-converting enzyme (ECE). ET1 binds to ETA receptors in the pulmonary arterial SMC, ultimately leading to contraction, proliferation and hypertrophy of the SMC and fibroblasts. ET1 can also bind to ETB receptors, located in both SMC and endothelium, mediating both vasodilatation and vasoconstriction.

Other vasoactive substances produced by the endothelium (not shown in Figure 9) include additional byproducts of arachidonic acid, such as thromboxane (TXA_2), other prostaglandins and leukotrienes and serotonin. The release of TXA2 results in vasoconstriction via phospholipase C signaling.

There is evidence that patients with PVD secondary to CCS and other types of PAH present a down-regulation of the NO-cGMP signaling cascades with reduced expression and activity of eNOS and prostacyclin synthase(48, 49), an up-regulation of the endothelin cascade with increased plasma ET-1 levels(50, 51), and an imbalance between TXA_2 and PGI_2 that favors vasoconstriction(52, 53). Thus, the earliest and most important consequence of endothelial injury is believed to be an imbalance in endothelium-derived vasoactive effectors that results in endothelial dysfunction or inability of the endothelium to mediate vasodilation, vascular cell proliferation and thrombosis(54).

1.2.4.2.2 Alterations in the Extracellular Matrix

Along with providing basic structural support to blood vessels, extracellular matrix (ECM) proteins interact with different sets of vascular cells via cell surface

receptors(55). Over the last few decades it has become apparent that the process of pulmonary vascular remodeling in PVD involves not only the endothelium and SMC layers, but all the compartments of the pulmonary arterial wall. Thus, in addition to intimal fibrosis and medial hypertrophy, there is an increased production and redistribution of extracellular matrix (ECM) with deposition of collagen and elastin, which contributes to the remodeling of the adventitia and the increase in PVR and PAP(56).

The observation by Rabinovitch et al of degradation of elastin in the pulmonary arterial media of patients with PVD pointed to a possibly important role for proteolysis of extracellular matrix proteins(57). Thus, it is postulated that an additional consequence of the shear stress-induced endothelial injury in CCS is the disruption of the pulmonary endothelial cell cytoskeleton, which leads to increased permeability, leakage of serum factors such as the endothelial vascular elastase to the sub-endothelial space, and subsequent activation of a SMC serine elastase(58). Elastases then cleave elastin and other extracellular matrix proteoglycans, releasing growth factors like fibroblastic growth factor 2 and TFGß that in turn induce SMC hypertrophy and proliferation, as well as synthesis of extracellular matrix proteins. Elastases also activate other proteolytic enzymes such as matrix metalloproteinases, which are involved in collagen degradation, regulation of extracellular matrix proteins and cellular migration and growth(56). In addition, degradation of collagen may lead to activation of ß3 integrins, which are involved in the inhibition of endothelial cell apoptosis and increased production of tenascin, an extracellular matrix glycoprotein associated with activation of SMC growth factor receptors found to be elevated in the media and neointima of pulmonary arteries in patients with PVD secondary to CCS(59). All these events

not only critically contribute to pulmonary vascular remodeling, but also add to the effects of endothelium-derived chemokines, attracting circulating inflammatory cells and platelets to promote an inflammatory repair reaction that involves all pulmonary arterial compartments(60).

1.2.4.2.3 Oxidative stress

Another determining process associated to endothelial injury is oxidative stress. Under normal conditions, reactive oxygen species (ROS), such as superoxide anion (0_2^-) and hydrogen peroxide (H_2O_2), are produced in the vasculature at low concentrations and function as signaling molecules that contribute to maintain vascular integrity, endothelial function and tone(61, 62). ROS are highly reactive due to their unpaired valence shell electron and can alter the function of specific proteins. Oxidative stress occurs when generation of ROS overwhelms the cells' natural antioxidant defenses, the two major being superoxide dismutase and catalase. In recent years, oxidative stress has been recognized as a hallmark of many cardiovascular diseases(63). In the pulmonary vasculature, excess ROS result in NO scavenging, eNOS uncoupling, peroxynitrite formation and cellular damage, all of which lead to a reduction of bioavailable NO, further oxidative stress and an aggravation of pulmonary endothelial dysfunction(64).

Four enzyme systems are thought to predominate in pulmonary vascular endothelial ROS generation: NADPH oxidase, xanthine oxidase, uncoupled eNOS and mitochondrial electron leakage.

Originally studied in polymorphonuclear cells and macrophages as vital in the innate immunity, the NADPH oxidase system is a transmembrane multimeric protein that constitutes a major source of 0_2^-, a highly reactive free radical, in pulmonary vascular SMC, fibroblasts and endothelial cells. NADPH oxidase-

derived O_2^- has consistently been shown to induce SMC proliferation in PAH models as well as impaired angiogenesis and disturbed fibrinolysis, suggesting it likely plays a key role in pulmonary vascular remodeling(65, 66).

Xanthine oxidase is another important source of ROS in the pulmonary vascular tree. This cytoplasmic enzyme catalyzes the transformation of hypoxanthine and xanthine to uric acid, releasing O_2^- and H_2O_2 as byproducts. Animal and human studies have suggested that xanthine oxidase-derived O_2^- can induce impaired pulmonary arterial relaxation, increase SMC proliferation and reduce apoptosis contributing to pulmonary vascular remodeling(66-68).

Figure 10: Generation of NO and O2$^-$ from coupled and uncoupled eNOS
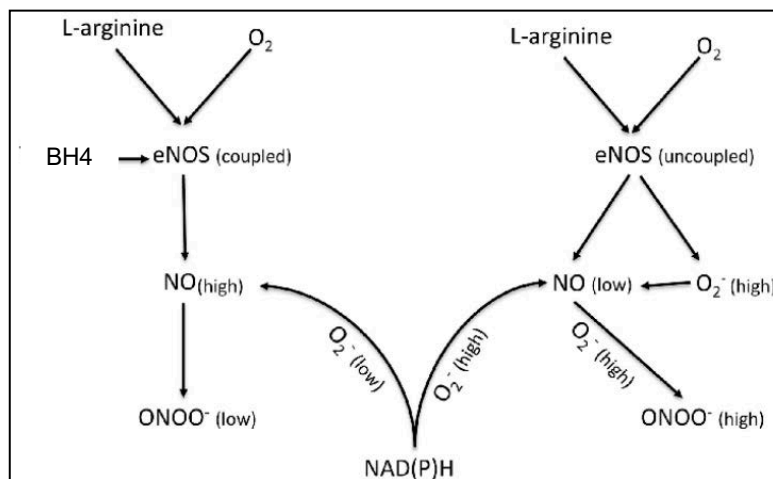
Schematic diagram showing the generation of NO and superoxide from a coupled eNOS and an uncoupled eNOS in a normal and a dysfunctional endothelium respectively. BH4: tetrahydrobiopterin. From Piechota-Polanczyk et al.(69)

Furthermore, endothelial nitric oxide synthase (eNOS) can also be an important source of pulmonary oxidative stress. In normal conditions, eNOS converts L-arginine to L-citrulline to generate NO and maintain a low pulmonary vascular tone. However, when either the substrate L-arginine or the cofactor tetrahydrobiopterin (BH$_4$) are deficient eNOS drives the production of O2$^-$ instead of NO(64). This state is referred to as "eNOS uncoupling" and it implies the dissociation of the ferrous–dioxygen complex from the heme group in the eNOS

oxidase domain to produce O_2^-. Optimal BH_4 levels, therefore, are essential to prevent eNOS uncoupling, as BH_4 increases L-arginine binding to eNOS, coupling L-arginine oxidation and NO synthesis to NADPH consumption. Once produced, O_2^- can rapidly bind to NO to form peroxynitrite (ONOO-) (Figure 10), a powerful oxidant able to modify protein structure and function through the nitration of tyrosine residues, leading to nitrosative stress and decreased NO bioavailability[70].

Uncoupling of eNOS is a recognised crucial contributor to endothelial dysfunction and cardiovascular disease, that not only reduces NO production but also potentiates oxidative stress creating a vicious cycle[71]. A number of pathways that lead to eNOS uncoupling have been identified. On one hand, animal data suggest that in systemic hypertension increased production of ROS from NADPH oxidase is responsible for the degradation or oxidation of BH_4 with subsequent eNOS uncoupling[72, 73]. In addition, oxidative stress has been associated in animal and human studies of PVD to increased levels of dimethyl-l-arginine (ADMA), an endogenous L-arginine analogue that competes with L-arginine for the substrate binding site on eNOS, promoting eNOS uncoupling and therefore further oxidative stress [74-76]. Besides, there is evidence that efficient eNOS activity requires the binding of heat shock protein 90 (HSP90), a chaperone molecule that acting as a scaffold augments coupled eNOS activity in an ATP-dependent process. HSP90 inhibition or decreased eNOS-HSP90 interactions in vitro result in eNOS uncoupling[77, 78]. Recently, S-glutathionylation of eNOS, a post-translational modification, has also been shown to be a key mechanism for eNOS uncoupling in several cardiovascular diseases[79].

Lastly, the role of mitochondrial derived ROS in the vascular endothelium has become in the last decade a relevant focus of study, with increasing number of animal and human studies indicating the importance of mitochondrial function in regulating NO signaling(80). Through oxidative phosphorylation, mitochondria are considered one of the major sources of ROS in the cardiovascular system(64, 81).

Figure 11: The potential role of mitochondrial dysfunction in systemic hypertension
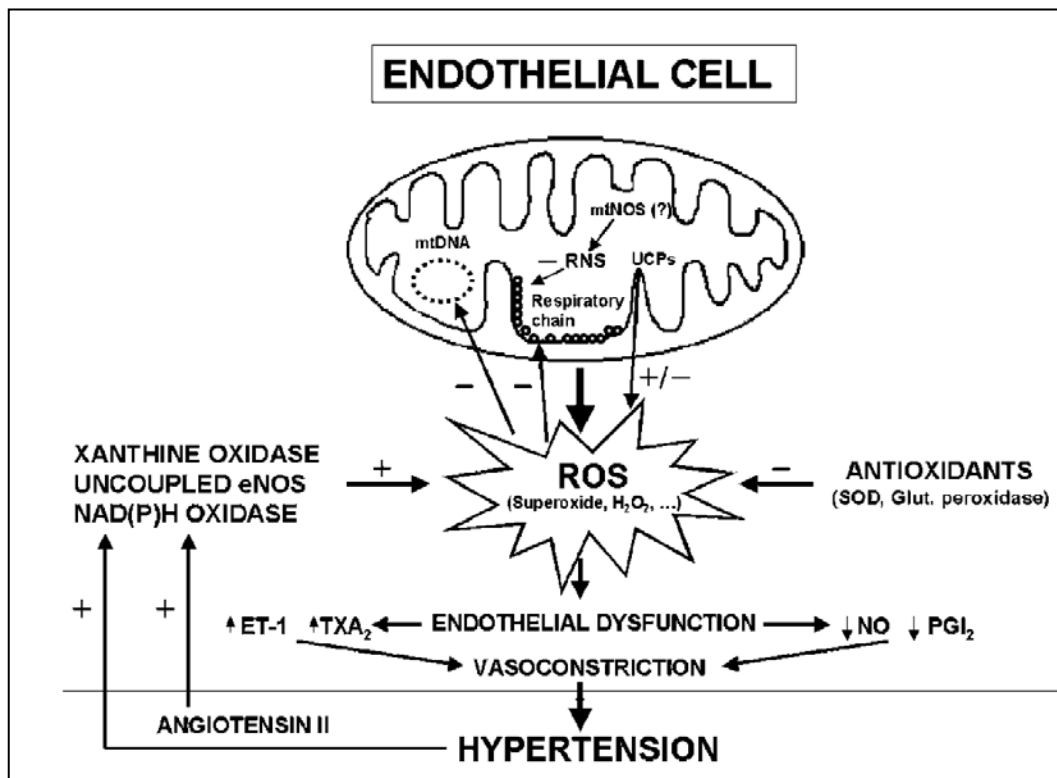
From Puddu et al.(82)

But at the same time, mitochondria are potential targets of ROS action with a clearly identified cross-talk between mitochondrial ROS and NADPH and xanthine oxidases that result in mitochondrial dysfunction(83). Interestingly in systemic hypertension, as in many other cardiovascular conditions, increasing evidence suggests that enhanced endothelial cell cytoplasm ROS generation can induce mitochondrial DNA damage, protein oxidation and lipid peroxidation, resulting in cell death or mitochondrial dysfunction. This implies disruptions in the respiratory

chain with decrease of electron transfer, altered membrane potential, aerobic glycolisis and reduced ATP production. Altogether this leads to exacerbated mitochondrial ROS production ("ROS-induced ROS release") and a consecutive vicious cycle of oxidative stress and energetic decline (Figure 11)(82, 84). In fact, disruption of mitochondrial function is now acknowledged as a critical event in numerous other pathologic conditions associated with oxidative stress, such as atherosclerosis, diabetes mellitus, chronic renal failure, stroke or neurodegenerative conditions(85-89).

In PH, the role of mitochondrial derived ROS is complex with several competing studies having indicated that mitochondrial ROS both increase and decrease during the progression of the disease(64, 90, 91). Despite this controversy, animal and human in-vitro studies have consistently demonstrated mitochondrial ROS induce pulmonary arterial vasoconstriction, as well as pulmonary vascular remodeling through mitochondrial membrane hyperpolarization and attenuated mitochondrial-mediated apoptosis(92-95).

In addition, in human pulmonary endothelial cells increased ADMA appears to induce mitochondrial dysfunction by stimulating redistribution of uncoupled eNOS to the mitochondrion, inducing mitochondrial oxidative stress and protein nitration, and ultimately resulting in reduction in cellular ATP levels and secondary disruption of HSP90-eNOS interactions(96). Furthermore, there is evidence of increased mitophagy (selective autophagy of damaged mitochondria) in human patients with PH(97) mitochondrial dysfunction has ben shown to underlie several cases of PH(98). Thus, despite not yet fully elucidated, growing evidence indicates that the contribution of mitochondrial derived oxidative stress and mitochondrial dysfunction to the pathogenesis of PVD is likely critical(99).

1.3   THE CARNITINE SYSTEM AND ITS ROLE IN MITOCHONDRIAL FUNCTION

L-carnitine   (β-hydroxy-γ-N-trimethylammonium-butyrate)   is   a   vitamin-like compound ubiquitous in mammalian species. In humans, L-carnitine derives from dietary sources (75%) and *de novo* biosynthesis (25%) in the kidney, liver and brain from the amino acid precursors lysine and methionine. Approximately 95% of the carnitine pool in the organism is present in the skeletal and cardiac muscle, 2-3% is contained in the liver and kidney and only 0.5-1% is present in the extracellular fluids(100). The endogenous pool of carnitines exists either as free L-carnitine (FC, non-esterified form) or as acylcarnitines (AC, esterified forms). The acylcarnitines are products of the reaction catalyzed by acyltransferases in which acyl moieties are transferred to carnitine from acyl-coenzymeA, and can vary in length from short (acetyl) to long chain (palmitoyl). Carnitines, along with plasma membrane transporters and the carnitine-dependent enzymes constitute the *carnitine system*, which plays a key role in cellular energy production and normal mitochondrial function (Figure 12).

A main role of the carnitine system is the transport of long-chain fatty acids from the cell cytosol to the mitochondrial matrix for subsequent β-oxidation and ATP production. This function is dependent on L-carnitine as well as on the enzymes carnitine palmitoyltransferases (CPT1 and CPT2) and carnitine acylcarnitine translocase (CACT). CPT1 is localized in the outer mithocondrial membrane, CACT is an integral inner membrane protein, and CPT2 is localized on the inner mitochondrial membrane. CPT1 conjugates carnitine with long acyl-CoA chains (>C12), CACT then transfers the acylcarnitines across the inner mitochondrial

membrane, and CPT2 conjugates the long acylcarnitine chains back to coenzyme A for subsequent β-oxidation.

Figure 12: The carnitine system and the role of carnitine in the mitochondrial oxidation of fatty acids
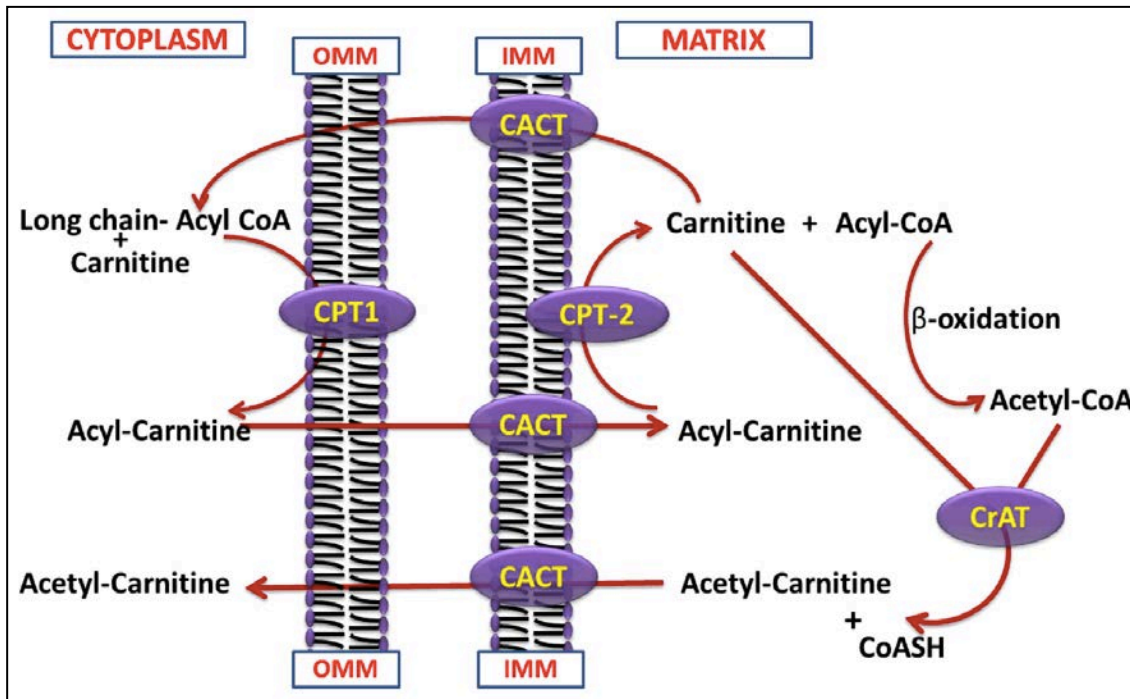
From Fratz et al.(70)

Besides, carnitines play a crucial regulatory role in mitochondrial function by helping to buffer and remove potentially toxic fatty acyl-CoA metabolites and by modulating the cellular acyl-CoA:CoA ratio. This function is mostly dependent on the freely reversible conversion of short-chain acyl-CoA and carnitine to free coenzyme-A (CoA) and acyl-carnitine, process catalyzed by the intra-mitochondrial enzyme carnitine acyltransferase (CrAT). CoA is an obligate cofactor for many enzymes involved in intermediary metabolism. It remains compartmentalized in limited pools within the cell, mainly in the mitochondria, and is normally kept in homeostasis with carnitine. As the mitochondria inner membrane is impermeable to CoA and its esters, the reversible transfer of acyl

moieties from CoA to carnitine ensures the vital maintenance of free CoA pools within the mitochondria and prevents the accumulation of poorly metabolized toxic short-chain acyl-CoA compounds, that can be exported out of the mitochondria as carnitine esters. This allows the maintenance of a balanced cellular acyl-CoA:CoA ratio, critical in the regulation of the activity of many mitochondrial enzymes involved in the Krebs cycle, the fatty oxidation, the gluconeogenesis, and the urea cycle(101).

Therefore, adequate carnitine levels as well as optimal activities of carnitine-dependent enzymes are instrumental for normal mitochondrial function. The accumulation of acyl groups and consequent unavailability of free CoA inhibit multiple enzymes involved in ß-oxidation resulting in a mitochondrial metabolic roadblock with mitochondrial oxidative stress and reduced energy production(102). In fact, a low acylcarnitines:free carnitine ratio, a reflection of a low acylCoA:CoA balance, is recognized as a marker of healthy mitochondrial function and viceversa.

Given the crucial interlink between the carnitine system and the mitochondrial function, a therapeutic role of carnitine supplementation on conditions characterized by oxidative stress and mitochondrial dysfunction has been explored in the last decades, with a beneficial effect reported in a variety of processes such as systemic hypertension, congestive heart failure, or myocardial and cerebral ischaemic reperfusion injury(103-106). No study to date, however, has yet explored the effects of carnitine therapy in the development of PVD associated with CHD with increased PBF.

1.4   LAMB MODEL OF PVD SECONDARY TO INCRASED PBF: LESSONS LEARNT

Many animal models of increased PBF and/or pressure have been attempted through the years. Most of these models involved the surgical placement of an aorta-to-pulmonary shunt in post-natal animals of different age. Models using adult animals had little success in producing elevations in PAP due to low PVR at surgical shunt placement, and the large left-to-right shunts produced usually resulted in early congestive heart failure and animal death(107, 108). Some younger animal models were able to achieve modest elevations in PAP with associated vascular smooth muscle remodeling(109-111). However, despite relevant all of these models failed to simulate true conditions of CHD with increased PBF, as the systemic-to-pulmonary shunt was placed once the drastic fall in PVR at birth had occurred and after a period of normal lung growth and development.

To achieve a better understanding of the pathophysiology of PVD secondary to CCS, Dr Fineman's group from the University of California San Francisco established in 1995 a clinically relevant animal model of a CHD with increased PBF by placing a large aorto-pulmonary vascular graft (shunt) in the late-gestation fetal lamb(112) (Figure 13). To the best of our knowledge, this is the first and only existing model of increased PBF to date in which the systemic-to-pulmonary communication is in place during intrauterine life, truly mimicking human disease and allowing the study of the early and sequential morphologic, physiologic and molecular derangements produced by increased PBF during growth and development before overt vascular remodeling occurs (24).

Figure 13: In-utero placement of an aorto-pulmonary shunt. Illustrations of surgical technique
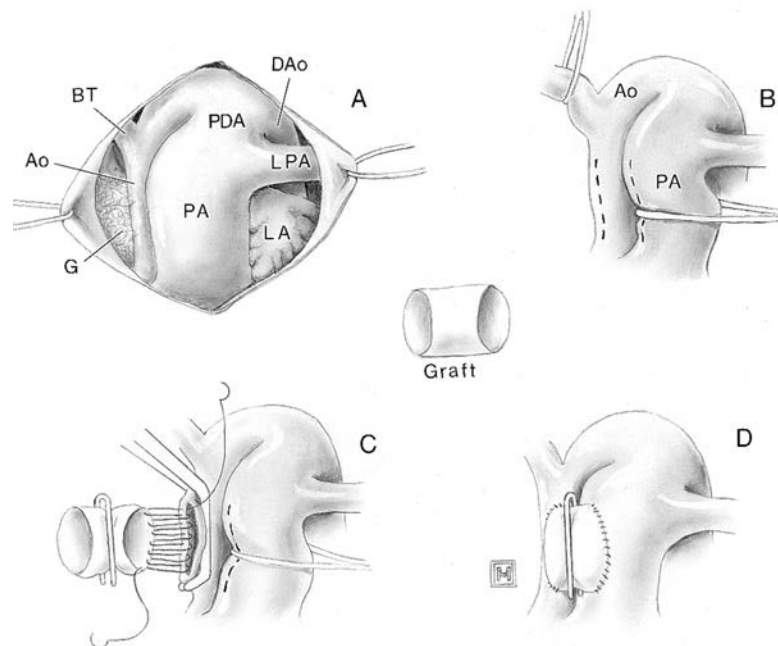
A. Exposure of fetal heart via left thoracotomy. Ao indicates ascending aorta; BT, bovine trunk; DAo, descending aorta; G, gauze sponge over the right atrium; LA, left atrial appendage; LPA, left pulmonary artery; PA, main pulmonary artery; and PDA, patent ductus arteriosus. B: Bovine trunk, aorta, and main pulmonary artery are dissected. Vessel loops are passed around the bovine trunk and main pulmonary artery. C. Continuous suture technique of the aorta to vascular graft anastamosis. D. Completed anastomosis. Vascular clip is subsequently removed to establish graft patency. From Reddy et al.(112)

In the initial study, at 4 weeks of age shunt lambs showed elevated pulmonary pressures, increased PBF (Qp/Qs ≈2.5-3.1), raised left and right atrial pressures, failure to thrive and biventricular cardiomegaly. In addition, shunt lambs showed an augmented response to pulmonary vasoconstricting stimuli like hypoxaemia or thromboxane A_2 infusion compared to control lambs. Moreover, morphometric analysis of the barium filled pulmonary artery bed revealed shunt lambs had early changes similar to those seen in children with PVD secondary to CCS: dilation of the proximal pulmonary arteries, increased medial wall thickness of the small muscular arteries, abnormal extension of muscle to peripheral pulmonary arteries,

an increased number of barium-filled intra-acinar pulmonary arteries (Figure 14)(112).

Figure 14: Pulmonary arteriolar vasculature of 4-week-old shunt lambs compared to control lambs
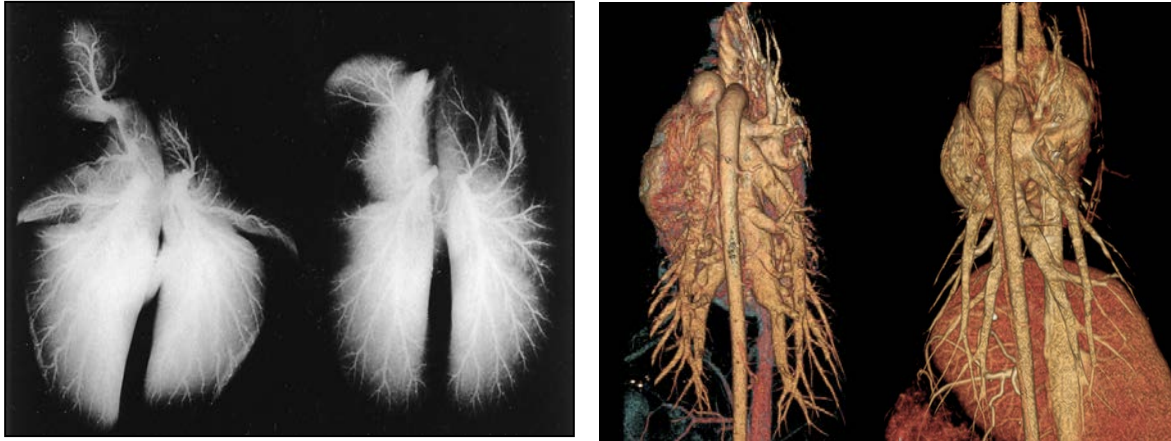
Left: pulmonary arteriogram of a 4-week-old shunt lamb (left) and its twin control lamb (right); from Reddy et al.(112). *Right*: CT-pulmonary angiogram of a 4-week-old shunt lamb (left) and an age-matched control (right); courtesy of Dr S. Datar. We observe dilation of the proximal pulmonary arteries as well as an increase in the number and size of the intra-acinar arteries in shunt lambs compared to control lambs, suggested by the increased background haziness observed in the pulmonary arteriogram and evidenced in the CT-angiogram images.

Over the last three decades, this model has extensively been used to study the early sequential evolution of PVD associated with CCS. We will next summarize the most relevant findings demonstrated by Dr Fineman's group in this lamb model over the last few decades.

1.4.1 Early selective impairment of endothelium-mediated pulmonary vasodilatation

Compared to age-matched sham-operated controls, by 4 weeks of age shunt lambs display significant attenuated pulmonary vasodilatory response to the administration of the endothelium-dependent vasodilator acetylcholine, an agonist that requires eNOS to produce NO. Pulmonary vasodilatory response to the administration of the endothelium-independent vasodilator iNO is however

preserved, indicating an early and selective impairment of endothelium-mediated pulmonary vasodilation in shunt lambs (Figure 15)(113, 114).

Figure 15: Selective impairment of endothelium-mediated pulmonary vasodilation in shunt lambs
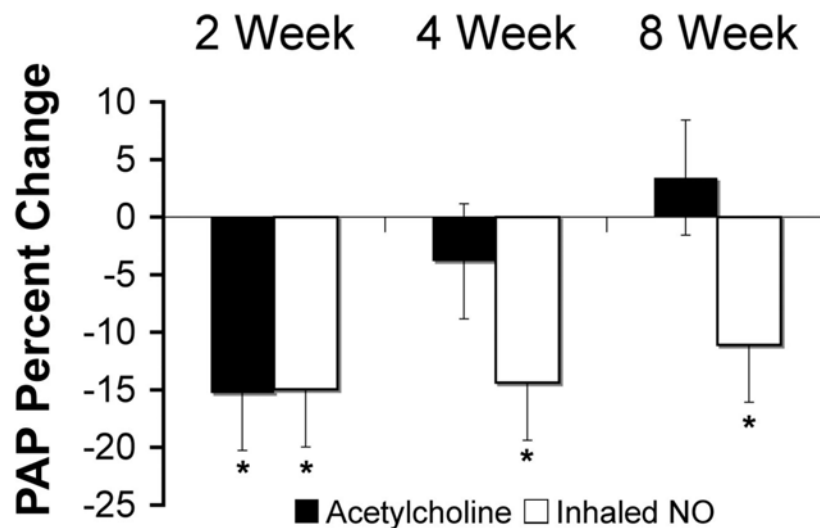
Changes in pulmonary arterial pressure (PAP) expressed as percent change from baseline in response to Ach (1 mcg/kg) iv and inhaled nitric oxide (40 ppm) in shunt lambs (filled bars) and sham-operated controls (white bars) at 2, 4, and 8 weeks of age. At 2 weeks of age, PAP decreased significantly from baseline in response to Ach and iNO. At 4 and 8 weeks of age, PAP decreased significantly in response only to iNO. Values are means ± SD; N=5 for each group. *p<0.05 compared with baseline. From Oishi et al(114).

1.4.2 Alterations in endothelin-1 cascade

Compared to age-matched controls, 4 weeks-old shunt lambs display an increased ET-1 production and increased ET-1 mediated vasoconstriction with increased levels of endothelin type A receptor (the receptor that mediates vasoconstriction) and loss of endothelin type B receptor-mediated vasodilatation(115, 116). By 8-weeks of age, shunt lambs present an emergence of ET_B receptors on SMC with strong ET_B-mediated pulmonary vasoconstriction(117). Interestingly, some of these changes in the ET-1 cascade can be observed already in 1-week old shunt lambs, indicating that increased PBF induces alterations in ET1 signaling before than in NO signaling, suggesting an

early role for ET1 in the altered vascular reactivity associated with increased PBF(118).

1.4.3 Progressive decline in NO signaling

Despite an early up-regulation of basal NO activity, over the first two months of life shunt lambs display a progressive decline in NO signaling in response to shear stress. Thus, compared to age-match sham-operated controls 2-weeks old shunt lambs have increased levels of plasma and lung tissue NOx (an indirect determinant of bioavailable NO) (Figure 16) and significantly increased peripheral lung eNOS gene expression and activity by 4 weeks of age (Figure 17). Plasma and lung NOx levels, however, decrease over the first 8 weeks in both shunt and control lambs. And when lung tissue NOx levels are assessed relative to total NOS activity, we observe that NOx levels are markedly lower in shunt lambs compared to control lambs at 4 and 8 weeks of age, indicative of a progressive impairment of NOS function that leads to reduced bioavailable NO (Figure 18)(113, 119, 120).

Figure 16: Plasma and lung tissue NOx levels at 2, 4, and 8 weeks of age in sham-operated control and shunt lambs
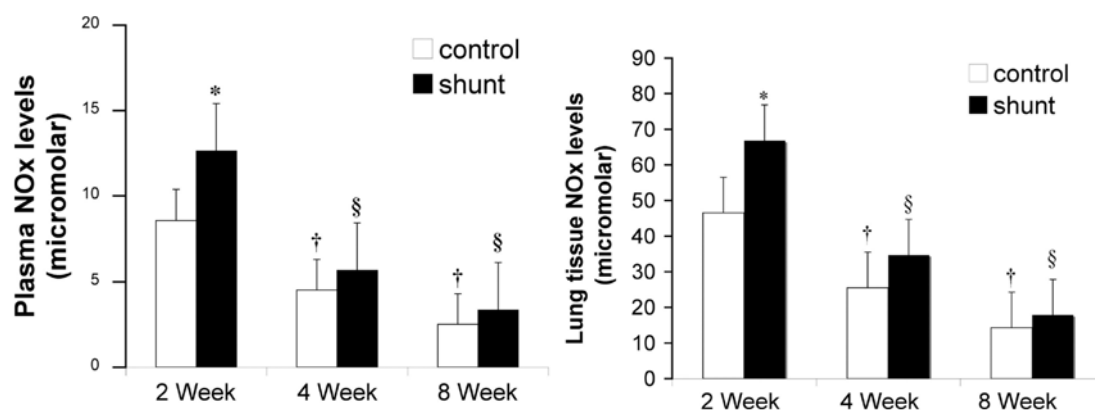
Plasma (left) and lung tissue (right) nitrite and nitrate (NOx) levels are significantly greater in shunt lambs than sham-operated controls at 2 weeks. Plasma and lung NOx levels decrease over the course of the first 2 months of age in both control and shunt lambs. N=5 for each group; *p< 0.05 compared with age-matched sham- operated control; †p<0.05 compared with 2-week sham-operated control; §p<0.05 compared with 2-week shunts. From Oishi et al(114).

Figure 17: Lung tissue eNOS expression and NOS activity in sham-operated control and shunt lambs at 2, 4 and 8 weeks of age
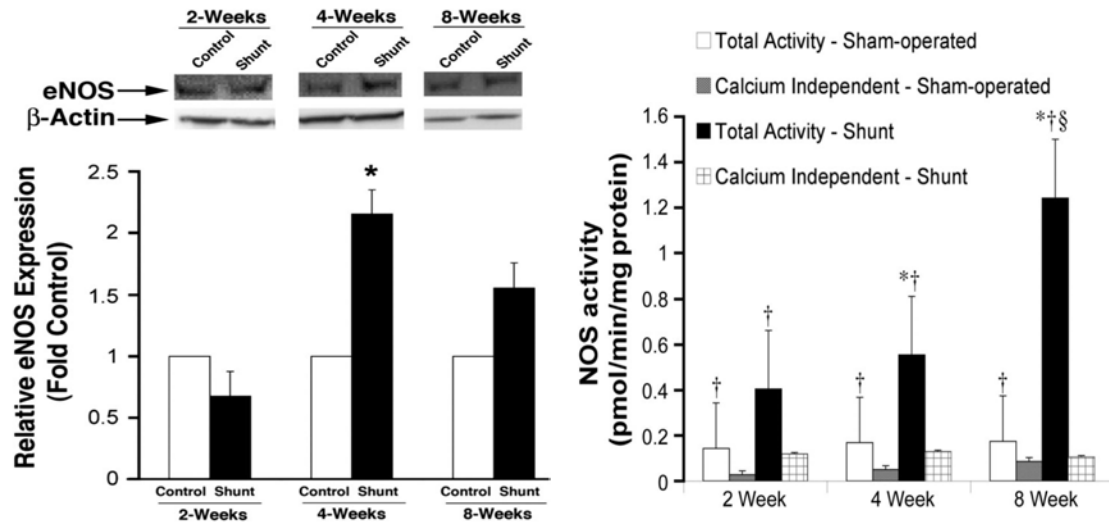
Left top: representative Western blots for eNOS protein extracts from lung tissue analyzed using a specific antiserum raised against eNOS and reprobed with β-actin to demonstrate equal loading. *Left bottom*: densitometric values for eNOS protein in shunt lambs (black bars) shown relative to control (white bars). *$p<0.05$ vs. age-matched control; n=5 for each group. Values are means ± SD.

Right: total NOS activity measured using the conversion of [³H]arginine to [³H]citrulline in control and shunt lambs. Total NOS activity increase from 2 to 8 weeks of age in shunt lambs (ANOVA). To determine the potential contribution of inducible NOS (calcium independent) to total NOS activity, assays were repeated without calcium supplementation, showing no change from 2 to 8 weeks of age in either control or shunt lambs and lower than total NOS activity at all ages for both groups. N=5 for each group. Values are means ± SD. *$p<0.05$ compared with 2-weeks shunt. From Oishi et al(114)

Figure 18: NOx levels expressed relative to total NOS activity at 2, 4, and 8 weeks of age in sham-operated control and shunt lambs
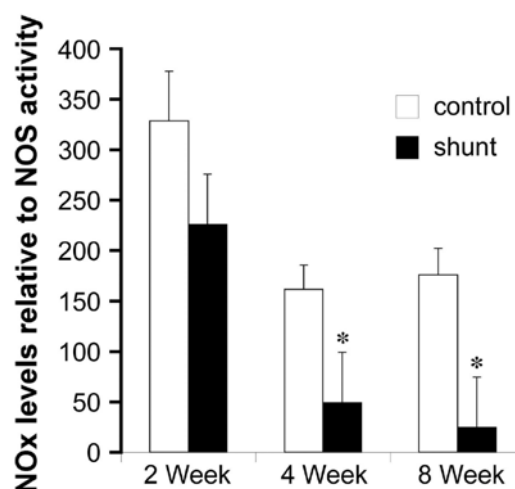
Relative NOx levels are lower than controls at 4 and 8 weeks of age. N= 5 for each group. *$p<0.05$ compared with age-matched sham-operated controls. From Oishi et al(114)

1.4.4 Oxidative stress

Over the last decade, a series of studies in shunt lambs have provided us with compelling evidence that oxidative stress plays a crucial role in pulmonary endothelial dysfunction secondary to increased PBF.

On one hand, from 2 to 8 weeks of age shunt lambs exhibit progressively elevated lung superoxide levels, which appear mainly to result from increased production via vascular xanthine oxidase, the NADPH oxidase complex and uncoupled eNOS(114, 121) (Figure 19). In addition, further evidence indicates that the developmental increase in eNOS uncoupling in shunt lambs is related to a diversity of factors including eNOS nitration (Figure 20), decreased BH₄ and L-arginine levels, enhanced ADMA levels, and reduced HSP90-eNOS interactions(114, 121-125).

Figure 19: Increased lung tissue superoxide levels in shunt lambs
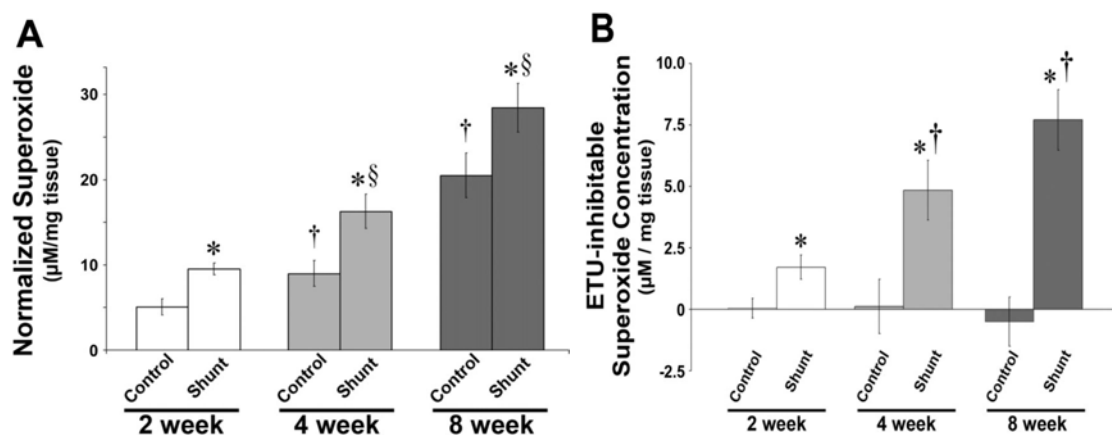
A: Superoxide levels in lung tissue in sham-operated control and shunt lambs at 2, 4, and 8 weeks of age estimated by electron paramagnetic resonance (EPR) assay. Superoxide concentrations increased from 2 to 8 wk of age in both sham-operated control and shunt lambs (ANOVA) and were greater in shunt lambs than sham-operated control lambs at each age. B: S-ethylisothiourea hydrobromide (ETU)-mediated inhibition of NOS resulted in almost no change in EPR amplitude of control lambs, whereas shunt lambs showed up to 30% reduction in signal, suggesting that uncoupled eNOS contributed to superoxide levels in shunt but not control lambs. N=5 for each group. Values are means ± SD. *p<0.05 compared with age-matched controls; †p<0.05 compared with previous controls; §p<0.05 compared with previous shunts.

Figure 20: Developmental increases in eNOS nitration in shunt lambs
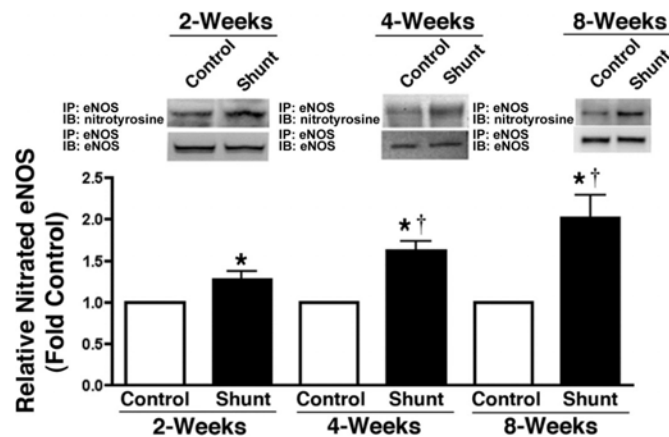
As an indirect measure of peroxynitrite formation and oxidative stress, nitrated eNOS protein levels were determined by immunoprecipation (IP) in lung tissue extracts prepared from 2- (n=4), 4- (n=5), and 8-wk-old (n=4) shunt and age-matched control lambs. Representative Western Blots are shown. Densitometric analysis indicates that the levels of nitrated eNOS protein are increased in shunt lambs and that this nitration increases over time, suggesting a developmental increase in eNOS uncoupling. Values are means ± SD. *$p<0.05$ vs. age matched control; †$p<0.05$ vs. previous age. IB, immunoblot.

In addition, recent data suggest that decreases in lung antioxidant enzymes and ROS scavenging may contribute to the oxidative stress described in shunt lambs(126). Interestingly, the treatment of isolated 5th generation pulmonary arteries harvested from 4-weeks old shunt lambs with superoxide scavengers has been shown to restore endothelial-dependent pulmonary vasodilatation, which indicates a role of oxidative stress in endothelial dysfunction(120, 122).

1.4.5 Disrupted carnitine homeostasis and mitochondrial dysfunction

Recently, we demonstrated a disruption in carnitine homeostasis in shunt lambs that correlates with mitochondrial dysfunction and decreased NO signaling(127). Specifically, at two weeks of age shunt lambs exhibit significantly reduced expression of the key enzymes involved in carnitine metabolism: CPT1, CPT2 and CrAT ($p<0.05$) (Figure 21). Moreover, CrAT activity is inhibited due to increased nitration, which suggests the presence of early nitrosative stress in shunt lambs (Figure 22).

46

Figure 21: CrAT expression and activity in peripheral lung tissue from control and shunt lambs at 2 weeks of age
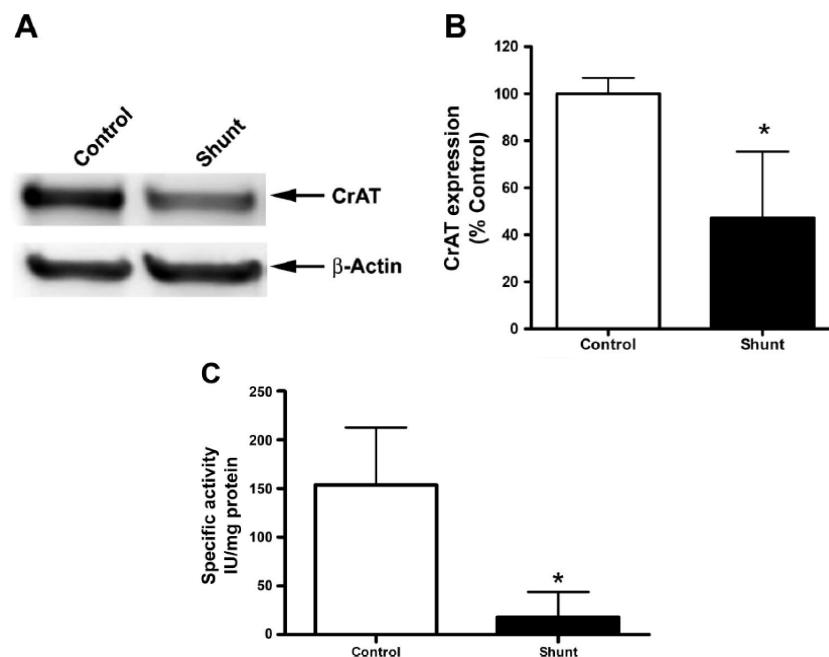
A: protein extracts (50 μg) prepared from peripheral lung of shunt and control lambs analyzed by Western blot using a specific antiserum raised against CrAT protein. CrAT expression was normalized for loading using ß-actin. A representative blot is shown. B: there was a significant decrease in normalized densitometric values for CrAT protein in peripheral lung tissue prepared from shunt compared with control lambs. Values are means ± SE; n=6 control and 6 shunt lambs. *P <0.05 vs. control. C: CrAT activity determined in protein extracts (40 μg) prepared from peripheral lung tissue from control and shunt lambs. There was a significant decrease in CrAT activity in peripheral lung tissue prepared from shunt compared with control lambs. Values are expressed as units of activity per μg of protein and are means ± SE; n=4 control and 4 shunt lambs. *p <0.05 vs. control. From Sharma et al(127)

Figure 22: Increased nitration of CrAT in peripheral lung tissue of shunt lambs at 2 weeks of age
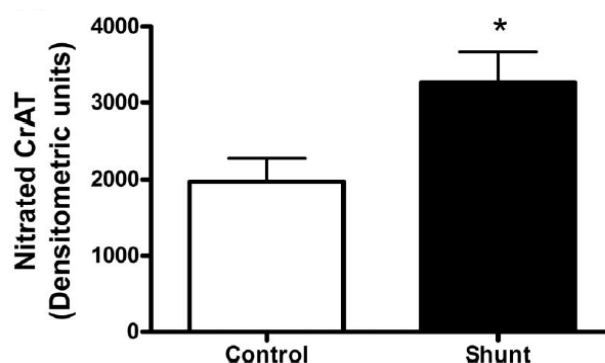
A: protein extracts (1,000 μg) prepared from peripheral lung of shunt and control lambs subjected to immunoprecipitation (IP) using an antibody specific to 3-nitrotyrosine (3-NT) and then analyzed by Western blot analysis using a specific antiserum raised against CrAT protein. There was a significant increase in nitrated CrAT protein in peripheral lung tissue prepared from shunt compared with control lambs. Values are means ± SE; n =6 control and 6 shunt lambs. *p<0.05 vs. control. From Sharma et al.(127)

Besides, free carnitine levels are significantly decreased in shunt lambs, while acylcarnitine levels are enhanced (Figure 23).

Figure 23: Carnitine levels in peripheral lungs of shunt and control lambs at 2 weeks of age

	Total Carnitines, nmol/g wet wt	Free Carnitine, nmol/g wet wt	L-Carnitine, nmol/g wet wt	Acylcarnitine, % of total
Control	60.54+8.45	67.57+13.43	56.42+12.27	6.2+4.7
Shunt	72.37+10.14	34.86+3.35*	20.21+4.29*	40.71+9*

Despite no differences observed in total carnitines, shunt lambs had significantly lower free carnitines and higher acylcarnitine levels. Acylcarnitines were calculated as total carnitine minus free carnitine. Values are means ± SE; n=5. *$p<0.05$ vs. control. From Sharma et al.(127)

The alterations in carnitine homeostasis observed in shunt lambs result in mitochondrial dysfunction by 2 weeks of life, as indicated not only by a significantly reduced free carnitine:acylcarnitine ratio (FC:AC), but also by a decreased pyruvate/lactate ratio suggestive of a shift to a glycolytic phenotype (Figure 24a). Moreover, shunt lambs exhibit reduced mitochondrial antioxidant superoxide dismutase-2 (SOD-2) levels, a well-recognized hallmark of decreased mitochondrial function(128), at the same time as increased levels of uncoupling protein-2 (UCP-2) (Figure 24b). Of note, up-regulation of UCP-2, a mitochondrial membrane proton transporter involved in clearance of mitochondrial ROS, is mediated by superoxide anion. Growing evidence suggests it can serve as a good marker of mitochondrial dysfunction(129).

Importantly, mitochondrial dysfunction in shunt lambs is associated with a progressive decrease in eNOS-HSP90 interactions that correlates with a progressive decrease in NO signaling (Figure 25)(127).

Figure 24: Markers of mitochondrial dysfunction are increased in shunt lambs at 2 weeks of age

24a: Lactate and pyruvate levels in peripheral lung of control and shunt lambs

	Lactate, μmol/g wet wt	Pyruvate, μmol/g wet wt	Lactate/Pyruvate Ratio
Control	1.79±0.34	0.144±0.03*	15.25±4.35:1
Shunt	3.1±0.86*	0.057±0.008*	51.8±10.92:1*

The relative changes in lactate levels were measured in homogenized lung tissues using a lactate assay kit (Biovision). Pyruvate levels were determined using the spectrophotometric enzymatic measurement assay at 340nm. Shunt lambs had significantly higher peripheral lung lactate levels as well as lactate:pyruvate ratio compared with control lambs. Values are means ± SE; n=5. *$p<0.05$ vs. control. From Sharma et al.(127)

24b: SOD-2 and UCP-2 levels in peripheral lung of control and shunt lambs
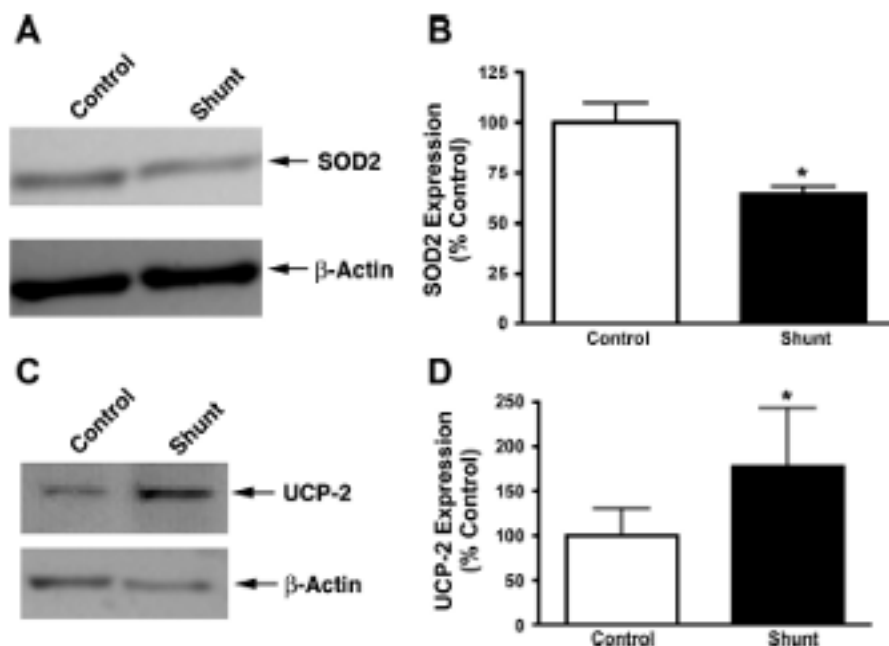
A: protein extracts (25 μg) prepared from peripheral lung of shunt and control lambs were analyzed by Western blot analysis using a specific antiserum raised against SOD2 protein. SOD2 expression was normalized for loading using ß-actin. A representative blot is shown. B: there was a significant decrease in normalized densitometric values for SOD2 protein in peripheral lung tissue prepared from shunt compared with control lambs. C: protein extracts (25 μg) prepared from peripheral lung of shunt and control lambs were analyzed by Western blot analysis using a specific antiserum raised against uncoupling protein-2 (UCP-2). UCP-2 expression was also normalized for loading using ß-actin. A representative blot is shown. D: there was a significant increase in normalized densitometric values for UCP-2 protein in peripheral lung tissue prepared from shunt compared with control lambs. Values are means ± SE; n=6 control and 6 shunt lambs. *$p<0.05$ vs. control. From Sharma et al.(127)

Figure 25: Progressive decreases in the interaction of eNOS with HSP90 in shunt compared with control lambs
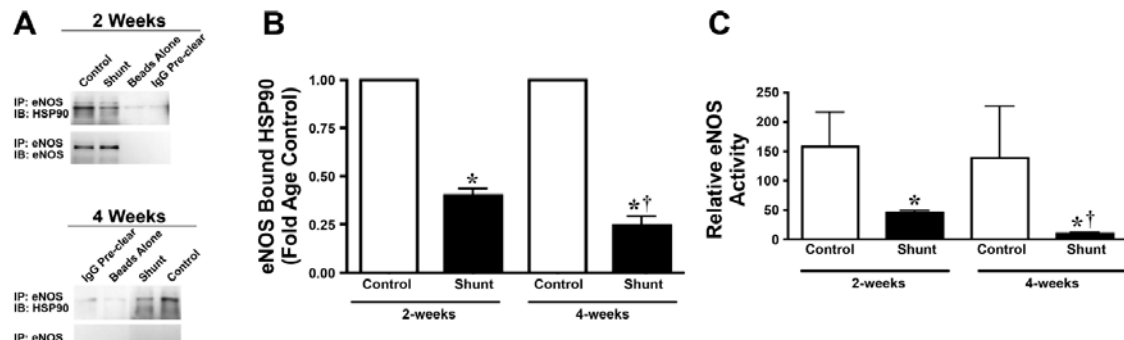
A: eNOS-HSP90 interaction determined by IP in peripheral lung of shunt and control lambs at 2 & 4 weeks of age. IP extracts were analyzed using antisera against either eNOS or HSP90. A representative image is shown. No specific protein bands were observed in the beads alone or in IgG preclear. B: levels of eNOS protein associated with HSP90 relative to total eNOS protein. The data indicate a progressive decrease in the association of eNOS with HSP90 in shunt compared with control lambs between 2 (bars at left) and 4 weeks of age (bars at right). Values are means ± SE; n=5 shunt and 5 control lambs at each age. *$p<0.05$ compared with age-matched control. †$p<0.05$ vs. 2-wk shunt. C: relative eNOS activity estimated in shunt and age-matched control lambs at 2 and 4 weeks of age by dividing peripheral lung tissue NOx levels by total lung eNOS activity (determined by calcium-dependent [3H]arginine to [3H]citrulline conversion). Relative eNOS activity was significantly lower in shunt lambs at both 2 and 4 weeks of age. Values are means ± SE; n =4 shunt and 4 control lambs at each age. *$p<0.05$ compared with age-matched control. †$p<0.05$ vs. 2-wk shunt. From Sharma et al(127).

In summary, carnitine undoubtedly plays a critical role in mitochondrial health and cellular energy metabolism. For this reason, carnitine supplementation has been proposed as a therapeutic tool for multiple disease processes characterized by oxidative stress and mitochondrial dysfunction. Previous data in our lamb model demonstrate that increased PBF leads to early disruption of carnitine homeostasis and this is associated with mitochondrial dysfunction, oxidative and nitrosative stress, eNOS uncoupling and a progressive decline in NO signaling(127). Thus, the purpose of this study is to determine if chronic supplementation with L-carnitine would preserve carnitine homeostasis, attenuating mitochondrial dysfunction and oxidative stress, and ameliorating NO signaling and endothelial function in our lamb model of CHD with increased PBF.

HYPOTHESIS

2 HYPOTHESIS

We hypothesize that in a lamb model of pulmonary vascular disease secondary to increased pulmonary blood flow, therapy with L-carnitine since post-natal day 1 of life will overcome the mitochondrial dysfunction associated with the disruption of pulmonary L-carnitine homeostasis, improving NO signalling and resulting in an ameliorated or restored pulmonary vascular endothelial function.

AIM AND OJBECTIVES

3 <u>AIM AND OBJECTIVES</u>

3.1 AIM:

To determine the effects of therapy with L-carnitine on pulmonary vascular endothelial function in a lamb model of pulmonary vascular disease secondary to increased pulmonary blood flow.

3.2 OBJECTIVES:

In a lamb model of pulmonary vascular disease secondary to increased pulmonary blood flow, our research objectives are:

3.2.1 To determine whether therapy with L-carnitine preserves carnitine homeostasis, increasing the FC:AC ratio and keeping the levels and/or activity of critical enzymes in the carnitine cycle.

3.2.2 To determine whether therapy with L-carnitine ameliorates mitochondrial dysfunction associated with shear stress.

3.2.3 To determine whether therapy with L-carnitine mitigates the oxidative stress associated with shear stress.

3.2.4 To determine whether therapy with L-carnitine preserves or ameliorates nitric oxide signalling.

3.2.5 To determine whether of L-carnitine therapy attenuates pulmonary vascular endothelial dysfunction.

METHODS

4 <u>METHODS</u>

4.1 LAMB MODEL OF INCREASED PULMONARY BLOOD FLOW

For the current study, a total of 24 mixed-breed Western neonatal lambs were used. These corresponded to 13 lambs with increased PBF (shunts), subdivided in two experimental groups receiving daily treatment with orl L-carnitine (n=7, 100mg/kg/day) or its vehicle (n=6). Eleven lambs with normal PBF served as controls.

The Committee on Animal Research of the University of California, San Francisco and the Georgia Health Sciences University (for the tissue studies) approved all protocols and procedures.

4.1.1 In utero placement of an aortic-pulmonary shunt

This procedure has been previously described in detail(112). In summary, 13 mixed-breed Western ewes in late gestation (131-139 days gestation) (term: 145 days) were operated on under sterile conditions with the use of local (2% lidocaine hydrochloride) and general anaesthesia (1-3% inhaled isoflurane). For initial sedation, ewes received 120 mg of intramuscular ketamine hydrochloride. Subsequently, a 16-gauge catheter was inserted into the maternal external jugular vein through which surgical prophylaxis with 1 million units Penicillin G + 100mg Gentamicin was immediately administered. A polyvinyl arterial catheter was inserted in one of the hind legs for invasive monitoring of arterial blood pressure. After gas induction endotracheal intubation was performed with a 9.0-mm-OD cuffed endotracheal tube and mechanically ventilated through the anesthesia machine (Figure 26). Ringer Lactate with 5% Dextrose was used as maintenance intravenous (iv) fluids through the case (2 liters). A midline

incision was made in the ventral abdomen (Figure 27) and the pregnant horn of

the uterus was exposed (Figure 28). Through a small uterine incision, the left

fetal forelimb and chest were exposed (Figure 29) and a left lateral thoracotomy

was performed in the third intercostal space (Figure 30). Fetal anesthesia

consisted of local anesthesia with 1% lidocaine hydrochloride and 0.25%

bupivacaine hydrochloride. The pericardium was incised along the main

pulmonary trunk and suspended with tacking sutures. The bovine arterial trunk

and the main pulmonary artery were dissected and controlled with vessel loops.

Figure 26: Anaesthesia machine used for fetal surgery

The ascending aorta was side-clamped with a side-biting vascular clamp (Figure

31). An aortotomy was performed with a No. 11 bladed knife. The aortotomy

was extended to ~8mm with fine scissors, and a strip of aortic wall was excised

to create an oval opening in the ascending aorta. The anastomosis between the

8.0-mm expanded polytetrafluoroethylene vascular graft (~2 mm length) (W. L.

Gore and Associates, Milpitas, CA) and ascending aorta was performed with

7.0-Prolene using a continuous suture technique (Ethicon, Somerville, NJ)

(Figure 32).

Figure 27: Midline incision in the ewe's ventral abdomen

Figure 28: Pregnant horn of uterus exposed

Figure 29: Uterus incision and fetal lamb exposure
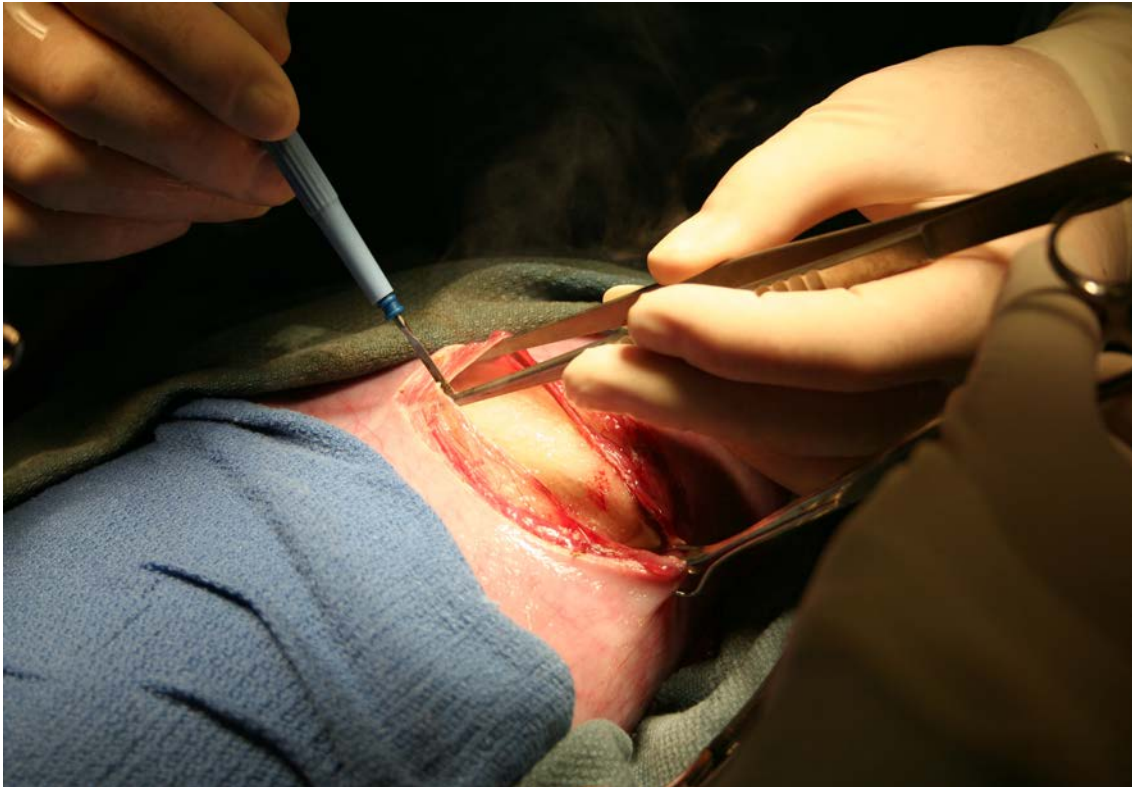
Figure 30: Fetal lamb left lateral thoracotomy
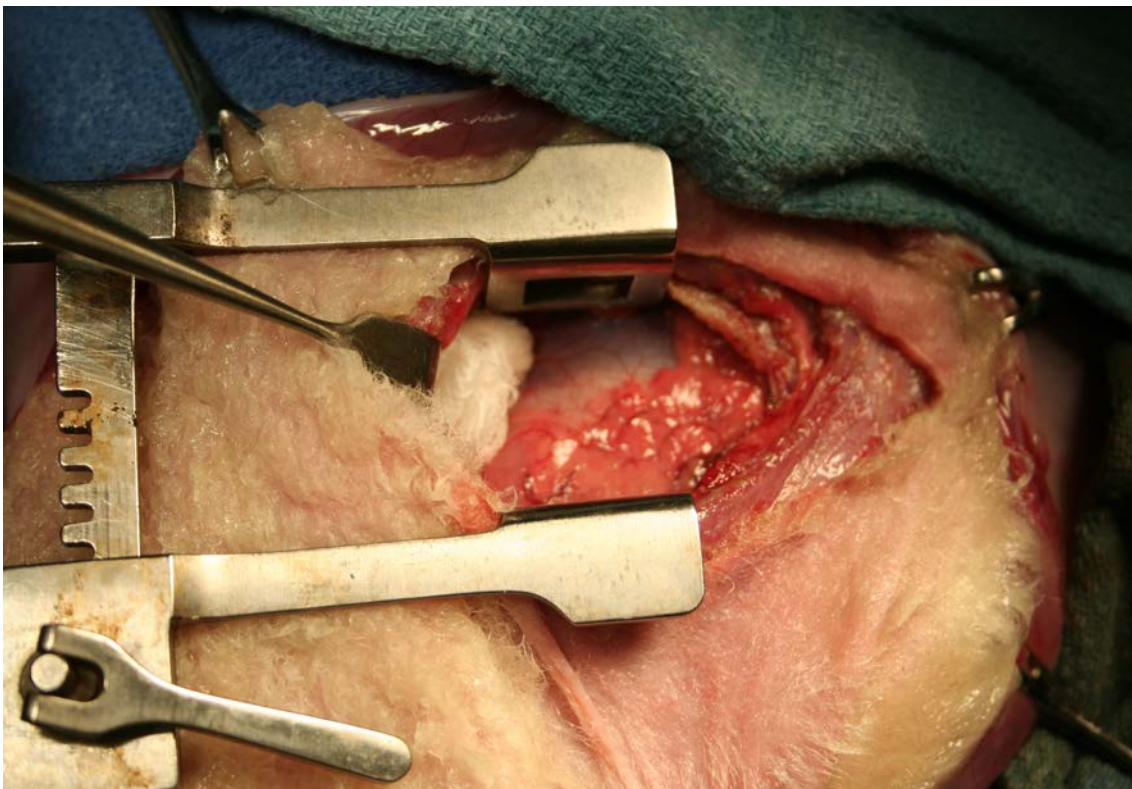
A large vascular clip was placed to temporarily occlude the graft, and the vascular clamp was gradually released to minimize any bleeding at the suture line. The vascular clamp then was applied to the pulmonary artery. A pulmonary arteriotomy was performed, a strip of the posterior wall was excised, and the free end of the graft was sutured to the pulmonary artery. The vascular clamp was gradually released, allowing any air in the graft to escape through the suture line and needle holes. The vascular clip then was removed, establishing the graft patency (Figure 33). The thoracotomy incision was closed in layers. Warm saline was infused to replace the lost amniotic fluid together with a second dose of surgical prophylaxis as described above. The uterine incision was then closed.

Figure 31: Ascending aorta side-clamped
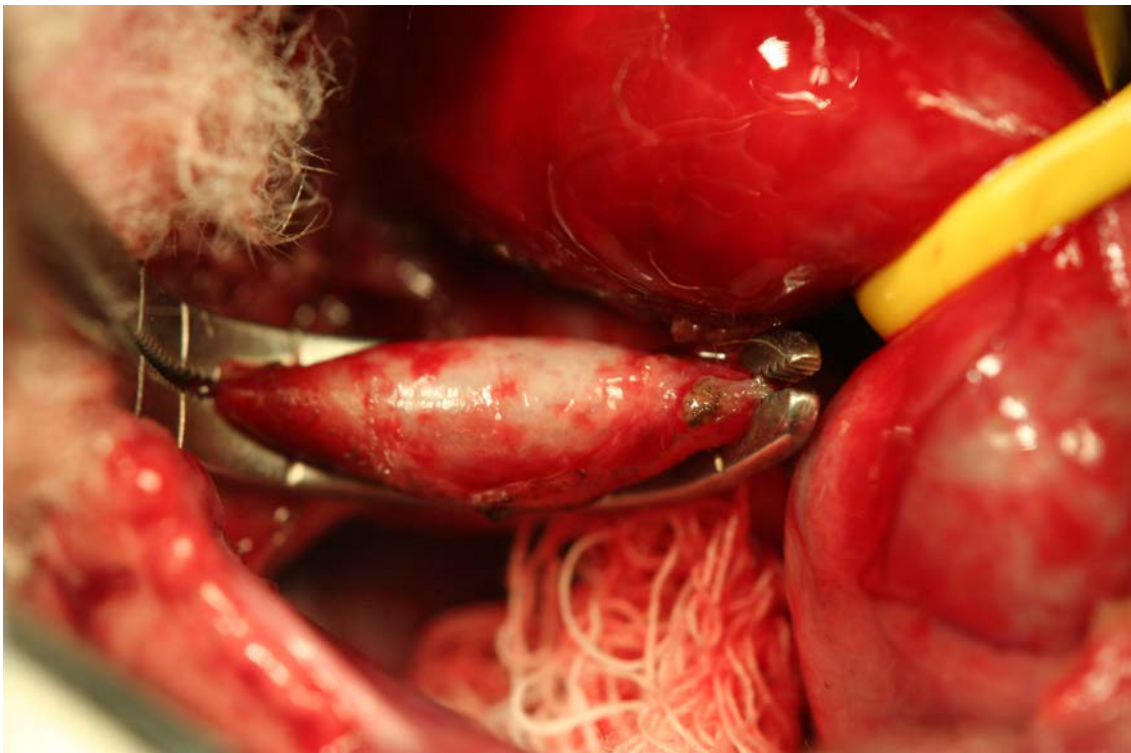
After recovery from anesthesia, the ewe was returned to the cage with free access to food and water until spontaneous delivery occurred. IM buprenorphine

(0.6 mg doses) was used for postoperative analgesia (first dose given before tracheal extubation, second dose 6 hours after, and third dose 12 hours post-second dose).

Figure 32: Anastomosis between vascular graft and ascending aorta
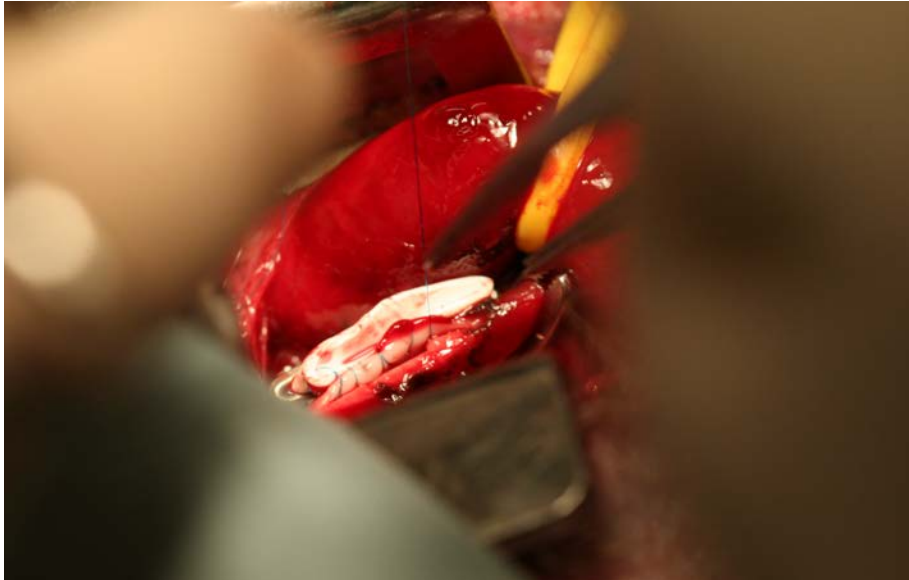
Figure 33: Aorto-pulmonary shunt in place
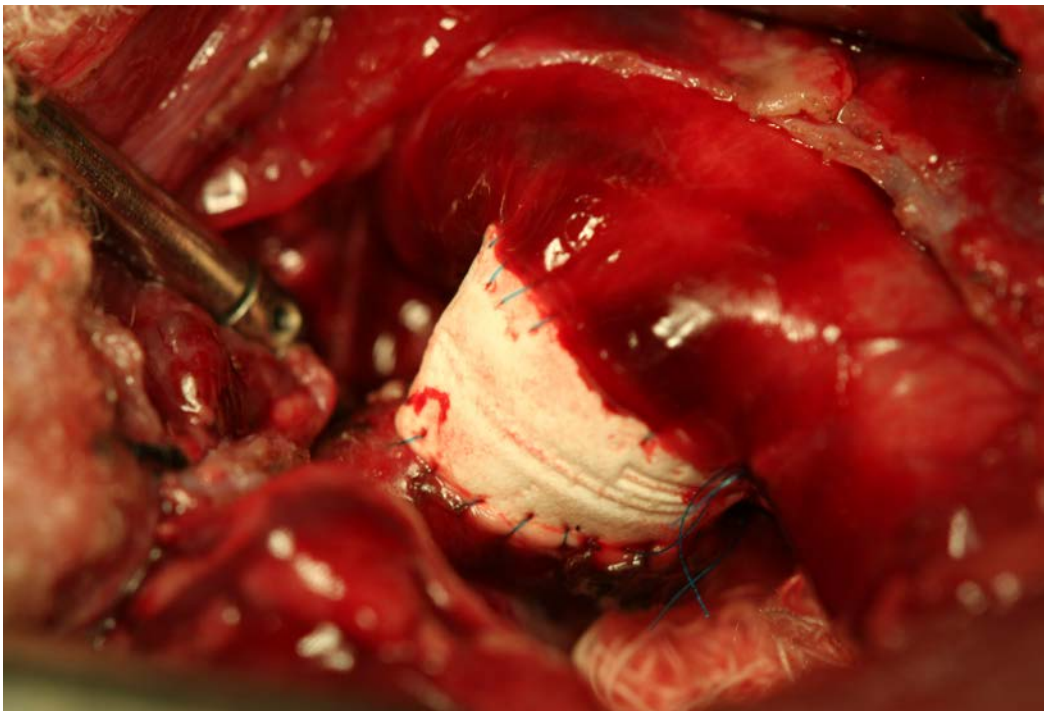
An additional group of five lambs with normal PBF served as age-matched controls.

4.1.2 Lamb intervention and surgical preparation

After spontaneous delivery, the 13 shunt-lambs were subdivided in two experimental groups receiving daily treatment with oral L-carnitine (n=7, 100 mg/kg/day) or its vehicle (n=6). 10 shunt-lambs died in-utero or before 4 weeks of age. Lambs were weighed daily, and the respiratory rate and heart rate were obtained. Elemental iron (100 mg IM) was given weekly to all lambs. Furosemide (1 mg/kg IM) was administered once or twice daily to lambs with signs of respiratory distress.

At 4 weeks of age (22-36 days), the 13 shunt lambs and 11 control lambs with normal PBF were instrumented for haemodynamic and pulmonary vascular reactivity measurements, as well as for blood and lung tissue sampling. For this, initial sedation with 10-15mg/kg of IM ketamine was administered to the lambs. Subsequently, polyurethane catheters were placed in two arteries and two veins of the hind legs. Arterial catheters were advanced to the femoral artery. Lambs were then anesthetized with ketamine hydrochloride (0.3 mg/kg/min), diazepam (0.002 mg/kg/min) and fentanyl citrate (1.0 µg/kg/h) infusions, intubated with a 6 to 7.5-mm-OD cuffed endotracheal tube, and mechanically ventilated with a Viasys, V.I.P. Bird Sterling (Palm Springs, CA) time-cycled, pressured-limited pediatric ventilator. Succinylcholine chloride (2 mg/kg per dose) was given intermittently for muscle relaxation. Ventilation with 21% oxygen was adjusted to maintain a $PaCO_2$ between 35 and 45 mm Hg. Dextrose 5% Ringer Lactate at 80-110ml/hour was administered as maintenance i.v. fluids. Surgical prophylaxis consisted of single dose of cefazolin 1G. The lambs were maintained normothermic (39ºC) with a heating blanket. With a strict aseptic technique, a mid-sternotomy incision was then performed and the pericardium

incised. Using a purse-string suture technique, two single-lumen polyurethane catheters were inserted directly into the right and left atrium respectively. Two additional single-lumen polyurethane catheters were placed in the main pulmonary artery distal to the vascular graft (one for administration of medication and one for pressure monitoring). An ultrasonic flow probe (Transonics Systems, Ithaca, NY) was placed around the left pulmonary artery to measure left pulmonary blood flow. After a 30-minute recovery, simultaneous blood was obtained from the left and right atria, distal pulmonary artery, right ventricle, and femoral artery for hemoglobin and oxyhemoglobin saturation determinations for Qp/Qs calculation. At this time, 20 additional ml of arterial blood and peripheral lung tissue from a randomly selected pulmonary lobe were harvested. Blood was centrifuged (4,000 g for 15 minutes) at 4°C, and plasma and serum supernatants were snap-frozen in liquid nitrogen and then stored in polypropylene storage tubes at -80°C for further analyses. Lung tissue was rinsed in cold, sterile PBS solution, cut in pieces using a sterile technique, snap-frozen in liquid nitrogen, and stored at -80°C for further analyses.

At the end of the experimental protocol, all lambs were euthanized with a lethal injection of sodium pentobarbital followed by bilateral thoracotomy as described in the NIH Guidelines for the Care and Use of Laboratory AnimalsNational Research Council (U.S.). Committee for the Update of the Guide for the Care and Use of Laboratory Animals., Institute for Laboratory Animal Research (U.S.) (130). Additional lung biopsies and isolated pulmonary arterial and venous vessels were collected post-mortem, processed, snap-frozen in liquid nitrogen, and stored at -80°C for further analyses.

4.2   HAEMODYNAMIC MEASUREMENTS

Pulmonary and systemic arterial, and right and left atrial pressures were measured using Sorenson Neonatal Transducers (Abbott Critical Care Systems, North Chicago, IL). Mean pressures were obtained by electrical integration. Heart rates were measured by a cardiotachometer triggered from the phasic systemic arterial pressure pulse wave. Left pulmonary blood flow was measured on an ultrasonic flow meter (Transonic Systems, Ithaca, NY). All hemodynamic variables were measured continuously utilizing the Gould Ponemah Physiology Platform (Version 4.2) and Acquisition Interface (Model ACG-16, Gould Inc., Cleveland, OH), and recorded with a Dell Inspiron 5160 computer (Dell Inc., Round Rock, TX). Blood gases and pH were measured on a Radiometer ABL5 pH/blood gas analyzer (Radiometer, Copenhagen, Denmark). Hemoglobin concentration and oxyhemoglobin saturation (SO_2) were measured by a co-oximeter (model 682, Instrumentation Laboratory, Lexington, MA). Pulmonary vascular resistance was calculated using standard formulas. Shunt fraction (Qp/Qs) was determined using the Fick principle [Qp/Qs= (femoral artery SO_2- right ventricle SO_2) / (left atria SO_2– pulmonary artery SO_2)]. Body temperature was monitored continuously with a rectal temperature probe. Baseline haemodynamic measurements were taken after 30-minutes recovery post lamb instrumentation.

4.3   PULMONARY VASCULAR REACTIVITY MEASUREMENTS

Pulmonary vascular responses were then assessed in response to ACh and inhaled NO. Acetylcholine (Ach) chloride (1µg/kg) followed by inhaled NO (40 ppm) were administered. Ach chloride (IOLAB, Claremont, CA) was diluted in

sterile 0.9% saline and delivered by rapid injection into the pulmonary artery. Inhaled NO was delivered to the inspiratory limb of the respiratory circuit (Inovent, Ohmeda Inc., Liberty, N.J.), and continued for 15 minutes. The inspired concentrations of NO and nitrogen dioxide were continuously quantified by electrochemical methodology (Inovent, Ohmeda Inc., Liberty, N.J.). The hemodynamic variables were monitored and recorded continuously. A minimum of 30 minutes separated the administration of ACh and inhaled NO, and the second agent was not given until baseline hemodynamics returned.

4.4   LABORATORY MEASUREMENTS

4.4.1   Preparation of protein extracts and Western Blot analysis

Lung protein extracts were prepared by homogenizing lamb peripheral lung tissues in lysis buffer (50mM Tris• HCl, pH 7.6, 0.5% Triton X-100, and 20% glycerol) containing Halt protease inhibitor cocktail (Pierce, Rockford, IL). Extracts were then clarified by centrifugation (15,000 G x 10 min at 4°C). Supernatant fractions were then assayed for protein concentration using the Bradford reagent (Bio-Rad, Richmond, CA) and used for Western blot analysis. Lung protein extracts (50µg) were separated on Long-Life 4–20% Tris-SDS-Hepes gels (Frenchs Forest, Australia). All gels were electrophoretically transferred to Immuno-Blot polyvinylidene difluoride membrane (Bio-Rad Laboratories, Hercules, CA). The membranes were blocked with 5% nonfat dry milk in Tris-buffered saline containing 0.1% Tween-20 (TBST). After blocking, the membranes were probed at room temperature with antibodies to eNOS (BD transduction Laboratories, San Jose, CA), CPT-1B (Affinity Bioreagents, Rockford, IL), CPT2 (Affinity Bioreagents), CrAT (Santa Cruz Biotechnology,

Santa Cruz, CA), Hsp70 (Enzo Life Sciences, Farmingdale, NY), or Hsp90 (BD transduction Laboratories), washed with TBS containing 0.1% Tween, and then incubated with an appropriate IgG conjugated to horseradish peroxidase. Protein bands were then visualized with chemiluminescence (SuperSignal West Femto Substrate Kit, Pierce Laboratories, Rockford, IL) on a Kodak 440CF Image Station (Kodak, Rochester, NY). Band intensity was quantified using Kodak 1D image processing software. All captured and analyzed images were determined to be in the dynamic range of the system. To normalize for protein loading, blots were re-probed with the housekeeping protein, β-actin.

4.4.2 Measurement of carnitine homeostasis

4.4.2.1 Sample purification and derivatization

For free carnitine (L-carnitine and acetyl-L-carnitine) determination, 100μl samples of peripheral lung tissue, 300μl water and 100μl of internal standard (Sigma ST 1093) were mixed. For total carnitine determination 100μl samples were hydrolyzed with 0.3 M KOH, heated at 45°C, pH neutralized using perchloric acid, the volume was made to 400μl and 100μl internal standard was added. All samples were purified using solid phase extraction columns, SAX 100mg/ml (Varian, Harbor City, CA) and derivatized using aminoanthracene in presence of EDCI (catalyst) and kept at 30°C for 1 hour to complete reaction of carnitines. Separation was carried out with an isocratic elution in 0.1M Tris-acetate buffer (pH 3.5): acetonitrile (68:32, vol/vol) at a flow rate of 0.9 ml/min as previously described(131, 132).

4.4.2.2 High Performance Liquid Chromatography detection

Detection of carnitines was then performed using an Amersham Biosciences

AKTA purifier system (GE Healthcare, Piscataway, NJ) with a 5-µm OmniSpher C18 column (250 x 4.6-mm OD) equipped with a Jasco FP-2020 fluorescence detector (Tokyo, Japan). Total and free carnitines levels were quantified in lung tissue homogenates by fluorescence detection at 248 (excitation) and 418 nm (emission) as described previously(131, 132). Acylcarnitines were calculated as total carnitine minus free carnitine.

4.4.3 Measurements of carnitine acyltransferase activity

Peripheral lung tissue was homogenized in 50 mM Tris•HCl (pH 7.5), 2 mM EDTA, 5 mM MgCl2, 0.8 mM DTT, and 0.25 mM PMSF with protease inhibitor cocktail. The homogenates were then centrifuged at 3,500 g for 5 min, and Coomassie protein estimation was carried out. CrAT activity was then determined using a modification of the method described by Liu et al(133). Briefly, the assay mixture consisted of 50 mM Tris.HCl, pH 7.5, 2 mM EDTA, 25 mM malate, 0.25 mM NAD, 12.5 g/ml rotenone, 0.04% Triton X-100, 12.5 g/ml malic dehydrogenase, 50 g/ml citrate synthase, 6.25 µM CoA, 200 µM CoA, 400 µM CoA, and 2 mM ALCAR. Sample (10 µl) with a protein concentration of 0.5 mg/ml was added to the assay mixture along with CoA (400 µM) with a constant concentration of 2 mM ALCAR (the Km value for CoA). Reactions were monitored at room temperature for 5 min in a Beckman DU series 600 spectrophotometer. The absorbance was measured at time intervals of 30 seconds, giving 10 readings per sample. The rate was calculated using linear regression to determine the best-fit line.

4.4.4 Immunoprecipitation analyses for nitrated CrAT

Peripheral lung tissues were homogenized in immunoprecipitation buffer [25

mM HEPES, pH 7.5, 150 mM NaCl, 1% Nonidet P-40, 10 mM MgCl2, 1 mM EDTA, and 2% glycerol supplemented with protease inhibitor cocktail (Pierce Laboratories, Rockford, IL)]. Tissue homogenates (1,000 µg of protein) were precipitated either with a rabbit antibody against 3-nitrotyrosine (5 µg; Upstate Biotechnology) or to eNOS (5µg; BD Transduction Laboratories) in 0.5 ml final volume at 4°C overnight. Protein G plus/protein A agarose (40 µl; Calbiochem) was added and rotated at 4°C for an additional 2 h. The precipitated protein was washed three times in 2X volume of immunoprecipitation buffer; the pellet was resuspended in Laemmli buffer (20 µl), boiled, and separated on a 4–20% SDS-PAGE gel (LongLife). CrAT protein levels were then detected using Western-blot analysis.

4.4.5 Determination of lactate and pyruvate levels

Peripheral lung tissues were homogenized in ice-cold 0.5 M perchloric acid and centrifuged at 14,000 rpm for 20 min. The supernatant were then neutralized with 3 M KHCO3 and used for lactate and pyruvate assays. The relative changes in lactate levels were measured using a lactate assay kit (Biovision). Pyruvate levels were determined using the spectrophotometric enzymatic measurement assay at 340 nm. NADH was used as a cofactor and lactate dehydrogenase as the coenzyme. Experimental conditions were as previously described(134).

4.4.6 Assay for Nitric Oxide Synthase (NOS) activity

NOS activity was determined using the conversion of [³H]L-arginine to [³H]L-citrulline as previously described(135). Briefly, peripheral lung tissues were homogenized in NOS assay buffer (50 mM Tris•HCl, pH 7.5, containing 0.1 mM

EDTA and 0.1 mM EGTA) with a protease inhibitor cocktail. Enzyme reactions were carried out at 37°C in the presence of total lung protein extracts (500 µg), 1 mM NADPH, 14 µM tetrahydrobiopterin, 100 µM FAD, 1 mM MgCl2, 5 µM unlabeled L-arginine, 15 nM [^{3}H]L-arginine, calmodulin (25 units), and 5 mM calcium to produce conditions that drive the reaction at maximal velocity. Duplicate assays were run in the presence of the NOS inhibitor nitro-L-arginine methyl ester (L-NAME) to detect nonspecific production of [^{3}H]citrulline. This value was then subtracted to obtain the final activity value. Assays were incubated for 60 min at 37°C such that no more than 20% of the [^{3}H]arginine was metabolized to insure that the substrate was not limiting. The reactions were stopped by the addition of iced stop buffer (20 mM sodium acetate, pH 5, 1 mM L-citrulline, 2 mM EDTA, and 0.2 mM EGTA) and then applied to columns containing 1 ml of Dowex AG 50W-X8 resin, Na$^+$ form, preequilibrated with 1 N NaOH. [^{3}H]L-citrulline was then quantitated by scintillation counting. All activities were normalized to the amount of protein in each lysate. To determine the potential contribution of iNOS to total NOS activity, assays were repeated without calcium supplementation.

4.4.7 Measurements of superoxide levels in peripheral lung tissue

Approximately 0.2 g of peripheral lung tissue was sectioned from fresh-frozen tissue and immediately immersed in normal EPR buffer [PBS supplemented with 5 µM diethydithiocarbamate (DETC; Sigma-Aldrich) and 25 µM desferrioxamine (Def MOS; Sigma-Aldrich)]. In addition, to determine the relative contribution of uncoupled NOS activity to superoxide production, equivalent samples were pre-incubated in 100 µM S-ethylisothiourea hydrobromide (ETU; Sigma), a non-specific inhibitor of NO synthases(136).

Superoxide levels were then estimated by electronic paramagnetic resonance (EPR) assay using the spin-trap compound 1-hydroxy-3-methoxycarbonyl-2,2,5,5-tetramethylpyrrolidine·HCl (CMH) as previously described(137, 138). NOS-derived superoxide levels were determined by subtracting the values in the presence of ETU from the values in the absence of ETU. To convert EPR waveforms into units of superoxide we used 1mU of xanthine oxidase to generate 1nM/min of superoxide over a 60 min period to generate a standard curve. Using this standard curve we were able to convert waveform amplitudes into nmol of superoxide produced/min/mg protein in each reaction condition.

4.4.8 Measurements of bioavailable NO (NOx)

Plasma samples were treated with cold ethanol for 1 h at −20°C and then centrifuged at 20,000g to remove proteins that can interfere with NO measurements. Potassium iodide–acetic acid reagent was prepared fresh daily by dissolving 0.05 g of potassium iodide in 7 ml of acetic acid. KI/AcOH mixture was added into a septum-sealed purge vessel and bubbled with nitrogen gas. The gas stream was connected via a trap containing 1 N NaOH to a Sievers 280i Nitric Oxide Analyzer (GE Analytical, Boulder, CO). Samples were injected with a syringe through a silicone–Teflon septum. Results were analyzed by measuring the area under the curve of the chemiluminescence signal using the Liquid software (GE). The resultant NOx value represents total nitric oxide and nitrite.

4.5   STATISTICAL ANALYSIS

Statistical analysis was performed using GraphPad Prism version 5.0 (GraphPad Software, San Diego, CA). The means ± SD or SEM were calculated. Statistical significance was determined either by the unpaired t-test, paired t-test (for 2 groups) or repeated measures ANOVA (for ≥3 groups) with Tukey's post-hoc testing as indicated. All tests were two-sided and statistical significance was evaluated at the 5% level ($p<0.05$).

RESULTS

5   RESULTS

5.1   HEMODYNAMIC MEASUREMENTS

The baseline hemodynamic data, arterial blood gases, hemoglobin and weights

for age-matched control lambs, vehicle-treated shunt lambs, and carnitine-

treated shunt lambs at 4 weeks of age are shown in Table 10.

Table 10: Baseline lamb hemodynamic and laboratory characteristics

Hemodynamic Variable	Control (n=5)	Shunt + Vehicle (n=6)	Shunt + Carnitine (n=7)
mPAP (mmHg)	15.3 ± 3.8	23.1 ± 4.3*	20.8 ± 3.5
mSAP (mmHg)	77.6 ± 7.7	70.7 ± 8.9	60.5 ± 6.3†
mRAP (mmHg)	3.5 ± 2	3.8 ± 1.4	3.6 ± 1.7
mLAP (mmHg)	4.1± 1.6	7.1 ± 1.7	8.5 ± 3.4†
HR	126 ±13	174 ± 26*	142 ± 37
LPA-Q (ml/min/kg)	0.8 ± 0.2	1.8 ± 0.6	2.56 ± 0.8†
LPVR (mmHg/ml/min/kg)	0.24 ± 0.10	0.14 ±0.06	0.088 ± 0.03†
Qp:Qs	-	2.8 ± 0.9	2.7 ± 0.5
pH (units)	7.36 ± 0.03	7.40± 0.02	7.41 ± 0.02
pCO_2 (torr)	42.3 ± 2.1	40.0 ± 3.7	42.0 ± 3.0
PO_2 (torr)	78.3 ± 12.2	71 ± 11	74.7 ± 11.2
Hb (mg/dl)	9.0 ± 1.7	9.8 ± 1.6	8.6 ± 1.4
Weight (kg)	15.7 ± 2.5	13.9 ± 2.1	14.1 ± 3.2

mPAP: mean pulmonary arterial pressure; mSAP: mean systemic arterial pressure; mRAP: mean right atrial pressure; mLAP: mean left atrial pressure; HR: heart rate; LPA-Q: blood flow through the left pulmonary artery; LPVR: left pulmonary vascular resistance; Qp:Qs: ratio of pulmonary to systemic blood flow; Hb: hemoglobin. Values are mean ± SD; *$p<0.05$ control vs. vehicle-treated shunt, †$p<0.05$ control vs. carnitine-treated shunt.

There were no statistically significant differences in baseline hemodynamic indices between both shunt lambs groups. There were also no statistically significant differences in hemoglobin, arterial blood gases or weights between the three groups, despite a trend for lower weight in shunt lambs. The shunt fraction (Qp/Qs) was close to 2.8 in each shunt group, demonstrating the presence of a large aorto-pulmonary shunt.

Compared to age-matched control lambs, however, vehicle-treated shunt lambs exhibited a significantly increased mean PAP and heart rate that were not observed in carnitine-treated shunt lambs. In addition, compared to age-matched control lambs, carnitine-treated shunts displayed decreased mean systolic arterial pressure and left PVR, as well as significantly higher left pulmonary artery flow and mean left pulmonary arterial pressure.

5.2 EVALUATION OF THE PROTEINS RESPONSIBLE FOR MAINTAINING CARNITINE HOMEOSTASIS

Compared to vehicle-treated shunt lambs, carnitine-treated shunt lambs displayed an increase in the peripheral lung protein levels of CrAT (Figure 34A). Further, in carnitine-treated lambs CrAT activity was significantly higher compared to vehicle-treated shunt lambs (Figure 34B), whereas nitrated CrAT levels were significantly reduced (Figure 34C).

Besides, although in carnitine-treated shunt lambs CrAT protein levels and nitrated CrAT were not significantly different to age-matched control lambs with normal PBF, CrAT activity was still significantly reduced (Figure 34B).

Furthermore, the peripheral lung protein levels of CPT1 were significantly higher in carnitine-treated shunt lambs compared to age-matched control lambs with normal PBF (Figure 35A). CPT2 levels, however, were unchanged in any of the

three groups (Figure 35B).

Figure 34: Carnitine acetyltransferase protein levels and activity, and relative nitrated CrAT levels in the lamb lung
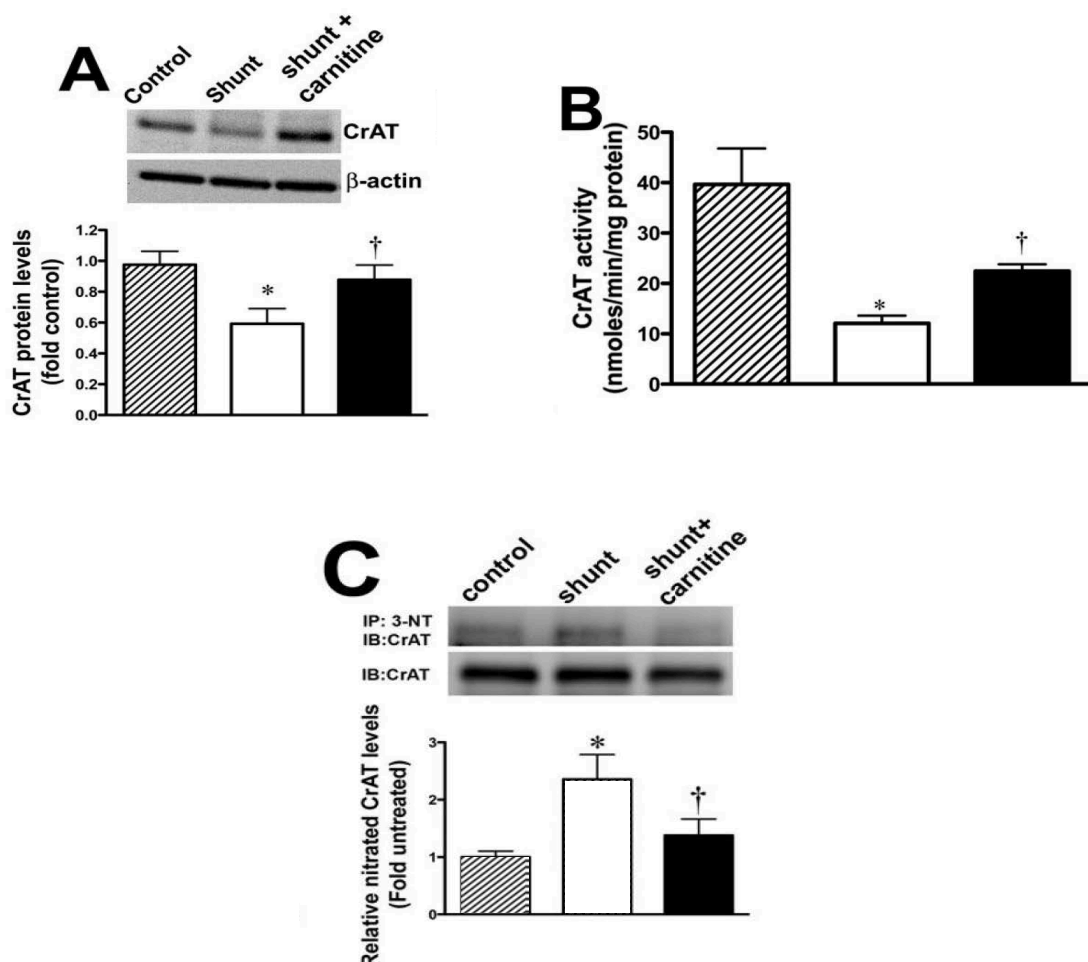
Protein extracts (50µg), prepared from peripheral lung of age-matched control lambs (diagonal lined), vehicle (white)- and carnitine (black)-treated shunt lambs were analyzed by Western blot analysis using a specific antiserum raised against CrAT protein. Blots were also normalized for loading using β-actin. A representative blot is shown (A). CrAT activity was determined in protein extracts (40 µg) prepared from peripheral lung tissue from all three groups of lambs (B). Protein extracts (1mg) were also subjected to immunoprecipitation using an antibody specific to 3-NT and then analyzed by Western blot analysis using a specific antiserum raised against CrAT protein. A representative blot is shown (C). Values are mean ± SEM; n=4 age-matched control lambs, n=6 vehicle-treated shunt lambs, and n=7 carnitine-treated shunt lambs. *$p<0.05$ vs. control; †$p <0.05$ versus vehicle-treated shunt lambs.

5.3 EVALUATION OF CARNITINE HOMEOSTASIS

In the current study we determined peripheral lung carnitine levels in carnitine- and vehicle-treated shunt lambs, as well as age-matched control lambs with normal PBF. We found that acyl-carnitine levels were significantly higher in

vehicle-treated shunt lambs than in either carnitine-treated shunt lambs or age-

matched control lambs with normal PBF (Figure 36A).

Figure 35: CPT1 and CPT2 protein levels in the lamb lung
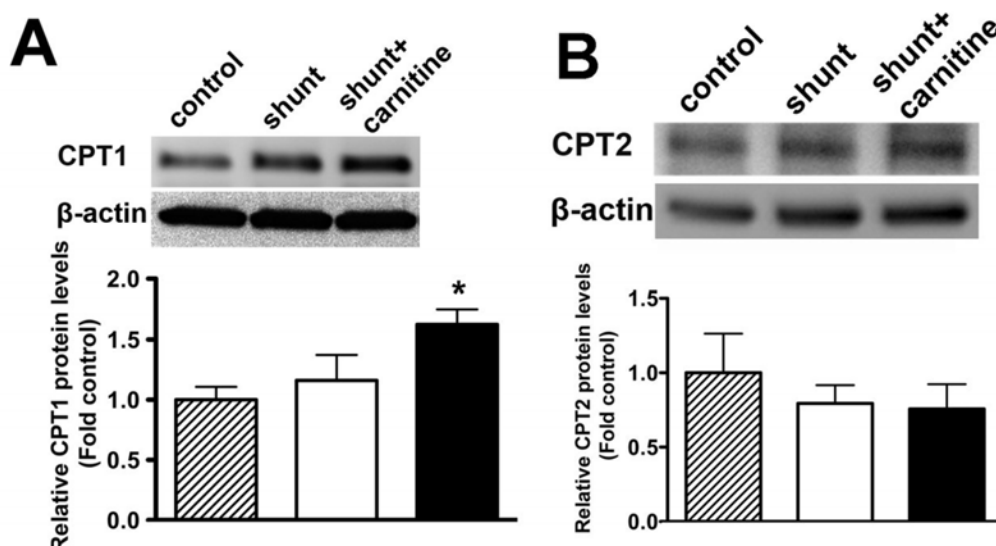
Protein extracts (50µg) prepared from peripheral lung of age-matched control lambs (diagonal lined), vehicle (white)-, and carnitine (black)-treated shunt lambs were analyzed by Western blot analysis using a specific antisera raised against carnitine palmitoyltransferase 1B (CPT-1) and carnitine palmitoyltransferase 2 (CPT-2). Blots were also normalized for loading using β-actin. Representative blots are shown (A & B). Values are mean ± SEM; n=5 age-matched control lambs, n=6 vehicle-treated shunt lambs, and n=7 carnitine-treated shunt lambs. *p<0.05 vs. control.

Figure 36: Carnitine homeostasis in the lamb lung
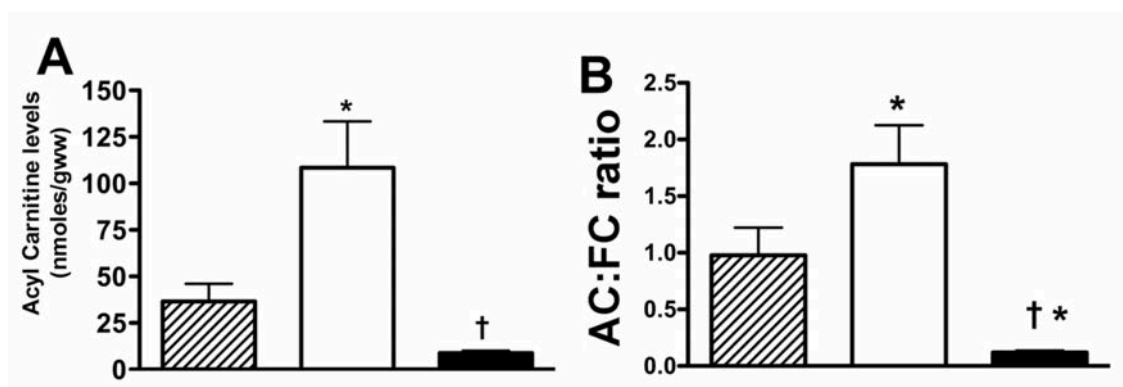
Acyl-carnitines (A), the AC:FC ratio (B) were determined in peripheral lung of age-matched control lambs (diagonal lined), vehicle (white)-, and carnitine (black)-treated shunt lambs. Values are mean ± SEM; n=6 vehicle-treated shunt lambs, n=7 carnitine-treated shunt lambs, and n=4 age matched control lambs. *p<0.05 vs. control; †p<0.05 vs. vehicle-treated shunt lambs

Similarly, the peripheral lung acyl-carnitine:free-carnitine (AC:FC) ratio was

significantly higher in vehicle-treated shunt lambs than in either carnitine-treated

shunt lambs or age-matched control lambs with normal PBF (Figure 36B). In addition, although the acyl-carnitine levels were unchanged between carnitine-treated shunt lambs and age-matched control lambs with normal PBF, the AC:FC ratio was significantly less (Figure 36B).

5.4   EVALUATION OF MITOCHONDRIAL FUNCTION

To estimate lung mitochondrial activity we determined and compared lung levels of lactate and pyruvate. As shown in Figure 37A, the lactate:pyruvate ratio was significantly higher in vehicle-treated shunt lambs than in either carnitine treated shunt lambs or age-matched control lambs with normal PBF (Figure 37A). The lactate:pyruvate ratio was unchanged in age-matched control lambs with normal PBF compared to carnitine-treated shunt lambs.

Figure 37: Mitochondrial function in the lamb lung
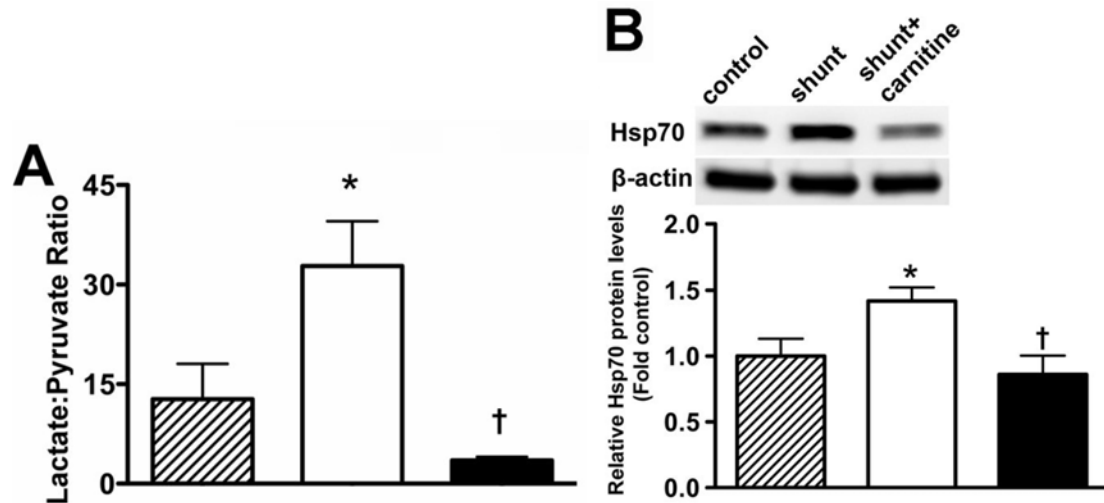
A. The lactate:pyruvate ratio was determined in peripheral lung of age-matched control lambs (diagonal lined), vehicle (white)-, and carnitine (black)-treated shunt lambs. B: Protein extracts (50µg), prepared from all three groups were also analyzed by Western blot analysis using a specific antisera raised against Hsp70. Blots were also normalized for loading using β-actin. A representative blot is shown (B). Values are mean ± SEM; n=4 age-matched control lambs, n=6 vehicle-treated shunt lambs, and n=7 carnitine-treated-shunt lambs. *p<0.05 vs. control; †p<0.05 vs. vehicle treated-shunt lambs.

In addition, we determined the levels of Hsp70, a mitochondrial chaperone protein that exerts protection against oxidative injury and whose gene

expression is induced by mitochondrial stress(139, 140). Our data indicate that Hsp70 protein levels were significantly higher in vehicle-treated shunt lambs than in either carnitine-treated shunt lambs or age-matched control lambs with normal PBF. The levels of Hsp70 were not different between carnitine-treated shunt lambs and age-matched control lambs with normal PBF (Figure 37B).

5.5   ASSESSMENT OF NO SIGNALING PATHWAY

To assess the NO signaling pathway, we determined and compared eNOS-HSP90 interactions, NOS activity, and NOx levels in carnitine- and vehicle-treated shunt lambs, as well as age-matched control lambs with normal PBF.

We found eNOS-bound-HSP90 was significantly lower in vehicle-treated shunt lambs compared to either carnitine-treated shunt lambs or age-matched control lambs with normal PBF. HSP90-eNOS interactions were not significantly different between carnitine-treated shunt lambs and age-matched control lambs with normal PBF (Figure 38A).

In addition, we found a decrease in NOS-dependent superoxide levels, indicative of decreased eNOS uncoupling in carnitine-treated shunt lambs compared to vehicle-treated shunt lambs. Again NOS-derived superoxide levels were not significantly different between carnitine-treated shunt lambs and age-matched control lambs with normal PBF (Figure 38B).

Furthermore, the maximal velocity (Vmax) for total NOS activity in the peripheral lung was also significantly higher in carnitine-treated shunt lambs compared to both vehicle-treated shunt lambs and age-matched control lambs with normal PBF (Figure 38C).

Figure 38: Determinations of eNOS-Hsp90 interactions, eNOS-dependent superoxide levels, NOS activity, and NOx levels in the lamb lung
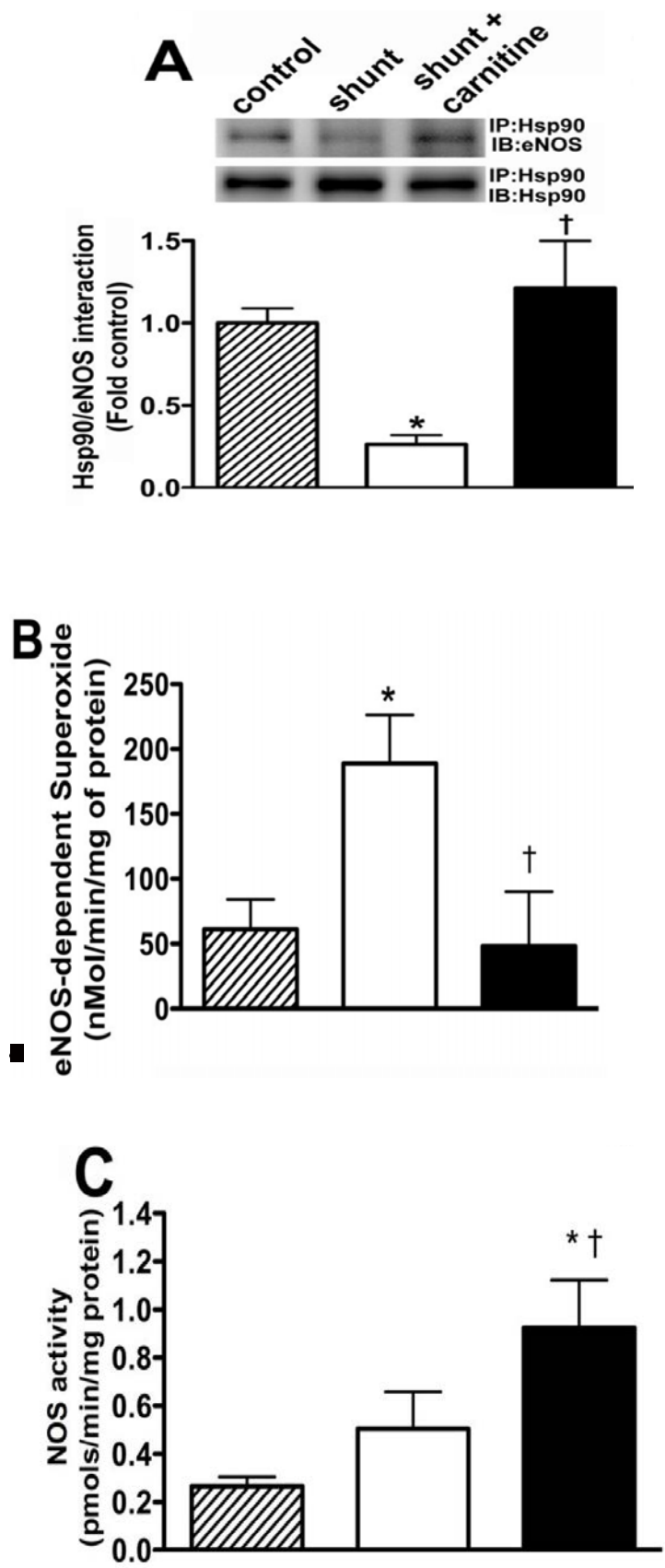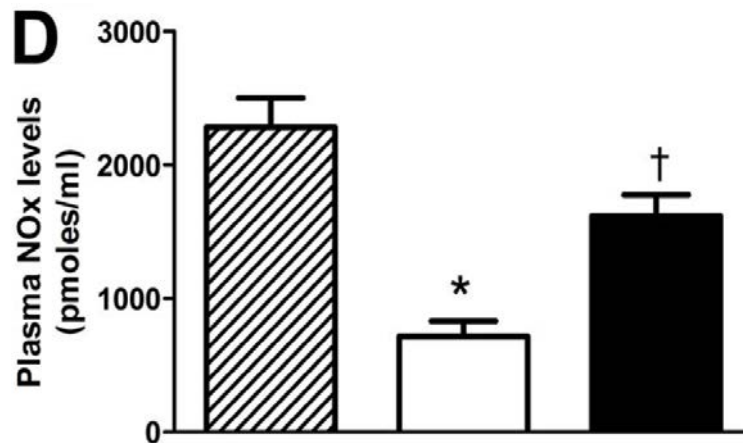
A: The interaction of eNOS with Hsp90 was determined by immunoprecipitation using specific antiserum raised against eNOS in the peripheral lung of age-matched control lambs (diagonal lined), vehicle (white)-, and carnitine (black)-treated shunt lambs. Immunoprecipitated extracts were analyzed using antisera against either eNOS or Hsp90 (to normalize for immunoprecipitation efficiency). A representative image is shown.

B: Superoxide anion levels were determined by EPR in snap-frozen lung tissue in each group of lambs in the presence and absence of the NOS inhibitor 2-Ethyl-2-thiopseudourea (ETU, 100µM). Values are mean ± SEM; n=6 age-matched control lambs, n=5 vehicle-treated, n=6 carnitine-treated shunt lambs. *p<0.05 vs. control; †p<0.05 vs. vehicle-treated shunt lambs

Total NOS activity (C) and NOx levels (D) were also determined in peripheral lung and plasma in all 3 groups. Values are mean ± SEM; n=6 age-matched control lambs, n=5 vehicle-treated, n=6 carnitine-treated shunt lambs. *p<0.05 vs. control; †p<0.05 vs. vehicle-treated shunt lambs.

Lastly, the increased eNOS-HSP90 interactions, decreased eNOS-derived superoxide production, and enhanced maximal NOS activity in carnitine-treated shunt lambs was associated with improved NO signaling, as demonstrated by increased plasma NOx levels compared to vehicle-treated shunt lambs (Figure 38D).

5.6   PULMONARY VASCULAR REACTIVITY

In the current study we found that the endothelium-dependent vasodilator acetylcholine chloride (1µg/kg) did not decrease PVR in vehicle-treated shunt lambs (Figure 39). However, in carnitine-treated shunt lambs PVR decreased significantly in response to acetylcholine. The acetylcholine-mediated decrease in PVR was not significantly different between carnitine-treated shunt lambs and age-matched control lambs with normal PBF (Figure 39).

Figure 39: Measurements of Left Pulmonary Vascular Resistance
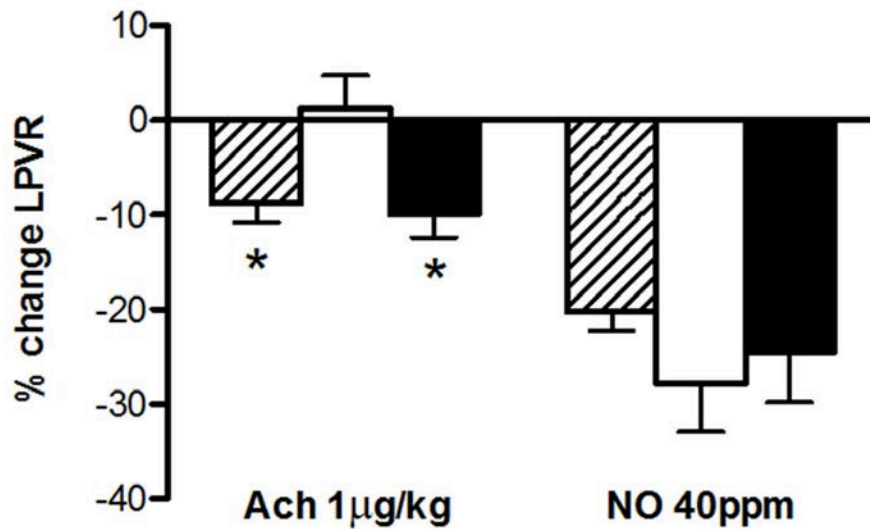
Changes in left pulmonary vascular resistance (LPVR), expressed as percent change from baseline, in response to injection of acetylcholine (1 µg/kg), an endothelium-dependent agent, and inhaled nitric oxide (40 ppm), an endothelium-independent agent, in age matched control lambs (n=5, diagonal lined), carnitine-treated (n=7, black), and vehicle treated (n=5, white) shunt lambs. Acetylcholine significantly decreased LPVR in the carnitine-treated-, but not in the vehicle-treated-shunt lambs. The decrease in PVR was not significantly different between carnitine-treated shunt lambs and age matched control lambs. All groups experienced a similar drop in PVR in response to inhaled NO (40ppm). Values are mean ± SD. *p<0.05 compared to baseline.

In contrast, in response to the endothelium-independent vasodilator inhaled nitric oxide (iNO) (40ppm), calculated PVR decreased similarly in all groups (Figure 39). These data are identical when analyzed for absolute change over time (data not shown).

DISCUSSION

6 <u>DISCUSSION</u>

The results of this study show that early treatment with L-carnitine prevents the disruption of lung carnitine homeostasis, improves mitochondrial function, enhances NO signaling, and ultimately results in better endothelial function in our lamb model of CHD with increased PBF.

The carnitine system is critical to maintain normal mitochondrial function and cellular energy metabolism. Under conditions of metabolic stress, the mitochondria accumulate acylCoA esters, which are normally maintained in homeostasis with free CoA by the carnitine system. This results in a state of relative carnitine insufficiency and reduced free CoA availability, that leads to impaired oxidative metabolism, decreased energy production and in turn enhanced secondary generation of ROS, mitochondrial dysfunction and/or cell death[141, 142]. In addition, recent data suggest that mitochondrial oxidative stress can damage CrAT, decreasing its binding affinity for substrates and resulting in further disruption of the carnitine system and mitochondrial function[133].

Although the high impact of the carnitine system is patent in the clinical manifestations of its inborn errors (encephalopaty, heart failure, muscle weakness and death[143]), in recent decades compromised carnitine metabolism has been implicated in the development of mitochondrial injury in conditions characterized by oxidative stress and mitochondria dysfunction such as hypoxic-ischaemic injury, neurodegenerative diseases, insulin resistance or aging[144-148]. Furthermore, animal and human studies have demonstrated protective effects of carnitine therapy in maintaining or improving mitochondrial

function in numerous of these conditions, including Alzheimer disease and other neurodegenerative conditions such as Parkinson and multiple sclerosis, stroke, insulin resistance, diabetic neuropathy, myocardial infarction, peripheral vascular disease, heart failure, systemic hypertension, male infertility or aging(80, 149, 150).

In our lamb model of CHD with increased PBF, we have previously demonstrated a disruption in carnitine homeostasis that results in mitochondrial dysfunction and impaired NO signalling (127, 151). As described in other metabolic stress conditions, shunt lambs display high acylcarnitine:free carnitine ratios, which reflect an imbalance in mitochondrial acylCoA:CoA. In addition, shunt lambs exhibit decreased expression of three key carnitine-dependent enzymes (CPT1, CPT2, CrAT), as well as a significantly reduction of CrAT activity, which is at least in part secondary to eNOS-dependent nitration. Moreover, evidence from prior work of our group indicates that eNOS is uncoupled in shunt lambs(121, 127). Through mechanisms not fully elucidated, uncoupled eNOS redistributes from the plasma membrane to the mitochondria, where it induces mitochondrial dysfunction, with increased mitochondrial-derived ROS generation, nitration of mitochondrial proteins and decreased ATP generation(96).

Altogether these data suggest that under the shear stress imposed by increased PBF, the endogenous lung endothelial pool of carnitine becomes insufficient for the acyl transfer demand in shunt lambs, resulting in insufficient free CoA and mitochondrial oxidative stress and dysfunction. In addition, nitration-dependent drop in CrAT activity leads to further disruption of the

carnitine system, worsening mitochondrial dysfunction, and further decline in ATP production.

Previous studies have shown the importance of ATP in pulmonary endothelial function, likely due to its role in eNOS activation(152). eNOS activity is tightly controlled through multiple mechanisms that include phosphorylation and protein-protein interactions(153). Hsp90, member of a molecular chaperone family, is among the key proteins that increase eNOS activity in a process ATP-dependent(77, 123). Therefore, as our findings suggest, it is plausible that if disruption in carnitine homeostasis leads to a decrease in mitochondrial ATP production and a subsequent decrease in Hsp90-eNOS interactions(127), chronic L-carnitine exogenous supplementation would result in increased NO signaling and improved endothelial function.

The same as eNOS, it is noteworthy that GTP cyclohydrolase I (GCHI) -the rate limiting enzyme in the *de novo* biosynthesis of the eNOS cofactor tetrahydrobiopterin (BH4)- is also chaperoned by Hsp90. We have previously shown that BH4 levels are reduced in shunt lambs, which contributes to eNOS uncoupling(154). Thus, the preservation of mitochondrial function and NO signaling in L-carnitine supplemented shunt lambs likely involves increases not only in eNOS/HSsp90-, but also in GCHI/Hsp90-interactions.

In fact, in a recent study from our group we showed that ADMA -an endogenous competitive eNOS inhibitor that induces mitochondria dysfunction- results in decreased ATP-dependent HSP90-GCH1 interactions and increased GCH1 degradation in ovine pulmonary arterial endothelial cells (PAEC), that lead to reduced BH4 levels and ultimately eNOS uncoupling(155). Interestingly, pre-treatment of PAEC with acetyl-L-carnitine abolished these phenomena,

preserving mitochondrial ATP production and HSP90 activity, increasing GCH1 and BH4 levels, and in agreement with our in-vivo data, improving eNOS coupling and NO signaling. Importantly, we extended the study to our lamb model and confirmed the same cell culture findings in peripheral lung tissue of carnitine-treated shunt lambs. Furthermore, additional data on the effects of carnitine on NO signalling have been recently reported by Calo et al. who has shown a direct stimulatory effect of carnitine on eNOS gene and protein expression in human endothelial cells(156). Importantly, our current work demonstrates that the described molecular changes translate functionally into enhanced endothelial function, as demonstrated by a conserved reduction of PVR in response to Ach. This physiologic improvement appears to be selective to the endothelium since the response to inhaled NO was unchanged.

Interestingly, our data is supported by animal research on systemic hypertension, where carnitine supplementation has been shown to induce endothelial-dependent vasodilatation, enhance NO and PGI_2 production, and improve endothelial dysfunction(157-159). Unfortunately, none of these studies assessed carnitine homeostasis or mitochondrial function, and authors ascribed the positive beneficial effects of carnitine on blood pressure to an observed concomitant reduction in ROS, acknowledging the mechanisms underlying the antioxidant properties of carnitine remain unclear.

In this regard, besides reducing the mitochondrial toxicity resulting from excess acyl-CoA, evidence suggests that carnitine and its acyl derivatives exert antioxidant properties through additional mechanisms that include direct free radical scavenging, inhibition and/or repair of peroxidized biomolecules(160, 161), and induction of gene and protein expression of oxidative stress related

proteins(156). Thus, as described in systemic hypertension, carnitine has shown protective effects in numerous conditions in which oxidative damage is thought to play a major role like myocardial and cerebral ischaemia-reperfusion injury, gentamycin and anthracycline toxicity, or chronic renal failure(162-165). In addition, carnitine has been shown to display anti-apoptotic effects for instance in the skeletal muscle of an animal model of heart failure, which authors believe occurs through its ability to attenuate oxidative stress(166).

Despite compelling evidence that oxidative stress plays a causal role in the development of PVD secondary to increased PBF(167), the work from our group is the first to suggest a mitochondrial component linked to alterations in the carnitine system in its pathogenesis, which in the current study we demonstrate is reversible, at least in part, by exogenous L-carnitine supplementation. Lung mitochondrial dysfunction had previously been described in some animal studies of PH, including a rat model of hypoxic pulmonary vasoconstriction(168) and the pulmonary hypertension syndrome of fast-growing broilers, which was interestingly attenuated by antioxidant therapy with vitamin E(169, 170). However, it is only in the last few years that rapidly emerging animal and human evidence is recognizing mitochondrial dysfunction as a central driver of PAH, with a new so-called *metabolic theory* gaining relevance among the scientific community(171, 172).

Specifically, the *metabolic theory* of PAH proposes that many apparently unrelated molecular abnormalities described to date in PAH converge to the mitochondria, either causing or promoting the suppression of glucose oxidation, which in turn results in secondary up-regulation of cytoplasmic glycolysis with increased lactate production(171-173). Besides, due to a reciprocal inhibitory

mechanism, the inhibition of glucose oxidation results in the activation of fatty acid oxidation and altered lipid metabolism.

This glycolytic phenotype occurring under normoxic conditions is known as the *Warburg effect* and it is a feature of cancer cells(174). Although more extensively studied in pulmonary SMC, in recent years the Warburg effect has been evidenced in PAH in all pulmonary arterial layers as well as in the remodeled right ventricle(175). Besides, animal and human data have also demonstrated altered pulmonary vasculature and right ventricle fatty acid metabolism in association with PAH(176, 177).

Thus, after the cancer paradigm, the *metabolic theory* proposes that in PAH the suppression of mitochondrial function secondary to the inhibition of mitochondrial oxidative phosphorylation results in a metabolic reprogramming that irrespectively of oxygen availability results in the anti-apoptotic, proliferative and inflammatory phenotype that defines pulmonary vascular cells in PAH(177-180). Some of the latest proposed mechanisms of mitochondrial damage in PAH include electron transport chain dysfunction, altered mitochondrial membrane potential, increased mitochondrial oxidative stress, damage mitochondrial DNA, impaired mitochondrial biogenesis and mitophagy, and altered mitochondrial dynamics via fission/fusion(172). Consequently, the *metabolic theory* supports that if multiple molecular abnormalities of PAH may be the result of a primary mitochondrial dysfunction, mitochondria-targeting therapies aimed to enhance glucose oxidation should be able to address them simultaneously, which is currently a promising research area(181).

Not only our previous findings of disrupted mitochondrial function and carnitine homeostasis in shunt lambs are consistent with the *metabolic theory*, the

present work showing how L-carnitine supplementation decreases the lactate:pyruvate ratio in our lamb model suggests an improved mitochondrial glucose oxidation and highlights the potential role of carnitine as a target *metabolic* therapy for PAH.

To date, however, only anecdotal reports have assessed the role of carnitine supplementation in PAH. On one hand, L-carnitine supplementation has shown beneficial effects on lipid peroxidation and pulmonary vascular remodeling in cold-exposed broilers with pulmonary hypertension syndrome, postponing the occurrence of disease despite not reducing cumulative mortality(182). On the other hand, two small human studies on children with sickle cell disease and β-thalassemia associated PAH suggested a benefit of L-carnitine therapy in decreasing PA systolic pressure(183, 184).

Importantly however, in agreement with our lamb data, several human in vivo studies have demonstrated in the last years an altered carnitine homeostasis associated to PAH, strengthening the argument of a randomized trial of carnitine therapy in PAH patients. Thus, in 2016 Brittain et al. evidenced increased circulating free fatty acids and long-chain acylcarnitines in patients with idiopathic and heritable PAH, alongside right ventricle lipotoxicity(185). To our knowledge, this study was the first to report altered carnitine homeostasis in humans with PHA, and authors attributed their findings to failure of fatty acid utilization at the mitochondrial level. Moreover, in 2017 a new study from our group demonstrated a disrupted carnitine and mitochondrial homeostasis in children with CHD and increased PBF (VSDs), linked to impaired NO signaling and oxidative stress(186). Lastly, Luo et al. reported in the same year significantly higher plasma concentrations of long-chain acylcarnitines in

patients with different subtypes of PAH compared to controls, suggesting the presence of unique metabolic abnormalities associated to the disease(187).

Our study has some potential limitations, especially regarding the oral delivery system we utilized (100mg/kg/day). It has been shown that oral administration of carnitine occurs both by carrier-mediated transport and through passive diffusion. However, this process appears to be relatively inefficient as previous studies using oral doses of 1–6g, resulted in only 5–18% bioavailability compared to the 75% bioavailability of L-carnitine ingested through dietary means. Therefore, supplemental doses of L-carnitine appear to be absorbed less efficiently(188). The dose for this study was chosen after three pilot studies in shunt lambs demonstrated that free and acyl-carnitine lung levels returned to values similar to non-operated controls.

There are also some unanswered questions that our study raised. On one hand, it is unclear how L-carnitine supplementation led to an increase in the expression of CPT1. It is possible that this may be mediated via an increase in the activity of peroxisome proliferator-activated receptor gamma (PPARγ), a subfamily of nuclear receptors that function as transcription factors regulating the expression of genes involved in fatty acid storage and glucose metabolism. We have previously shown that PPARγ expression and activity are reduced in shunt lambs(189), and we recently demonstrated how expression of some of the carnitine homeostasis genes can be regulated by PPAR(190). In fact, the promoter region of the CPT1 gene appears to contain a PPAR response element (PPRE), DNA sequences in target genes to which PPAR binds(191). However, a PPRE has not been identified in the CrAT gene and thus it remains to be elucidated how L-carnitine preserves CrAT expression in shunt lambs.

Alternatively, these genes may be down-regulated in response to oxidative stress, which is reduced in the presence of L-carnitine.

It is also worth noting that L-carnitine supplementation did not preserve all the parameters we measured to the levels of those observed in age-matched control lambs with normal PBF. Interestingly, although maximal NOS activity was enhanced in carnitine supplemented lambs, NOx levels did not increase above those observed in age-matched control lambs with normal PBF. However, the fact that the reduction in PVR in response to Ach was still preserved suggests that there is sufficient bioavailable NO produced in carnitine-supplemented shunt lambs to induce SMC relaxation.

Finally, it is unclear why and noteworthy that none of the mitochondrial inborn errors of metabolism associated with carnitine deficiencies have been shown to be associated with the development of pulmonary hypertension. Although unlikely, it is possible that this correlation has not been investigated or that the standard therapy with high dose L-carnitine prevents the potential development of pulmonary hypertension for carnitine homeostasis defects. Alternatively, altered lung carnitine homeostasis in PVD is a tissue-specific phenomenon and a consequence of multiple pathways that converge in the mitochondria and lead to mitochondrial oxidative stress and disrupted function through diverse mechanisms. Therefore, alone systemic carnitine deficiency may not lead to PVD, but in the context of increased PBF exogenous and altered carnitine homeostasis, it is plausible that carnitine supplementation contributes to palliate or prevent the associated lung mitochondrial oxidative stress and dysfunction. Besides, similarly to what has been seen with several trialed antioxidant therapies, it is likely that despite showing promising effects in vitro and in

animals, treatment with L-carnitine is not able to revert established pulmonary vascular remodeling and only provide a therapeutic benefit when initiated early in the disease process and administered chronically.

CONCLUSIONS

7 <u>CONCLUSIONS</u>

1. Early treatment with L-carnitine during the first month of extra-uterine life attenuates the alterations in lung carnitine homeostasis previously demonstrated in our lamb model of CHD with increased PBF.

2. Early treatment with L-carnitine during the first month of extra-uterine life improves pulmonary mitochondrial function in our lamb model of CHD with increased PBF.

3. Early treatment with L-carnitine during the first month of extra-uterine life mitigates the oxidative stress associated with the chronic exposure of the lung vasculature to increased pulmonary blood that characterizes our lamb model of CHD.

4. Early treatment with L-carnitine during the first month of extra-uterine life ameliorates lung vasculature NO signaling in our lamb model of CHD with increased PBF.

5. The improvement in NO signaling observed with early treatment with L-carnitine in the lung vasculature ultimately results in improved endothelial function in our lamb model of CHD with increased PBF.

6. Early chronic L-carnitine therapy may prevent and/or attenuate the progressive decline in endothelial function that occurs during the development of PVD in children with CCS, and thus has potential important clinical implications that warrant further investigation.

REFERENCES

8   REFERENCES

1.   Sharma S, Aramburo A, Rafikov R, Sun X, Kumar S, Oishi PE, et al. L-carnitine preserves endothelial function in a lamb model of increased pulmonary blood flow. Pediatr Res. 2013;74(1):39-47.

2.   Hansmann G, Apitz C, Abdul-Khaliq H, Alastalo TP, Beerbaum P, Bonnet D, et al. Executive summary. Expert consensus statement on the diagnosis and treatment of paediatric pulmonary hypertension. The European Paediatric Pulmonary Vascular Disease Network, endorsed by ISHLT and DGPK. Heart. 2016;102 Suppl 2:ii86-100.

3.   Adatia I, Kothari SS, Feinstein JA. Pulmonary hypertension associated with congenital heart disease: pulmonary vascular disease: the global perspective. Chest. 2010;137(6 Suppl):52S-61S.

4.   van Loon RL, Roofthooft MT, Hillege HL, ten Harkel AD, van Osch-Gevers M, Delhaas T, et al. Pediatric pulmonary hypertension in the Netherlands: epidemiology and characterization during the period 1991 to 2005. Circulation. 2011;124(16):1755-64.

5.   Li L, Jick S, Breitenstein S, Hernandez G, Michel A, Vizcaya D. Pulmonary arterial hypertension in the USA: an epidemiological study in a large insured pediatric population. Pulm Circ. 2017;7(1):126-36.

6.   Beghetti M, Tissot C. Pulmonary arterial hypertension in congenital heart diseases. Semin Respir Crit Care Med. 2009;30(4):421-8.

7.   del Cerro Marin MJ, Sabate Rotes A, Rodriguez Ogando A, Mendoza Soto A, Quero Jimenez M, Gavilan Camacho JL, et al. Assessing pulmonary hypertensive vascular disease in childhood. Data from the Spanish registry. Am J Respir Crit Care Med. 2014;190(12):1421-9.

8.   Fasnacht MS, Tolsa JF, Beghetti M, Swiss Society for Pulmonary Arterial H. The Swiss registry for pulmonary arterial hypertension: the paediatric experience. Swiss Med Wkly. 2007;137(35-36):510-3.

9.   Hatano S ST, eds. Primary Pulmonary Hypertension. Report on a WHO Meeting. Geneva, World Health Organization. 1975.

10.   Kovacs G, Berghold A, Scheidl S, Olschewski H. Pulmonary arterial pressure during rest and exercise in healthy subjects: a systematic review. Eur Respir J. 2009;34(4):888-94.

11.   Simonneau G, Montani D, Celermajer DS, Denton CP, Gatzoulis MA, Krowka M, et al. Haemodynamic definitions and updated clinical classification of pulmonary hypertension. Eur Respir J. 2019;53(1).

12.   Rosenzweig EB, Abman SH, Adatia I, Beghetti M, Bonnet D, Haworth S, et al. Paediatric pulmonary arterial hypertension: updates on definition, classification, diagnostics and management. Eur Respir J. 2019;53(1).

13.   Cerro MJ, Abman S, Diaz G, Freudenthal AH, Freudenthal F, Harikrishnan S, et al. A consensus approach to the classification of pediatric pulmonary hypertensive vascular disease: Report from the PVRI Pediatric Taskforce, Panama 2011. Pulm Circ. 2011;1(2):286-98.

14.   Hoeper MM, Bogaard HJ, Condliffe R, Frantz R, Khanna D, Kurzyna M, et al. Definitions and diagnosis of pulmonary hypertension. J Am Coll Cardiol. 2013;62(25 Suppl):D42-50.

15.   Galie N, Humbert M, Vachiery JL, Gibbs S, Lang I, Torbicki A, et al. 2015 ESC/ERS Guidelines for the diagnosis and treatment of pulmonary hypertension: The Joint Task Force for the Diagnosis and Treatment of Pulmonary Hypertension of the European Society of Cardiology (ESC) and the

European Respiratory Society (ERS): Endorsed by: Association for European Paediatric and Congenital Cardiology (AEPC), International Society for Heart and Lung Transplantation (ISHLT). Eur Respir J. 2015;46(4):903-75.

16.   Abman SH, Hansmann G, Archer SL, Ivy DD, Adatia I, Chung WK, et al. Pediatric Pulmonary Hypertension: Guidelines From the American Heart Association and American Thoracic Society. Circulation. 2015;132(21):2037-99.

17.   Townsley MI. Structure and composition of pulmonary arteries, capillaries, and veins. Compr Physiol. 2012;2(1):675-709.

18.   Miller OI, Tang SF, Keech A, Pigott NB, Beller E, Celermajer DS. Inhaled nitric oxide and prevention of pulmonary hypertension after congenital heart surgery: a randomised double-blind study. Lancet. 2000;356(9240):1464-9.

19.   Suesaowalak M, Cleary JP, Chang AC. Advances in diagnosis and treatment of pulmonary arterial hypertension in neonates and children with congenital heart disease. World J Pediatr. 2010;6(1):13-31.

20.   Daliento L, Somerville J, Presbitero P, Menti L, Brach-Prever S, Rizzoli G, et al. Eisenmenger syndrome. Factors relating to deterioration and death. Eur Heart J. 1998;19(12):1845-55.

21.   Konstantinos Dimopoulos G-PD. Pulmonary hypertension in adult congenital heart disease. First ed. Massimo Chessa HB, Andreas Eicken, Alessandro Giamberti, editor. Cham, Switzerland: Springer; 2017. 368 p.

22.   Yamaki S, Endo M, Takahashi T. Different grades of medial hypertrophy and intimal changes in small pulmonary arteries among various types of congenital heart disease with pulmonary hypertension. Tohoku J Exp Med. 1997;182(1):83-91.

23.   Friedman WF, Heiferman MF. Clinical problems of postoperative pulmonary vascular disease. Am J Cardiol. 1982;50(3):631-6.

24.   Steinhorn RH, Fineman JR. The pathophysiology of pulmonary hypertension in congenital heart disease. Artif Organs. 1999;23(11):970-4.

25.   Yamaki S, Abe A, Tabayashi K, Endo M, Mohri H, Takahashi T. Inoperable pulmonary vascular disease in infants with congenital heart disease. Ann Thorac Surg. 1998;66(5):1565-70.

26.   Egito ES, Aiello VD, Bosisio IB, Lichtenfels AJ, Horta AL, Saldiva PH, et al. Vascular remodeling process in reversibility of pulmonary arterial hypertension secondary to congenital heart disease. Pathol Res Pract. 2003;199(8):521-32.

27.   Own BcsMgoBMWoMDwl--. 2014.

28.   Hislop A. Developmental biology of the pulmonary circulation. Paediatr Respir Rev. 2005;6(1):35-43.

29.   Rabinovitch M. Pathobiology of pulmonary hypertension. Annu Rev Pathol. 2007;2:369-99.

30.   Heath D EJ. The pathology of hypertensive pulmonary vascular disease. Circulation. 1958;18:533-47.

31.   Heath D, Helmholz HF, Jr., Burchell HB, Dushane JW, Kirklin JW, Edwards JE. Relation between structural change in the small pulmonary arteries and the immediate reversibility of pulmonary hypertension following closure of ventricular and atrial septal defects. Circulation. 1958;18(6):1167-74.

32.   Rabinovitch M, Haworth SG, Castaneda AR, Nadas AS, Reid LM. Lung biopsy in congenital heart disease: a morphometric approach to pulmonary vascular disease. Circulation. 1978;58(6):1107-22.

33.   Rabinovitch M, Keane JF, Norwood WI, Castaneda AR, Reid L. Vascular structure in lung tissue obtained at biopsy correlated with pulmonary

hemodynamic findings after repair of congenital heart defects. Circulation. 1984;69(4):655-67.

34.   Rabinovitch M, Bothwell T, Hayakawa BN, Williams WG, Trusler GA, Rowe RD, et al. Pulmonary artery endothelial abnormalities in patients with congenital heart defects and pulmonary hypertension. A correlation of light with scanning electron microscopy and transmission electron microscopy. Lab Invest. 1986;55(6):632-53.

35.   Celermajer DS, Cullen S, Deanfield JE. Impairment of endothelium-dependent pulmonary artery relaxation in children with congenital heart disease and abnormal pulmonary hemodynamics. Circulation. 1993;87(2):440-6.

36.   Hanley FL, Heinemann MK, Jonas RA, Mayer JE, Jr., Cook NR, Wessel DL, et al. Repair of truncus arteriosus in the neonate. J Thorac Cardiovasc Surg. 1993;105(6):1047-56.

37.   Hassoun PM, Mouthon L, Barbera JA, Eddahibi S, Flores SC, Grimminger F, et al. Inflammation, growth factors, and pulmonary vascular remodeling. J Am Coll Cardiol. 2009;54(1 Suppl):S10-9.

38.   Oishi P, Datar SA, Fineman JR. Pediatric pulmonary arterial hypertension: current and emerging therapeutic options. Expert Opin Pharmacother.12(12):1845-64.

39.   Furchgott RF, Zawadzki JV. The obligatory role of endothelial cells in the relaxation of arterial smooth muscle by acetylcholine. Nature. 1980;288(5789):373-6.

40.   Beghetti M, Black SM, Fineman JR. Endothelin-1 in congenital heart disease. Pediatr Res. 2005;57(5 Pt 2):16R-20R.

41.   Higenbottam TW, Laude EA. Endothelial dysfunction providing the basis for the treatment of pulmonary hypertension: Giles F. Filley lecture. Chest. 1998;114(1 Suppl):72S-9S.

42.   Humbert M, Morrell NW, Archer SL, Stenmark KR, MacLean MR, Lang IM, et al. Cellular and molecular pathobiology of pulmonary arterial hypertension. J Am Coll Cardiol. 2004;43(12 Suppl S):13S-24S.

43.   Klinger JR. The nitric oxide/cGMP signaling pathway in pulmonary hypertension. Clin Chest Med. 2007;28(1):143-67, ix.

44.   Moncada S, Higgs A. The L-arginine-nitric oxide pathway. N Engl J Med. 1993;329(27):2002-12.

45.   Oishi P, Datar SA, Fineman JR. Advances in the management of pediatric pulmonary hypertension. Respir Care.56(9):1314-39; discussion 39-40.

46.   Ignarro LJ, Byrns RE, Buga GM, Wood KS. Endothelium-derived relaxing factor from pulmonary artery and vein possesses pharmacologic and chemical properties identical to those of nitric oxide radical. Circ Res. 1987;61(6):866-79.

47.   McGoon MD, Kane GC. Pulmonary hypertension: diagnosis and management. Mayo Clin Proc. 2009;84(2):191-207.

48.   Giaid A, Saleh D. Reduced expression of endothelial nitric oxide synthase in the lungs of patients with pulmonary hypertension. N Engl J Med. 1995;333(4):214-21.

49.   Kiettisanpipop P, Lertsapcharorn P, Chotivittayatarakorn P, Poovorawan Y. Plasma levels of nitric oxide in children with congenital heart disease and increased pulmonary blood flow. J Med Assoc Thai. 2007;90(10):2053-7.

50.   Giaid A, Yanagisawa M, Langleben D, Michel RP, Levy R, Shennib H, et al. Expression of endothelin-1 in the lungs of patients with pulmonary hypertension. N Engl J Med. 1993;328(24):1732-9.

51.   Yoshibayashi M, Nishioka K, Nakao K, Saito Y, Matsumura M, Ueda T, et al. Plasma endothelin concentrations in patients with pulmonary hypertension associated with congenital heart defects. Evidence for increased production of endothelin in pulmonary circulation. Circulation. 1991;84(6):2280-5.

52.   Christman BW, McPherson CD, Newman JH, King GA, Bernard GR, Groves BM, et al. An imbalance between the excretion of thromboxane and prostacyclin metabolites in pulmonary hypertension. N Engl J Med. 1992;327(2):70-5.

53.   Adatia I, Barrow SE, Stratton PD, Miall-Allen VM, Ritter JM, Haworth SG. Thromboxane A2 and prostacyclin biosynthesis in children and adolescents with pulmonary vascular disease. Circulation. 1993;88(5 Pt 1):2117-22.

54.   Farber HW, Loscalzo J. Pulmonary arterial hypertension. N Engl J Med. 2004;351(16):1655-65.

55.   Xu J, Shi GP. Vascular wall extracellular matrix proteins and vascular diseases. Biochim Biophys Acta. 2014;1842(11):2106-19.

56.   Hassoun PM. Deciphering the "matrix" in pulmonary vascular remodelling. Eur Respir J. 2005;25(5):778-9.

57.   Rabinovitch M. Elastase and the pathobiology of unexplained pulmonary hypertension. Chest. 1998;114(3 Suppl):213S-24S.

58.   Rabinovitch M. EVE and beyond, retro and prospective insights. Am J Physiol. 1999;277(1):L5-12.

59.   Jones PL, Cowan KN, Rabinovitch M. Tenascin-C, proliferation and subendothelial fibronectin in progressive pulmonary vascular disease. Am J Pathol. 1997;150(4):1349-60.

60.   Beghetti M. Pulmonary Arterial Hypertension Related to Congenital Heart Disease. London, United Kingdom: Elsevier Health Sciences; 2006 31 Oct 2006.

61.   Touyz RM. Reactive oxygen species as mediators of calcium signaling by angiotensin II: implications in vascular physiology and pathophysiology. Antioxid Redox Signal. 2005;7(9-10):1302-14.

62.   Touyz RM, Schiffrin EL. Reactive oxygen species and hypertension: a complex association. Antioxid Redox Signal. 2008;10(6):1041-4.

63.   Griendling KK, FitzGerald GA. Oxidative stress and cardiovascular injury: Part I: basic mechanisms and in vivo monitoring of ROS. Circulation. 2003;108(16):1912-6.

64.   Aggarwal S, Gross CM, Sharma S, Fineman JR, Black SM. Reactive oxygen species in pulmonary vascular remodeling. Compr Physiol. 2013;3(3):1011-34.

65.   Fresquet F, Pourageaud F, Leblais V, Brandes RP, Savineau JP, Marthan R, et al. Role of reactive oxygen species and gp91phox in endothelial dysfunction of pulmonary arteries induced by chronic hypoxia. Br J Pharmacol. 2006;148(5):714-23.

66.   Sharma S, Kumar S, Wiseman DA, Kallarackal S, Ponnala S, Elgaish M, et al. Perinatal changes in superoxide generation in the ovine lung: Alterations associated with increased pulmonary blood flow. Vascul Pharmacol. 2010;53(1-2):38-52.

67.   Gabrielli LA, Castro PF, Godoy I, Mellado R, Bourge RC, Alcaino H, et al. Systemic oxidative stress and endothelial dysfunction is associated with an attenuated acute vascular response to inhaled prostanoid in pulmonary artery hypertension patients. J Card Fail. 2011;17(12):1012-7.

68.   Hartney T, Birari R, Venkataraman S, Villegas L, Martinez M, Black SM, et al. Xanthine oxidase-derived ROS upregulate Egr-1 via ERK1/2 in PA smooth

muscle cells; model to test impact of extracellular ROS in chronic hypoxia. PLoS One. 2011;6(11):e27531.

69.   Piechota-Polanczyk A, Jozkowicz A, Nowak W, Eilenberg W, Neumayer C, Malinski T, et al. The Abdominal Aortic Aneurysm and Intraluminal Thrombus: Current Concepts of Development and Treatment. Front Cardiovasc Med. 2015;2:19.

70.   Fratz S, Fineman JR, Gorlach A, Sharma S, Oishi P, Schreiber C, et al. Early determinants of pulmonary vascular remodeling in animal models of complex congenital heart disease. Circulation.123(8):916-23.

71.   Huige Li UF. Uncoupling of eNOS in Cardiovascular Disease. In: Inc. E, editor. Nitric Oxide2017. p. 117-24.

72.   Landmesser U, Dikalov S, Price SR, McCann L, Fukai T, Holland SM, et al. Oxidation of tetrahydrobiopterin leads to uncoupling of endothelial cell nitric oxide synthase in hypertension. J Clin Invest. 2003;111(8):1201-9.

73.   Nandi M, Miller A, Stidwill R, Jacques TS, Lam AA, Haworth S, et al. Pulmonary hypertension in a GTP-cyclohydrolase 1-deficient mouse. Circulation. 2005;111(16):2086-90.

74.   Wang D, Li H, Weir EK, Xu Y, Xu D, Chen Y. Dimethylarginine dimethylaminohydrolase 1 deficiency aggravates monocrotaline-induced pulmonary oxidative stress, pulmonary arterial hypertension and right heart failure in rats. Int J Cardiol. 2019;295:14-20.

75.   Pullamsetti S, Kiss L, Ghofrani HA, Voswinckel R, Haredza P, Klepetko W, et al. Increased levels and reduced catabolism of asymmetric and symmetric dimethylarginines in pulmonary hypertension. FASEB J. 2005;19(9):1175-7.

76.   Shao Z, Wang Z, Shrestha K, Thakur A, Borowski AG, Sweet W, et al. Pulmonary hypertension associated with advanced systolic heart failure: dysregulated arginine metabolism and importance of compensatory dimethylarginine dimethylaminohydrolase-1. J Am Coll Cardiol. 2012;59(13):1150-8.

77.   Garcia-Cardena G, Fan R, Shah V, Sorrentino R, Cirino G, Papapetropoulos A, et al. Dynamic activation of endothelial nitric oxide synthase by Hsp90. Nature. 1998;392(6678):821-4.

78.   Pritchard KA, Jr., Ackerman AW, Gross ER, Stepp DW, Shi Y, Fontana JT, et al. Heat shock protein 90 mediates the balance of nitric oxide and superoxide anion from endothelial nitric-oxide synthase. J Biol Chem. 2001;276(21):17621-4.

79.   Chen CA, Wang TY, Varadharaj S, Reyes LA, Hemann C, Talukder MA, et al. S-glutathionylation uncouples eNOS and regulates its cellular and vascular function. Nature. 2010;468(7327):1115-8.

80.   Sharma S, Black SM. Carnitine Homeostasis, Mitochondrial Function, and Cardiovascular Disease. Drug Discov Today Dis Mech. 2009;6(1-4):e31-e9.

81.   Duchen MR. Mitochondria in health and disease: perspectives on a new mitochondrial biology. Mol Aspects Med. 2004;25(4):365-451.

82.   Puddu P, Puddu GM, Cravero E, De Pascalis S, Muscari A. The putative role of mitochondrial dysfunction in hypertension. Clin Exp Hypertens. 2007;29(7):427-34.

83.   Dikalov S. Cross talk between mitochondria and NADPH oxidases. Free Radic Biol Med. 2011;51(7):1289-301.

84.   Genova ML, Pich MM, Bernacchia A, Bianchi C, Biondi A, Bovina C, et al. The mitochondrial production of reactive oxygen species in relation to aging and pathology. Ann N Y Acad Sci. 2004;1011:86-100.

85.   Puddu P, Puddu GM, Cravero E, De Pascalis S, Muscari A. The emerging role of cardiovascular risk factor-induced mitochondrial dysfunction in atherogenesis. J Biomed Sci. 2009;16:112.
86.   Maiese K, Chong ZZ, Shang YC. Mechanistic insights into diabetes mellitus and oxidative stress. Curr Med Chem. 2007;14(16):1729-38.
87.   Hasselwander O, Young IS. Oxidative stress in chronic renal failure. Free Radic Res. 1998;29(1):1-11.
88.   Sims NR, Muyderman H. Mitochondria, oxidative metabolism and cell death in stroke. Biochim Biophys Acta.1802(1):80-91.
89.   Mancuso C, Scapagini G, Curro D, Giuffrida Stella AM, De Marco C, Butterfield DA, et al. Mitochondrial dysfunction, free radical generation and cellular stress response in neurodegenerative disorders. Front Biosci. 2007;12:1107-23.
90.   Waypa GB, Marks JD, Guzy RD, Mungai PT, Schriewer JM, Dokic D, et al. Superoxide generated at mitochondrial complex III triggers acute responses to hypoxia in the pulmonary circulation. Am J Respir Crit Care Med. 2013;187(4):424-32.
91.   Archer SL, Gomberg-Maitland M, Maitland ML, Rich S, Garcia JG, Weir EK. Mitochondrial metabolism, redox signaling, and fusion: a mitochondria-ROS-HIF-1alpha-Kv1.5 O2-sensing pathway at the intersection of pulmonary hypertension and cancer. Am J Physiol Heart Circ Physiol. 2008;294(2):H570-8.
92.   Firth AL, Yuill KH, Smirnov SV. Mitochondria-dependent regulation of Kv currents in rat pulmonary artery smooth muscle cells. Am J Physiol Lung Cell Mol Physiol. 2008;295(1):L61-70.
93.   Hu HL, Zhang ZX, Chen CS, Cai C, Zhao JP, Wang X. Effects of mitochondrial potassium channel and membrane potential on hypoxic human pulmonary artery smooth muscle cells. Am J Respir Cell Mol Biol. 2010;42(6):661-6.
94.   Bonnet S, Rochefort G, Sutendra G, Archer SL, Haromy A, Webster L, et al. The nuclear factor of activated T cells in pulmonary arterial hypertension can be therapeutically targeted. Proc Natl Acad Sci U S A. 2007;104(27):11418-23.
95.   McMurtry MS, Bonnet S, Wu X, Dyck JR, Haromy A, Hashimoto K, et al. Dichloroacetate prevents and reverses pulmonary hypertension by inducing pulmonary artery smooth muscle cell apoptosis. Circ Res. 2004;95(8):830-40.
96.   Sud N, Wells SM, Sharma S, Wiseman DA, Wilham J, Black SM. Asymmetric dimethylarginine inhibits HSP90 activity in pulmonary arterial endothelial cells: role of mitochondrial dysfunction. Am J Physiol Cell Physiol. 2008;294(6):C1407-18.
97.   Ryan JJ, Archer SL. Emerging concepts in the molecular basis of pulmonary arterial hypertension: part I: metabolic plasticity and mitochondrial dynamics in the pulmonary circulation and right ventricle in pulmonary arterial hypertension. Circulation. 2015;131(19):1691-702.
98.   Sproule DM, Dyme J, Coku J, de Vinck D, Rosenzweig E, Chung WK, et al. Pulmonary artery hypertension in a child with MELAS due to a point mutation of the mitochondrial tRNA((Leu)) gene (m.3243A > G). J Inherit Metab Dis. 2008.
99.   Marshall JD, Bazan I, Zhang Y, Fares WH, Lee PJ. Mitochondrial dysfunction and pulmonary hypertension: cause, effect, or both. Am J Physiol Lung Cell Mol Physiol. 2018;314(5):L782-L96.
100.   Calvani M, Benatti P, Mancinelli A, D'Iddio S, Giordano V, Koverech A, et al. Carnitine replacement in end-stage renal disease and hemodialysis. Ann N Y Acad Sci. 2004;1033:52-66.

101.   Steiber A, Kerner J, Hoppel CL. Carnitine: a nutritional, biosynthetic, and functional perspective. Mol Aspects Med. 2004;25(5-6):455-73.
102.   Szewczyk A, Wojtczak L. Mitochondria as a pharmacological target. Pharmacol Rev. 2002;54(1):101-27.
103.   Bueno R, Alvarez de Sotomayor M, Perez-Guerrero C, Gomez-Amores L, Vazquez CM, Herrera MD. L-carnitine and propionyl-L-carnitine improve endothelial dysfunction in spontaneously hypertensive rats: different participation of NO and COX-products. Life Sci. 2005;77(17):2082-97.
104.   Ferrari R, Merli E, Cicchitelli G, Mele D, Fucili A, Ceconi C. Therapeutic effects of L-carnitine and propionyl-L-carnitine on cardiovascular diseases: a review. Ann N Y Acad Sci. 2004;1033:79-91.
105.   Mingorance C, Rodriguez-Rodriguez R, Justo ML, Alvarez de Sotomayor M, Herrera MD. Critical update for the clinical use of L-carnitine analogs in cardiometabolic disorders. Vasc Health Risk Manag.7:169-76.
106.   Ames BN, Liu J. Delaying the mitochondrial decay of aging with acetylcarnitine. Ann N Y Acad Sci. 2004;1033:108-16.
107.   Michel RP, Hakim TS, Hanson RE, Dobell AR, Keith F, Drinkwater D. Distribution of lung vascular resistance after chronic systemic-to-pulmonary shunts. Am J Physiol. 1985;249(6 Pt 2):H1106-13.
108.   Damman JF Jr. BJ, Muller WH Jr. Pulmonary vascular changes induced by experimentally produced pulmonary arterial hypertension. Surg Gynecol Obstet.105:16-26.
109.   Fasules JW, Tryka F, Chipman CW, Van Devanter SH. Pulmonary hypertension and arterial changes in calves with a systemic-to-left pulmonary artery connection. J Appl Physiol (1985). 1994;77(2):867-75.
110.   Friedli B, Kent G, Kidd BS. The effect of increased pulmonary blood flow on the pulmonary vascular bed in pigs. Pediatr Res. 1975;9(6):547-53.
111.   Rendas A, Lennox S, Reid L. Aorta-pulmonary shunts in growing pigs. Functional and structural assessment of the changes in the pulmonary circulation. J Thorac Cardiovasc Surg. 1979;77(1):109-18.
112.   Reddy VM, Meyrick B, Wong J, Khoor A, Liddicoat JR, Hanley FL, et al. In utero placement of aortopulmonary shunts. A model of postnatal pulmonary hypertension with increased pulmonary blood flow in lambs. Circulation. 1995;92(3):606-13.
113.   Reddy VM, Wong J, Liddicoat JR, Johengen M, Chang R, Fineman JR. Altered endothelium-dependent responses in lambs with pulmonary hypertension and increased pulmonary blood flow. Am J Physiol. 1996;271(2 Pt 2):H562-70.
114.   Oishi PE, Wiseman DA, Sharma S, Kumar S, Hou Y, Datar SA, et al. Progressive dysfunction of nitric oxide synthase in a lamb model of chronically increased pulmonary blood flow: a role for oxidative stress. Am J Physiol Lung Cell Mol Physiol. 2008;295(5):L756-66.
115.   Wong J, Reddy VM, Hendricks-Munoz K, Liddicoat JR, Gerrets R, Fineman JR. Endothelin-1 vasoactive responses in lambs with pulmonary hypertension and increased pulmonary blood flow. Am J Physiol. 1995;269(6 Pt 2):H1965-72.
116.   Black SM, Bekker JM, Johengen MJ, Parry AJ, Soifer SJ, Fineman JR. Altered regulation of the ET-1 cascade in lambs with increased pulmonary blood flow and pulmonary hypertension. Pediatr Res. 2000;47(1):97-106.
117.   Black SM, Mata-Greenwood E, Dettman RW, Ovadia B, Fitzgerald RK, Reinhartz O, et al. Emergence of smooth muscle cell endothelin B-mediated

vasoconstriction in lambs with experimental congenital heart disease and increased pulmonary blood flow. Circulation. 2003;108(13):1646-54.

118.   Ovadia B, Reinhartz O, Fitzgerald R, Bekker JM, Johengen MJ, Azakie A, et al. Alterations in ET-1, not nitric oxide, in 1-week-old lambs with increased pulmonary blood flow. Am J Physiol Heart Circ Physiol. 2003;284(2):H480-90.

119.   Black SM, Fineman JR, Steinhorn RH, Bristow J, Soifer SJ. Increased endothelial NOS in lambs with increased pulmonary blood flow and pulmonary hypertension. Am J Physiol. 1998;275(5 Pt 2):H1643-51.

120.   Steinhorn RH, Russell JA, Lakshminrusimha S, Gugino SF, Black SM, Fineman JR. Altered endothelium-dependent relaxations in lambs with high pulmonary blood flow and pulmonary hypertension. Am J Physiol Heart Circ Physiol. 2001;280(1):H311-7.

121.   Grobe AC, Wells SM, Benavidez E, Oishi P, Azakie A, Fineman JR, et al. Increased oxidative stress in lambs with increased pulmonary blood flow and pulmonary hypertension: role of NADPH oxidase and endothelial NO synthase. Am J Physiol Lung Cell Mol Physiol. 2006;290(6):L1069-77.

122.   Lakshminrusimha S, Wiseman D, Black SM, Russell JA, Gugino SF, Oishi P, et al. The role of nitric oxide synthase-derived reactive oxygen species in the altered relaxation of pulmonary arteries from lambs with increased pulmonary blood flow. Am J Physiol Heart Circ Physiol. 2007;293(3):H1491-7.

123.   Sud N, Sharma S, Wiseman DA, Harmon C, Kumar S, Venema RC, et al. Nitric oxide and superoxide generation from endothelial NOS: modulation by HSP90. Am J Physiol Lung Cell Mol Physiol. 2007;293(6):L1444-53.

124.   Sharma S, Kumar S, Sud N, Wiseman DA, Tian J, Rehmani I, et al. Alterations in lung arginine metabolism in lambs with pulmonary hypertension associated with increased pulmonary blood flow. Vascul Pharmacol. 2009;51(5-6):359-64.

125.   Sun X, Kellner M, Desai AA, Wang T, Lu Q, Kangath A, et al. Asymmetric Dimethylarginine Stimulates Akt1 Phosphorylation via Heat Shock Protein 70-Facilitated Carboxyl-Terminal Modulator Protein Degradation in Pulmonary Arterial Endothelial Cells. Am J Respir Cell Mol Biol. 2016;55(2):275-87.

126.   Sharma S, Grobe AC, Wiseman DA, Kumar S, Englaish M, Najwer I, et al. Lung antioxidant enzymes are regulated by development and increased pulmonary blood flow. Am J Physiol Lung Cell Mol Physiol. 2007;293(4):L960-71.

127.   Sharma S, Sud N, Wiseman DA, Carter AL, Kumar S, Hou Y, et al. Altered carnitine homeostasis is associated with decreased mitochondrial function and altered nitric oxide signaling in lambs with pulmonary hypertension. Am J Physiol Lung Cell Mol Physiol. 2008;294(1):L46-56.

128.   Hinerfeld D, Traini MD, Weinberger RP, Cochran B, Doctrow SR, Harry J, et al. Endogenous mitochondrial oxidative stress: neurodegeneration, proteomic analysis, specific respiratory chain defects, and efficacious antioxidant therapy in superoxide dismutase 2 null mice. J Neurochem. 2004;88(3):657-67.

129.   Sreedhar A, Zhao Y. Uncoupling protein 2 and metabolic diseases. Mitochondrion. 2017;34:135-40.

130.   National Research Council (U.S.). Committee for the Update of the Guide for the Care and Use of Laboratory Animals., Institute for Laboratory Animal Research (U.S.), National Academies Press (U.S.). Guide for the care and use of laboratory animals. Washington, D.C.: National Academies Press,; 2011. Available from: http://www.ncbi.nlm.nih.gov/books/NBK54050.

131.   Longo A, Bruno G, Curti S, Mancinelli A, Miotto G. Determination of L-carnitine, acetyl-L-carnitine and propionyl-L-carnitine in human plasma by high-performance liquid chromatography after pre-column derivatization with 1-aminoanthracene. J Chromatogr B Biomed Appl. 1996;686(2):129-39.

132.   Minkler PE, Brass EP, Hiatt WR, Ingalls ST, Hoppel CL. Quantification of carnitine, acetylcarnitine, and total carnitine in tissues by high-performance liquid chromatography: the effect of exercise on carnitine homeostasis in man. Anal Biochem. 1995;231(2):315-22.

133.   Liu J, Killilea DW, Ames BN. Age-associated mitochondrial oxidative decay: improvement of carnitine acetyltransferase substrate-binding affinity and activity in brain by feeding old rats acetyl-L- carnitine and/or R-alpha -lipoic acid. Proc Natl Acad Sci U S A. 2002;99(4):1876-81.

134.   Marbach EP, Weil MH. Rapid enzymatic measurement of blood lactate and pyruvate. Use and significance of metaphosphoric acid as a common precipitant. Clin Chem. 1967;13(4):314-25.

135.   Bush PA, Gonzalez NE, Ignarro LJ. Biosynthesis of nitric oxide and citrulline from L-arginine by constitutive nitric oxide synthase present in rabbit corpus cavernosum. Biochem Biophys Res Commun. 1992;186(1):308-14.

136.   Garvey EP, Oplinger JA, Tanoury GJ, Sherman PA, Fowler M, Marshall S, et al. Potent and selective inhibition of human nitric oxide synthases. Inhibition by non-amino acid isothioureas. J Biol Chem. 1994;269(43):26669-76.

137.   Wiseman DA, Wells SM, Hubbard M, Welker JE, Black SM. Alterations in zinc homeostasis underlie endothelial cell death induced by oxidative stress from acute exposure to hydrogen peroxide. Am J Physiol Lung Cell Mol Physiol. 2007;292(1):L165-77.

138.   Wiseman DA, Wells SM, Wilham J, Hubbard M, Welker JE, Black SM. Endothelial response to stress from exogenous Zn2+ resembles that of NO-mediated nitrosative stress, and is protected by MT-1 overexpression. Am J Physiol Cell Physiol. 2006;291(3):C555-68.

139.   Veereshwarayya V, Kumar P, Rosen KM, Mestril R, Querfurth HW. Differential effects of mitochondrial heat shock protein 60 and related molecular chaperones to prevent intracellular beta-amyloid-induced inhibition of complex IV and limit apoptosis. J Biol Chem. 2006;281(40):29468-78.

140.   Lee YJ, Corry PM. Metabolic oxidative stress-induced HSP70 gene expression is mediated through SAPK pathway. Role of Bcl-2 and c-Jun NH2-terminal kinase. J Biol Chem. 1998;273(45):29857-63.

141.   Pande SV, Blanchaer MC. Reversible inhibition of mitochondrial adenosine diphosphate phosphorylation by long chain acyl coenzyme A esters. J Biol Chem. 1971;246(2):402-11.

142.   Ramsay RR, Zammit VA. Carnitine acyltransferases and their influence on CoA pools in health and disease. Mol Aspects Med. 2004;25(5-6):475-93.

143.   Ramsay RR, Gandour RD, van der Leij FR. Molecular enzymology of carnitine transfer and transport. Biochim Biophys Acta. 2001;1546(1):21-43.

144.   Wainwright MS, Kohli R, Whitington PF, Chace DH. Carnitine treatment inhibits increases in cerebral carnitine esters and glutamate detected by mass spectrometry after hypoxia-ischemia in newborn rats. Stroke. 2006;37(2):524-30.

145.   Rubio JC, de Bustos F, Molina JA, Jimenez-Jimenez FJ, Benito-Leon J, Martin MA, et al. Cerebrospinal fluid carnitine levels in patients with Alzheimer's disease. J Neurol Sci. 1998;155(2):192-5.

146.   Mingrone G. Carnitine in type 2 diabetes. Ann N Y Acad Sci. 2004;1033:99-107.

147.   Binienda ZK. Neuroprotective effects of L-carnitine in induced mitochondrial dysfunction. Ann N Y Acad Sci. 2003;993:289-95; discussion 345-9.

148.   Calabrese V, Giuffrida Stella AM, Calvani M, Butterfield DA. Acetylcarnitine and cellular stress response: roles in nutritional redox homeostasis and regulation of longevity genes. J Nutr Biochem. 2006;17(2):73-88.

149.   Reuter SE, Evans AM. Carnitine and acylcarnitines: pharmacokinetic, pharmacological and clinical aspects. Clin Pharmacokinet. 2012;51(9):553-72.

150.   Pekala J, Patkowska-Sokola B, Bodkowski R, Jamroz D, Nowakowski P, Lochynski S, et al. L-carnitine--metabolic functions and meaning in humans life. Curr Drug Metab. 2011;12(7):667-78.

151.   Sharma S, Sun X, Agarwal S, Rafikov R, Dasarathy S, Kumar S, et al. Role of carnitine acetyl transferase in regulation of nitric oxide signaling in pulmonary arterial endothelial cells. Int J Mol Sci. 2012;14(1):255-72.

152.   Konduri GG, Mattei J. Role of oxidative phosphorylation and ATP release in mediating birth-related pulmonary vasodilation in fetal lambs. Am J Physiol Heart Circ Physiol. 2002;283(4):H1600-8.

153.   Gratton JP, Fontana J, O'Connor DS, Garcia-Cardena G, McCabe TJ, Sessa WC. Reconstitution of an endothelial nitric-oxide synthase (eNOS), hsp90, and caveolin-1 complex in vitro. Evidence that hsp90 facilitates calmodulin stimulated displacement of eNOS from caveolin-1. J Biol Chem. 2000;275(29):22268-72.

154.   Sun X, Fratz S, Sharma S, Hou Y, Rafikov R, Kumar S, et al. C-terminus of heat shock protein 70-interacting protein-dependent GTP cyclohydrolase I degradation in lambs with increased pulmonary blood flow. Am J Respir Cell Mol Biol. 2011;45(1):163-71.

155.   Sharma S, Sun X, Kumar S, Rafikov R, Aramburo A, Kalkan G, et al. Preserving mitochondrial function prevents the proteasomal degradation of GTP cyclohydrolase I. Free Radic Biol Med.53(2):216-29.

156.   Calo LA, Pagnin E, Davis PA, Semplicini A, Nicolai R, Calvani M, et al. Antioxidant effect of L-carnitine and its short chain esters: relevance for the protection from oxidative stress related cardiovascular damage. Int J Cardiol. 2006;107(1):54-60.

157.   Herrera MD, Bueno R, De Sotomayor MA, Perez-Guerrero C, Vazquez CM, Marhuenda E. Endothelium-dependent vasorelaxation induced by L-carnitine in isolated aorta from normotensive and hypertensive rats. J Pharm Pharmacol. 2002;54(10):1423-7.

158.   de Sotomayor MA, Mingorance C, Rodriguez-Rodriguez R, Marhuenda E, Herrera MD. l-carnitine and its propionate: improvement of endothelial function in SHR through superoxide dismutase-dependent mechanisms. Free Radic Res. 2007;41(8):884-91.

159.   Gomez-Amores L, Mate A, Miguel-Carrasco JL, Jimenez L, Jos A, Camean AM, et al. L-carnitine attenuates oxidative stress in hypertensive rats. J Nutr Biochem. 2007;18(8):533-40.

160.   Gulcin I. Antioxidant and antiradical activities of L-carnitine. Life Sci. 2006;78(8):803-11.

161.   Arduini A. Carnitine and its acyl esters as secondary antioxidants? Am Heart J. 1992;123(6):1726-7.

162.   Ferrari R, Ceconi C, Cargnoni A, Pasini E, Boffa GM, Curello S, et al. The effect of propionyl-L-carnitine on the ischemic and reperfused intact

myocardium and on their derived mitochondria. Cardiovasc Drugs Ther. 1991;5 Suppl 1:57-65.

163.   Reznick AZ, Kagan VE, Ramsey R, Tsuchiya M, Khwaja S, Serbinova EA, et al. Antiradical effects in L-propionyl carnitine protection of the heart against ischemia-reperfusion injury: the possible role of iron chelation. Arch Biochem Biophys. 1992;296(2):394-401.

164.   Kopple JD, Ding H, Letoha A, Ivanyi B, Qing DP, Dux L, et al. L-carnitine ameliorates gentamicin-induced renal injury in rats. Nephrol Dial Transplant. 2002;17(12):2122-31.

165.   Sener G, Paskaloglu K, Satiroglu H, Alican I, Kacmaz A, Sakarcan A. L-carnitine ameliorates oxidative damage due to chronic renal failure in rats. J Cardiovasc Pharmacol. 2004;43(5):698-705.

166.   Vescovo G, Ravara B, Gobbo V, Sandri M, Angelini A, Della Barbera M, et al. L-Carnitine: a potential treatment for blocking apoptosis and preventing skeletal muscle myopathy in heart failure. Am J Physiol Cell Physiol. 2002;283(3):C802-10.

167.   Black SM, Fineman JR. Oxidative and nitrosative stress in pediatric pulmonary hypertension: roles of endothelin-1 and nitric oxide. Vascul Pharmacol. 2006;45(5):308-16.

168.   Ward JP, McMurtry IF. Mechanisms of hypoxic pulmonary vasoconstriction and their roles in pulmonary hypertension: new findings for an old problem. Curr Opin Pharmacol. 2009;9(3):287-96.

169.   Iqbal M, Cawthon D, Wideman RF, Jr., Bottje WG. Lung mitochondrial dysfunction in pulmonary hypertension syndrome. I. Site-specific defects in the electron transport chain. Poult Sci. 2001;80(4):485-95.

170.   Bottje W, Enkvetchakul B, Moore R, McNew R. Effect of alpha-tocopherol on antioxidants, lipid peroxidation, and the incidence of pulmonary hypertension syndrome (ascites) in broilers. Poult Sci. 1995;74(8):1356-69.

171.   Paulin R, Michelakis ED. The metabolic theory of pulmonary arterial hypertension. Circ Res. 2014;115(1):148-64.

172.   Suliman HB, Nozik-Grayck E. Mitochondrial Dysfunction: Metabolic Drivers of Pulmonary Hypertension. Antioxid Redox Signal. 2019;31(12):843-57.

173.   Culley MK, Chan SY. Mitochondrial metabolism in pulmonary hypertension: beyond mountains there are mountains. J Clin Invest. 2018;128(9):3704-15.

174.   Vander Heiden MG, Cantley LC, Thompson CB. Understanding the Warburg effect: the metabolic requirements of cell proliferation. Science. 2009;324(5930):1029-33.

175.   Freund-Michel V, Khoyrattee N, Savineau JP, Muller B, Guibert C. Mitochondria: roles in pulmonary hypertension. Int J Biochem Cell Biol. 2014;55:93-7.

176.   Singh N, Singh H, Jagavelu K, Wahajuddin M, Hanif K. Fatty acid synthase modulates proliferation, metabolic functions and angiogenesis in hypoxic pulmonary artery endothelial cells. Eur J Pharmacol. 2017;815:462-9.

177.   Sutendra G, Bonnet S, Rochefort G, Haromy A, Folmes KD, Lopaschuk GD, et al. Fatty acid oxidation and malonyl-CoA decarboxylase in the vascular remodeling of pulmonary hypertension. Sci Transl Med. 2010;2(44):44ra58.

178.   Xu W, Koeck T, Lara AR, Neumann D, DiFilippo FP, Koo M, et al. Alterations of cellular bioenergetics in pulmonary artery endothelial cells. Proc Natl Acad Sci U S A. 2007;104(4):1342-7.

179.   Archer SL, Marsboom G, Kim GH, Zhang HJ, Toth PT, Svensson EC, et al. Epigenetic attenuation of mitochondrial superoxide dismutase 2 in pulmonary arterial hypertension: a basis for excessive cell proliferation and a new therapeutic target. Circulation. 2010;121(24):2661-71.

180.   Ryan JJ, Marsboom G, Fang YH, Toth PT, Morrow E, Luo N, et al. PGC1alpha-mediated mitofusin-2 deficiency in female rats and humans with pulmonary arterial hypertension. Am J Respir Crit Care Med. 2013;187(8):865-78.

181.   Huetsch JC, Suresh K, Bernier M, Shimoda LA. Update on novel targets and potential treatment avenues in pulmonary hypertension. Am J Physiol Lung Cell Mol Physiol. 2016;311(5):L811-L31.

182.   Tan X, Hu SH, Wang XL. The effect of dietary l-carnitine supplementation on pulmonary hypertension syndrome mortality in broilers exposed to low temperatures. J Anim Physiol Anim Nutr (Berl). 2008;92(2):203-10.

183.   El-Beshlawy A, Abd El Raouf E, Mostafa F, Talaat M, Isma'eel H, Aoun E, et al. Diastolic dysfunction and pulmonary hypertension in sickle cell anemia: is there a role for L-carnitine treatment? Acta Haematol. 2006;115(1-2):91-6.

184.   El-Beshlawy A, Youssry I, El-Saidi S, El Accaoui R, Mansi Y, Makhlouf A, et al. Pulmonary hypertension in beta-thalassemia major and the role of L-carnitine therapy. Pediatr Hematol Oncol. 2008;25(8):734-43.

185.   Brittain EL, Talati M, Fessel JP, Zhu H, Penner N, Calcutt MW, et al. Fatty Acid Metabolic Defects and Right Ventricular Lipotoxicity in Human Pulmonary Arterial Hypertension. Circulation. 2016;133(20):1936-44.

186.   Black SM, Field-Ridley A, Sharma S, Kumar S, Keller RL, Kameny R, et al. Altered Carnitine Homeostasis in Children With Increased Pulmonary Blood Flow Due to Ventricular Septal Defects. Pediatr Crit Care Med. 2017;18(10):931-4.

187.   Luo N, Craig D, Ilkayeva O, Muehlbauer M, Kraus WE, Newgard CB, et al. Plasma acylcarnitines are associated with pulmonary hypertension. Pulm Circ. 2017;7(1):211-8.

188.   Evans AM, Fornasini G. Pharmacokinetics of L-carnitine. Clin Pharmacokinet. 2003;42(11):941-67.

189.   Tian J, Smith A, Nechtman J, Podolsky R, Aggarwal S, Snead C, et al. Effect of PPARgamma inhibition on pulmonary endothelial cell gene expression: gene profiling in pulmonary hypertension. Physiol Genomics. 2009;40(1):48-60.

190.   Sharma S, Sun X, Rafikov R, Kumar S, Hou Y, Oishi PE, et al. PPAR-gamma Regulates Carnitine Homeostasis and Mitochondrial Function in a Lamb Model of Increased Pulmonary Blood Flow. PLoS One.7(9):e41555.

191.   Mascaro C, Acosta E, Ortiz JA, Marrero PF, Hegardt FG, Haro D. Control of human muscle-type carnitine palmitoyltransferase I gene transcription by peroxisome proliferator-activated receptor. J Biol Chem. 1998;273(15):8560-3.

APPENDIX

9 APPENDICES

9.1 APPENDIX 1: UCSF INSTITUTIONAL ANIMAL CARE AND USE PROGRAM (IACUC) PROTOCOL APPROVAL*

IACUC Application Details AN077410-03A

	Summary
Principal Investigator:	Fineman, Jeffrey R.
Title:	Physiologic Effects of Chronic Systemic to Pulmonary Shunting in Newborn Lambs
Purpose:	Research
Objectives:	Pulmonary hypertension (high blood pressure in the lungs) is a very serious disorder in some children with congenital heart defects. It occurs in those defects that have communications between the heart structures going to the body and the heart structures going to the lungs. This results in increased blood flow to the lungs. If uncorrected, progressive abnormalities of the vessels in the lungs result in obliteration of these vessels and death. After surgical correction, early vascular changes are reversible, but more severe changes are not. Even those children with reversible vascular changes suffer significant morbidity and mortality immediately after surgery. Recent evidence suggests that vasoactive factors produced by the vascular endothelium (the cells that line the blood vessels) are important mediators of pulmonary vascular tone. Our aim is to sequentially assess the physiologic and biochemical alterations in these factors, such as Nitric Oxide (NO), Endothelin-1 (ET-1), Peroxisome proliferator-activated receptors (PPARs), and VEGF (vascular endothelial growth factor) in the lungs of normal lambs (controls) and lambs with increased pulmonary blood flow (shunted). A secondary goal is to determine the mechanisms for the physiologic and biochemical alterations in endothelial function by investigating the changes in gene expression and morphologic changes of these cascades, as well as their interactions, in the normal and shunt lambs. To this end, agonists and antagonists of these factors will be delivered. This information may lead to improved treatments and prevention strategies for post-surgical pulmonary hypertension, and decrease peri-operative morbidity and mortality of children with congenital heart disease. Lastly, increased lung water (pulmonary edema) is a significant clinical problem in children with congenital heart disease and increased pulmonary blood flow. This results in tachypnea (fast breathing), pulmonary infections, and inability to feed. There have been significant advances in our understanding of normal lung fluid clearance mechanisms and how these are perturbed under conditions

* Only the principal investigator and the author's names are included. Personally identifiable information from all other members of the team has been omitted.

Objectives:	of acute lung injury. However, nothing is known about potential changes in lung fluid clearance mechanisms under chronic conditions of increased pulmonary blood flow and pressure. In select studies, we will characterize these changes, which may lead to the investigation of novel prevention and treatment strategies that minimize lung water.
Status:	Approved With Conditions
Expiration Date:	10/24/2009

Application History			
Project Number	**Approval Type**	**Approval Date**	**Expiration Date**
AN077410-03A	Modification	09/24/2008	10/24/2009
AN077410-03	Annual Review	09/16/2008	10/24/2009
AN077410-02A	Modification	08/12/2008	10/24/2008
AN077410-02	Annual Review/Modify	09/27/2007	10/24/2008
AN077410-01H	Modification	08/10/2007	10/24/2007
AN077410-01G	Modification	07/24/2007	10/24/2007
AN077410-01F	Modification	03/23/2007	10/24/2007
AN077410-01E	Modification	03/13/2007	10/24/2007
AN077410-01D	Modification	02/21/2007	10/24/2007
AN077410-01C	Modification	02/15/2007	10/24/2007
AN077410-01B	Modification	01/04/2007	10/24/2007
AN077410-01A	Modification	12/05/2006	10/24/2007
AN077410-01	New Approval	10/24/2006	10/24/2007

Modification Description and Rationale

Are contacts and personnel changes only?	Yes

The following is a brief description of the Protocol changes and the justification for these changes.

A. Funding

Type:
Federal, State or Other Government

122

Funding Agency/Sponsor	Grant or Contract Number	Source has Approved Method for Scientific Merit Review
NIH	HL61284	Yes

You have selected at least one Project Funding Sources with an IACUC approved Method for Scientific Merit Review.

B. Regulated Materials and Stem Cell Info

Regulated Materials	Approval Number	Legacy Number	Expiration Date

Will data from this study be used to apply for Food and Drug Administration (FDA) approval of a drug or device, or will animal studies be outsourced?
No

Use of Human Embryonic Stem Cells:	
Will human embryonic stem cells or human somatic cells be used under this protocol?	No
Are the human embryonic stem cells on the NIH Human Embryonic Stem Cell Registry?	No
Does this protocol involve the transfer of a human somatic cell nucleus into an animal egg?	No
Does this protocol involve the combination of human embryonic stem cells with an animal embryo?	No

C. Animals

Species	USDA Type	Acquired	Bred	Total
Sheep	C	90	0	90
Sheep	D	90	180	270
	Total:	180	180	360

As required by federal regulations, describe the statistical tests (e.g. Power analyses) and/or other rationales (e.g. Tissue collection needs, breeding efficiency) that you used to determine the number of animals requested above. Note: The IACUC may require that you consult with a statistician from the UCSF Division of Biostatistics (476-8671).

90 of the 180 Category D acquired sheep represent pregnant ewes that will undergo uterine surgery for fetal intervention. The 90 Category D bred sheep represent the fetuses of these ewes, who will spontaneously deliver and be studied as shunted lambs. The other 90 Category D bred sheep represent the age-matched control lambs that will be studied following spontaneous delivery. The 90 acquired Category C sheep represent the mothers of these control lambs. These ewes will not be operated on, and will have blood drawn as their only procedure (Category C). Please note that if the acquired category D ewes (that undergo fetal surgery) have twin gestations, the unoperated twin will serve as the control lamb. Therefore, the 90 Category C acquired ewes and their 90 offspring represent the maximum number needed. We always request twin gestations, and utilize twin gestations whenever available. Therefore, these numbers will likely be reduced significantly.

Group I: Chronic NLA (NO inhibitor) infusion - n=10 shunt lambs and n=10 control

lambs (TOTAL 20 LAMBS)

Group II: Chronic Arginine (precursor to NO) - n=10 shunt lambs and n=10 control lambs (TOTAL 20 LAMBS)

Group III: Chronic IV Vehicle infusion - n=10 shunt lambs and n=10 control lambs (TOTAL 20 LAMBS)

Group IV: Chronic oral vehicle - n=10 shunt lambs and n=10 control lambs (TOTAL 20 LAMBS)

Group V: Chronic PPAR agonist treatment - n=10 shunt lambs and n=10 control lambs (TOTAL 20 LAMBS)

Group VI: Chronic PPAR antagonist treatment - n=10 shunt lambs and n=10 control lambs (TOTAL 20 LAMBS)

Group VII: Chronic VEGF treatment - n=10 shunt lambs and n=10 control lambs (TOTAL 20 LAMBS)

Group VIII: Chronic VEGF antagonist treatment - n=10 shunt lambs and n=10 control lambs (TOTAL 20 LAMBS)

Group IX: Isolated lung preparations for fluid clearance studies - n=10 shunt lambs and n=10 control lambs (TOTAL 20 LAMBS)

Power analysis based on preliminary data suggests that 8 lambs will be needed in each of the 9 study groups (a=0.05, b=0.2).

This chronic model has a 10-20% mortality due to the difficulty of the surgical preparation. In addition, the lambs may develop congestive heart failure and are susceptible to pulmonary infections. Therefore the total number of animals needed per group is estimated at 10 to yield a final number of 8.

Therefore total study lambs: 180 (90 from ewes undergoing uterine surgery:Cat D, and 90 from unoperated ewes: Cat C). Data over time will be compared by ANOVA. Comparisons between study groups will be made using the unpaired t-test.

Will you be using any animals transferred from another PI or protocol, from your previous protocol, or transferred from another Investigator or Institution?

No

Will animals have undergone any procedures?

No

Describe the prior experimental procedures, justify the use of the animals for your research and submit a completed LARC Animal Transfer Form with your application or at the time of animal transfer.

Justify also if the animal(s) is/are used in more than one protocol involving a major operative procedure from which it is allowed to recover.

D. Contacts & Personnel

Animal Procedures for Aramburo, Angela:

Surgery, monitoring, anesthesia, performance of physiologic studies.

Animal Training for Aramburo, Angela:
2 years of sheep work experience.

If emergency euthanasia is required for an animal and the LARC vet staff is unable to contact the PI or any member of their staff, please indicate which tissues/samples need to be collected from the animal, and specifically how they should be stored, e.g. Formalin, refrigeration, EDTA tube.
Heart and lungs frozen in liquid nitrogen. Carcur placed in refrigeration.

E. Justifications and Alternatives

Sources			
Date of Most Recent Search	**Key Words**	**Search Site**	**Years Covered**
9/15/2007	Pulmonary hypertension, nitric oxide, endothelin-1, lamb, vascular endothelium, congenital heart disease, VEGF, PPAR, lung fluid clearance	Medline	1980-present
9/15/2007	Pulmonary hypertension, nitric oxide, endothelin-1, lamb, vascular endothelium, congenital heart disease, VEGF, PPAR, lung fluid clearance	Vitual library of Veterinary Medicine	1980-present

Other Resources		
Date	**Topics**	**Resource (e.g. Attendance at meetings, consultation w/ colleagues)**
11/5/2007	Pulmonary hypertension, congenital heart disease.	Attendance at annual AHA and Pediatric Research meetings

Explain why animals are required for your studies, and why replacements, such as cell culture or computer modeling, cannot fully replace animals.
Pregnant ewes and lambs will be used. In utero placement of an aortopulmonary graft has provided a unique animal model that truly simulates congenital heart disease. Since this is a whole animal model of a disease, there are no other alternatives. There exist no in vitro systems which adequately simulate the physiology and morphology of the pulmonary circulation. Therefore, there are no alternatives to the use of live animals for these experiments. Based on these physiologic observations, we do utilize cell culture systems and molecular biological techniques to further delineate downstream mechanisms.

Describe how your proposal minimizes animal pain and distress (e.g. use of in vitro procedures, reduction of animal numbers, refinement of experimental design, refinement of procedural techniques). Please be specific.
REDUCTION NUMBER OF ANIMALS:
Refined surgical technique and improved post-operative care have decreased morbidity and increased survival rates of this procedure. In vitro procedures such as an isolated vessel studies and mRNA gene expression will be performed on peripheral lung tissue and 4th-5th generation arteries and veins, allowing many interventions on a single piece of tissue. This integrated physiologic and molecular approach allows a great deal of information to be gathered from a minimum number of animsl. Lastly, we will perform only the necessary number of studies to reach statistical significance, and utilize twin gestations when ever possible.

RELIEF METHOD:
All experiments have been designed to minimize trauma and discomfort. Anesthetics and analgesics appropriate to the species will be used where applicable. Close, daily monitoring and post-operative analgesics are used to minimize discomfort and ensure proper supportive care. At the conclusion of the last study, the ewe and lamb are euthanized by an overdose of pentobarbital sodium, followed by a bilateral thoracotomy.

Explain why the proposed species are the most appropriate.
Sheep are the ideal species for fetal survival surgery, allowing manipulation of the fetus without spontaneous abortion. Fetal and young lambs demonstrate many hemodynamic and hormonal functions similar to the human. Normal fetal and young lamb physiology and pathophysiology have been extensively studied. These studies provide the experimental background upon which this project is based. This information is not available in other species. Fetal and young lamb size and anatomy allow easy access to perform the necessary procedures, so that a high success rate can be achieved.

You have USDA Category C Animals.

You have USDA Category D Animals that would receive relief from pain, discomfort or distress.

You do not have USDA Category E Animals.

F. IACUC/LARC Standard Procedures (see Appendix - Section F for full text)

Sheep
Standard Procedures

Sub-mandibular Blood Collection is the IACUC-preferred technique for blood collection. If you intend to use Retro-Orbital Blood Collection, please justify below.

The techniques listed above have established IACUC/LARC Standard Procedures defined for them. You must follow the procedures as specified or you will be out of compliance. Any variation must be described and justified below, and approved by the IACUC.

G. Procedures Involving Living Animals

Species: Sheep   Group: C
Ewe blood drawing

Approximately 400 ml of whole blood will be obtained from the lamb's ewe for blood drawing replacement. The ewe is routinely housed in the lab with the nursing lamb until study. On the day of the study, the ewe is medicated with an IM injection of Ketamine hydrochloride and placed on a surgical table. The neck is shaved and disinfected. A 14-18 gauge angiocath is placed percutaneously into the external jugular vein, and blood is drained into a standard blood collection bag by gravity. At the end of the procedure, the catheter is removed, and hemostasis is obtained with direct pressure. The ewe is then returned to its cage and monitored every 15 minutes until

standing without signs of bleeding. All ewes will then be returned to the farm, when possible.

Species: Sheep   Group: D

In accordance with UCSF guidelines, pregnant ewes will have an acclimation period of at least 24-48 hours, after being delivered by the vendor, to avoid parturient paresis and pregnancy toxemia. Time-dated pregnant ewes (130-140 days gestation) are fasted for 12-24 hours prior to surgery. The ewes are anesthetized for surgery under sterile conditions. First the ewe is given ketamine hydrochloride for pre-anesthesia. The neck is then shave, and a 14-18g angiocath is placed percutaneously in the external jugular vein for IV fluids. The ewe is then allowed to breathe isoflurane via a facemask, and, when sufficiently anesthetized, intubated with an appropriate sized endotracheal tube. The ewe is mechanically ventilated with 1-3% isoflurane in oxygen to maintain anesthesia. A hallowell EMC animal ventilator is utilized with a Summitt Medical Vaporizer. After the induction of the anesthetic regimen, intravenous replacement fluids (D5 lactated ringer's) is begun. After infiltration of 1-2 ml of 2% lidocaine, a 0.05 id polyvinyl catheter is placed in the femoral artery of the left hindlimb, and systemic arterial pressure and heart are monitored continuously. The ewe is given intravenous antibiotics (penicillin G sodium, and gentamicin). The ewe is given an injection of 2% lidocaine along the midline prior to incision. A midline incision along the ventral abdomen is made and the uterus exposed. Through a uterine incision, the left fetal forelimb and chest are exposed. The fetus is given a local anesthetic (2% lidocaine hydrochloride) for skin incisions. A left lateral thoracotomy is performed in the fourth intercostal space. The pericardium is incised along the main pulmonary trunk, and the main pulmonary artery and ovine trunk of the ascending aorta are dissected free and controlled with vessel loops. The ascending aorta is partially clamped with a side biting vascular clamp. The aorta is incised and an anastomosis between a segment of 8.0 mm Gore-tex graft, (temporarily occluded with a vascular clip), and the aorta is performed with 7.0 surgilene suture. The vascular clamp is gradually released to minimize bleeding along the suture line. The vascular clamp is then applied to the pulmonary artery. The pulmonary artery is incised and the free end of the graft is sutured to the pulmonary artery. The clamp is gradually released, and, after a suitable period, the vascular clip is removed from the graft, establishing systemic to pulmonary blood flow. The thoracotomy is closed in layers, and an intercostal nerve block is performed (bupivacaine, 0.5%). In fetal lambs that will be receiving chronic infusions, a hindlimb is exposed through a second small uterine incision. Following infiltration with 2% lidocaine, a venous catheter is placed and advanced into the vena cava. The external catheter is coiled and sutured to the external skin. This insures that the catheter is not dislodged during delivery. The fetal limb and chest is returned to the uterus, warm saline is infused to replace any lost amniotic fluid, and the uterine incision closed. After recovery from anesthesia, the ewe is returned to the cage with free access to food and water. Antibiotics (penicillin, gentamicin, IM) is given daily for three consecutive days following surgery. Buprenorphine is given immediately after surgery 4-6 hours later, and ~every 8hours (not to exceed 12 hours) for the next 24 hours. Thereafter the ewe is assessed daily for the need for analgesia until it is deemed no longer needed. This assessment includes the ewe's activity and appetite. The ewe is allowed to spontaneously deliver the lamb(s).
Lambs: Furosemide (IM) is administered to the lambs 1-2 times daily prn for increasing respiratory effort and decreased activity. Elemental iron (1 ml, IM) is given once per week after birth. Weekly, venous blood (10 ml) may be obtained for the

sequential determination of plasma nitrate, cGMP and ET-1 concentrations.

Immediately following spontaneous delivery of the lambs, they will either undergo a continuous infusion of an experimental agent (via an ambulatory infusion pump), intermittent IV dosing of an experimental agent, or oral administration of an experimental agent.

Occasionally, the leg catheters are not placed during fetal surgery because of concern of dislodgement during spontaneous delivery. If the catheters are not placed in utero, they are placed on day one of life (for those protocols requiring intravenous dosing). For this procedure, ketamine ~15 mg/kg is given IM for sedation, and 2% lidocaine is infiltrated locally. A venous catheter is then placed and advanced into the vena cava.

From 2-8 weeks after spontaneous delivery, the lamb is studied. Polyurethane catheters are placed in a vein and artery of each hind leg of the lamb under anesthesia induced by ketamine hydrochloride (M) and local infiltration of local anesthetic (2% lidocaine). The lambs are given an IV boluses of fentanyl citrate and diazepam and then anesthetized with continuous intravenous infusions of fentanyl citrate, ketamine hydrochloride and diazepam and local infiltration of local anesthetic (2% lidocaine). Heart rate and blood pressure are continuously monitored, and doses adjusted with changes in these parameters. The lambs are intubated with a 4.5-5.5 mm OD cuffed endotracheal tube and mechanically ventilated with a pediatric time-cycled, pressure-limited ventilator. Pancuronium bromide is given intermittently for muscle relaxation. Ventilation with 21% oxygen is adjusted to maintain a systemic arterial PCO2 between 35 and 45 torr. Inhalational anesthesia is not utilized for the treatment studies because of their effects on the pulmonary vasculature and the ability to compare data that has been obtained over the past 10 years with IV anesthesia.

A midsternotomy incision is performed, and polyurethane catheters are placed in the pulmonary artery, and left and right atrium. An ultrasonic flow probe (Transonics Systems, Ithaca, NY) is placed on the left pulmonary artery to measure pulmonary blood flow. All procedures are performed using strict aseptic techniques. After 60 minutes of stable ventilation, hemoglobin and oxygen saturation measurements are made. Then, blood is collected from the pulmonary artery and aorta for plasma nitrate, cGMP and ET-1 determinations, and a peripheral lung biopsy is obtain for tissue nitrate, cGMP, and ET-1 determinations. The lamb will then receive a group of vasoactive stimuli. Stimuli that assess the NO cascade (Acetylcholine, Nitric Oxide, and 8-Bromo cGMP), stimuli that assess the ET-1 cascade and those that assess differences in vascular reactivity (ET-1, 4-Ala ET-1, and PD 156707) will be administered. At the termination of the last study, the ewe and lamb are killed by an intravenous overdose of pentobarbital sodium (Veterinary Euthanasia-6 Solution, 150 mg/ kg), followed by a bilateral thoracotomy. Blood will be drained by direct cardiac puncture. The heart and lungs will then be removed for morphologic evaluation.

Lung fluid clearance studies:
The day prior to study, some lambs (shunt and control) will have ~150 ml of blood withdrawn as follows: the lamb is medicated with an IM injection of Ketamine hydrochloride and placed on a surgical table. The neck is shaved and disinfected. A 16-22 gauge angiocath is placed percutaneously into the external jugular vein, and blood is drained into a standard blood collection bag by gravity. At the end of the

procedure, the catheter is removed, and hemostasis is obtained with direct pressure. The lamb is then returned to its cage and monitored every 15 minutes until standing without signs of bleeding. The serum is separated and mixed with Evans Blue dye and/or I125 labeled albumin.

For the lung fluid clearance studies, the lambs will be anesthetized with isoflurane after the initial ketamine premedication. In these lambs, Pancuronium bromide is also given intermittently for muscle relaxation, and ventilation with 21% oxygen is adjusted to maintain a systemic arterial PCO2 between 35 and 45 torr. Instrumentation is as above. However, the lambs will undergo a second thoracotomy for cannulation of the caudal mediastinal lymph node efferent duct.

Additional procedures involve flexible bronchoscopy with instillation and withdrawal of serum, I125 labelled albumin, and/or Lactated Ringer's solution into selected lung lobes. All procedures are performed while the lamb is under general anesthesia, and the lamb will not be allowed to recover from anesthesia.

H. Surgery and Post-Operative Care

Sheep	
Surgery Performed:	Yes
Surgery Type:	Survival (Single)
What is the duration of the surgery?	The ewe and fetal surgery will take ~2-3 hours. Some lambs will have a continuous IV infusion from birth for 2-8 weeks. The lamb physiologic study at 2 days-8 weeks of age will take ~4-6 hours. Blood drawing from the ewe takes 10-30 minutes. The ewe and fetal surgery will take ~2-3 hours.
For how long will the animals survive after surgery?	The ewe will survive 2-8 weeks after spontaneous deliver of the lamb.
Describe post-operative care and the frequency of monitoring in the days or weeks until the animals recover from the surgery (e.g. wound care, infection, etc.)	The ewe is monitored twice daily after surgery by the PI staff for two days. Thereafter, we will monitor the ewe once per day. This will be increased if clinical conditions warrant it. A minimum of daily assessemnts will be documented. After birth the lamb is monitored daily for condition of incision site and respiratory pattern. In addition, the hindlimb catheter (in select studies) is checked daily. The lamb is weighed 3 times per week the first week, and once per week thereafter if weight gain is normal. If weight gain does not appear normal, we will resume the 3 times per week regimen.
Will you follow IACUC/LARC Guidelines for Post-Operative Analgesia:	Yes
Will you follow IACUC/LARC Guidelines for Animal Surgery:	Yes

I. Pre-Anesthetics and Anesthetics, Neuromuscular Blocking Drugs, Therapeutics, Analgesics and Experimental Agents

Sheep: Pre-Anesthetics and Anesthetics						
Agent	**Dose Range (mg/kg)**	**Route**	**Frequency / Total Duration**	**Recover From Agent**	**Use IACUC Monitor Form**	**Anesthesia Recovery Time**
Bupivicaine (Marcaine)	2-3 ml Bupivicaine 0.5%	Nerve block	X1 at fetal surgery	Yes	No	The effect should last ~24 hours.
Diazepam	0.1 mg/kg (lamb studies)	IV	Bolus x1	No	No	N/A
Diazepam	0.002-0.005 mg/kg/min (lamb studies)	IV	Continuous	No	No	N/A
Fentanyl-Droperidol	5 µg/kg (lamb studies)	IV	Bolus X1	No	No	N/A
Fentanyl-Droperidol	1-3 µg/kg/hr (lamb studies)	IV	Continuous	No	No	N/A
Isoflurane	1-5%	Inhalational	Continuous during ewe surgery.	Yes	No	30-90 minutes.
Ketamine	(hydrochloride) 0.3-0.6 mg/kg/min (lamb studies)	IV	Continuous	No	No	N/A
Ketamine	(hydrochloride) ~15 mg/kg	IM	X1 Lambs and ewe PRE-OP, including leg catheterization.	Yes	No	Post-operatively, pregnant ewes recover quickly and are ambulatory and feeding usually within 1 hour after being returned to their pen. The lamb will not recover from anesthesia in the postnatal physiologic

						studies.
Ketamine	(hydrochloride) ~15 mg/kg	IM	X1 to ewes for blood drawing	Yes	No	15-30 minutes
Lidocaine (Xylocaine)	(2%, hydrochloride) 0.5-1.0 ml	SC	Skin incisions (ewe, fetus, and lamb)	Yes	No	Post-operatively, pregnant ewes recover quickly and are ambulatory and feeding usually within 1 hour after being returned to their pen. The lamb will not recover from anesthesia in the postnatal physiologic studies.

Sheep: Pre-Anesthetics and Anesthetics Monitoring Details					
Agent	**Variable Monitored**	**Monitoring Frequency [Anesthesia]**	**Monitoring Frequency [Recovery]**	**Doc/Charting Frequency [Anesthesia]**	**Doc/Charting Frequency [Recovery]**

Sheep: Neuromuscular Blocking Drugs			
Agent	**Dose Range (mg/kg)**	**Route**	**Frequency / Total Duration**
Pancuronium	0.05-0.1 mg/kg	IV	PRN movement in lamb studies

Sheep: Therapeutic			
Agent	**Dose Range (mg/kg)**	**Route**	**Frequency / Total Duration**
Furosemide (Lasix)	0.5-1.0 mg/kg	IM	1-2 times daily to lamb prn, for increased work of breathing and/or poor weight gain.
Gentamicin	100 mg (ewe only)	IV/IM	1X during surgery, and QD for 3 days post-op.
Iron Dextran	1 ml elemental iron	IM	weekly to lambs
Lactated Ringer's	2-10 ml/kg/hr Dextrose/Lactated Ringers	IV	Continuous during ewe surgery and lamb

Solution			surgery and study.
Penicillin	~10,000-20,000 u/kg (usually one million units) Penicillin G (ewe only)	IV/IM	1X during surgery, and QD for 3 days post-op.

Sheep: Analgesics			
Agent	**Dose Range (mg/kg)**	**Route**	**Frequency / Total Duration**
Buprenorphine (Buprenex)	0.05-0.1 mg/kg	IM/IV	After ewe surgery, 4-6 hours later, and ~every 8 hours (not tp exceed 12 hours) for 24 hours.

Sheep: Experimental Agents			
Agent	**Dose Range (mg/kg)**	**Route**	**Frequency / Total Duration**
Inhaled Nitric Oxide	40 ppm	Inhalational	X1 during study
LNA	0.1 mg/kg/hr	IV	Continuous for 2-8 weeks
0.9% saline	3 ml/hr	IV	Continuous for 2-8 weeks
Packed RBCs	5-20 ml/kg	IV	PRN anemia (hemoglobin lower than baseline value)
4-Ala-ET-1	1750 ng/kg	IV	X1 during study
Endothelin-1	250 ng/kg	IV	X1 study
Acetycholine	1ug/kg/min	IV	10 minutes during study
8-bromo-cGMP	2mg/kg	IV	X1 study
PD 156707	1mg/kg/min	IV	10 minutes during study
rosiglitazone	3 mg/kg	po	once per day for 28 days
arginine	50-250 mg/kg/hr	IV	Continuous for 2-8 weeks
Oral placebo (sugar pill)	capsule	PO	Once daily for 2-8 weeks
VEGF	TBD	IV	2-8 weeks
VEGF antagonist EYE-001	TBD	IV	2-8 weeks
PPARγ antagonist GW9662	TBD	IV	2-8 weeks

All Species: Pre-Anesthetics and Anesthetics	
Will you follow IACUC/LARC Guidelines for Anesthetizing Animals for Research Procedures:	Yes

All Species: Neuromuscular Blocking Drugs	
The need for NMBD must be scientifically justified:	The use of muscle relaxants is necessary in this protocol to insure that ventilation is completely controlled. One of our primary outcome variables is pulmonary vascular resistance, which is altered by changes in systemic arterial pH. Therefore, PCO_2 must be controlled. Once muscle relaxants are given, the infusion rates of ketamine, diazepam, and fentanyl will not be reduced. As always, we will use changes (~20% increases) in heart rate and systemic blood pressure as indicating a need for more anesthetics. Previous studies without muscle relaxants resulted in an inability to

	adequately control PaCO2. Since one of our primary outcome variables is pulmonary vascular resistance, the variability in our studies without muscle relaxants has required more animals to be studied to obtain statistical significance. We believe that the use of muscle relaxants will result in a reduction in the number of animals needed.
The anesthetic protocol, NMBD regimen, and method of ventilation must be specified.	As above. The lambs will be mechanically ventilated.
Description of the method(s)	
Will you follow IACUC/LARC Guidelines for use of Neuromuscular Blocking Drugs (NMBD):	Yes

J. Management and Monitoring of Adverse Effects of Procedures and Experimental Agents

Adverse Effects: Sheep Experimental Group: C		
Procedure, Agent or Phenotype	**Potential Adverse Effects**	**Management**
Ketamine sedation	Respiratory depression.	Supplemental oxygen

Monitoring Parameters: Sheep Experimental Group: C		
Monitoring Parameters	**Frequency**	**PI/Lab will Document**
Activity and respirations	q 15 minutes until standing	Yes

Describe the conditions, complications, and criteria (e.g. uncontrolled infection, loss of more than 15% body weight, etc.) that would lead to removal of an animal from the study, and describe how this will be accomplished (e.g. stopping treatment, euthanasia).

For all investigators housing animals with tumor formation, skin lesions, neurological deficits, or that are in Category E, list the expected characteristics/clinical presentations and endpoints of the animal model and the criteria for euthanasia. Note: The IACUC also requires such lists to be posted in the respective animal rooms and monitored by the IACUC compliance staff and LARC, to assure PI adherence to the endpoints listed.

Adverse Effects: Sheep Experimental Group: D		
Procedure, Agent or Phenotype	**Potential Adverse Effects**	**Management**
Surgical Instrumentation (ewe)	Ketosis, hypocalcemia	IV fluids, dextrose, calcium, polyethylene glycol, vet consultation.
Surgical instrumentation (ewe)	Incision infection/dehisense	Antibiotics, wound cleaning, and dressing
Ewe surgery and Lamb surgical study	Bleeding	Volume, blood transfusion, cauterize bleeding sight.
Catheter dislodgement (lamb)	Blood loss	Transfusion of RBCs

Aortopulmonary graft	Congestive heart failure	IV lasix (~1 mg/kg)
Chronic experimental agents	Decrease in pulmonary vascular resistance.	Increase lasix therapy

Monitoring Parameters: Sheep Experimental Group: D		
Monitoring Parameters	**Frequency**	**PI/Lab will Document**
Lamb weight	3x per week for the first week; once a week thereafter. If weight appears inappropriate, 3x per week schedule will be resumed.	Yes
Lamb activity/apetite	Daily	Yes
Ewe activity, appetite, and incision.	Daily	Yes

Describe the conditions, complications, and criteria (e.g. uncontrolled infection, loss of more than 15% body weight, etc.) that would lead to removal of an animal from the study, and describe how this will be accomplished (e.g. stopping treatment, euthanasia). Infection that cannot be controlled by antibiotics. Nonresponsive ketoacidosis hypocalcemia in the ewe following surgery. Evidence of fascial or cutaneous dehiscence not surgically repairable. Congestive heart failure that is not controlled with lasix therapy (poor weight gain, increased respiratory rate, decreased activity) in the lamb. Excessive blood loss that is not controlled with blood transfusion.

For all investigators housing animals with tumor formation, skin lesions, neurological deficits, or that are in Category E, list the expected characteristics/clinical presentations and endpoints of the animal model and the criteria for euthanasia. Note: The IACUC also requires such lists to be posted in the respective animal rooms and monitored by the IACUC compliance staff and LARC, to assure PI adherence to the endpoints listed.

K. Species Locations

Sheep - "LARC Space" Locations
Use LARC Space for Animal Housing of this species.
Use LARC Space for Extended Study of this species.
Use LARC Space for Survival Surgery on this species.
Use LARC Space for Non-Surgical Procedures on this species.

Sheep - "Non-LARC Space" Locations		
Building/Room	**Proposed Use**	**Space Owner**
PSB/Parnassus Service Building 330AB	Survival Surgery	PI Space
PSB/Parnassus Service Building 351	Animal Housing	PI Space
PSB/Parnassus Service Building 363	Animal Housing	PI Space

Sheep - Animal Housing - PSB/Parnassus Service Building 351	
Will animals be kept in the room for more than 12 hours?	No
Special attention is required for the strain or model:	No
Special post-procedural care is required:	No
Special environmental needs are required (light, temperature, sound, etc.):	No
Hazardous substance containment (Radiation, chemical or	No

biosafety containment) is required:	
Chronic preparation of animal is required (more than 12 hours):	No
Other requirements of the experiment, phenotype or model:	No
Maximum number of animals housed at a given time:	0
Justify this number:	
Animals are continuously housed:	No
LARC will provide animal husbandry services:	No
Other relevant details:	

Sheep - Animal Housing - PSB/Parnassus Service Building_363	
Will animals be kept in the room for more than 12 hours?	No
Special attention is required for the strain or model:	No
Special post-procedural care is required:	No
Special environmental needs are required (light, temperature, sound, etc.):	No
Hazardous substance containment (Radiation, chemical or biosafety containment) is required:	No
Chronic preparation of animal is required (more than 12 hours):	No
Other requirements of the experiment, phenotype or model:	No
Maximum number of animals housed at a given time:	0
Justify this number:	
Animals are continuously housed:	No
LARC will provide animal husbandry services:	No
Other relevant details:	

Sheep - "Transporting"
You will NOT be transporting animals in your own vehicles.

L. Reportable Exceptions for Procedures

Sheep

M. Physical Restraint of Conscious Animals

Sheep

N. Euthanasia

Sheep	
Will you conform to the UCSF Guidelines for Euthanasia?	Yes

Chemical Method	**Physical Method**	**Comments**
IV overdose of sodium pentobabital 260 mg/ml (50-100 mg/kg)	Bilateral thoracotomy	IV overdose of sodium pentobabital 260 mg/ml (50-100 mg/kg) followed by bilateral thoracotomy. When isolated vessels will be harvested, sodium thiopental (50-100 mg/kg) will be administered, and blood will be

		drained by direct cardiac puncture following euthansia.

O. Environmental Enrichment

Sheep	
Will you conform to the UCSF Guidelines for Environmental Enrichment?	Yes

P. Tissue Sharing and Live Animal Disposition

Sheep	
Name and telephone number of the contact person to discuss tissue-sharing arrangements:	
Contact Name:	
Contact Telephone:	
Live Animal Disposition	
Describe your plan, if you are willing to make live animals available after your study:	The unoperated ewes will be returned to the farm.

Sheep - Available Tissues						
Strain	**Gender**	**Age**	**Weight**	**Tissues Not Available**	**Form of Euthanasia**	**Tissue Alterations**
mixed breed	Both	newborn, 3-6 weeks, >6 months	4-50 kg	lungs, heart	pentobarbitol	Pulmonary alterations

Q. Roles & Training

Aramburo, Angela - Details	
Admin Role:	
MHS Questionnaire:	Completed on Apr 2 2008 11:23AM
BRER I Training:	Course Taken; BRER I course is required for all IACUC Personnel [every 3 years].
BRER II Training:	Course Taken; BRER II course is required for IACUC Personnel involved with Anesthesia, Surgery and/or Post Surgical Care [every 3 years].

Aramburo, Angela - Training Records	
Course Title	**Date**
Controlled Substances Safety (Online)	08/29/2007
IACUC - BRER I (Online)	03/22/2007
IACUC - BRER II (Online)	03/22/2007
Lab Safety for Researchers (Online)	08/29/2007
Protecting Human Research Subjects	11/29/2007

9.2 LAMB PULMONARY VASCULAR REACTIVITY TESTING PROTOCOL

- **Instrument Lamb**
  - Hind-limb catheters
    - Bilateral arterial lines (marked as 2 short lines)
    - Bilateral venous lines (3 short lines)
  - Intra-cardiac catheters
    - Right atrial (4 short lines)
    - Left atrial (no line)
    - 2 Pulmonary artery (long line)
      - One for medication administration, one for monitoring
  - Left pulmonary artery flow probe

- **Calibrate transducers** (at level of the heart)

- **Set-up computer**
  - Make sure each file is saved with its new animal number
  - In data section update details
    - Animal number, date of birth, weight, type of prep, treatments, sex, age, hemoglobin
  - Make sure logging rate is at 1-second intervals

- **Baseline**
  - Based on hemodynamics and arterial blood gas, make appropriate adjustments in minute ventilation, fluid status and hemoglobin
  - Once at steady state, record baseline hemodynamics
  - Obtain blood and/or tissue as appropriate for the study
    - Collect in a sterile manner. Separate into aliquots, depending on the biopsy size, label, and flash freeze in liquid nitrogen
    - Labeling:
      - ❖ Use the label maker whenever possible
      - ❖ At minimum should include:

- Animal number, Type of prep (control, shunt, etc), Age of animal, Treatment given, tissue
- Example: #3309, 4wk shunt-carnitine, lung
  - Spin and separate blood, put into labeled (as above) tubes, flash freeze
- If appropriate, perform Qp/Qs:
  - Simultaneous blood draws for blood gas analysis from: femoral artery, right ventricle, left atrium, pulmonary artery
  - Formula: (Femoral %sat - RV %sat) / (LA %sat - PA %sat)

- **Administer vasoactive agents**:

   Prior to administration of drug:
  - Obtain arterial blood gas
  - Check function of each catheter:
    - Confirm zero
    - Draw from and flush each line (to assure they are patent)
  - Intravenous agents are given by rapid push into the pulmonary artery (dedicated medication line) catheter. Mark a point on the computer that represents a baseline (usually letter A) immediately prior to administration, and mark the point when the agent is given/started
    - Acetylcholine: 1 microgram/kg/dose bolus
    - Acetylcholine continuous infusion at 1.5 mcg/kg/min, 5 minutes
    - Inhaled NO 40 ppm for 10 minutes
    - Hypoxia 10% FiO2 for 10 minutes (draw blood gas just prior to discontinuing hypoxia, in addition to blood gas at baseline)
    - Thromboxane: 1 microgram/kg/min until steady state achieved
  - Ensure return to baseline prior to administration of each agent